Design and development of nucleic acid amplification-based assays for the detection and characterization of plant viruses

PhD thesis

by Marianna Szemes

supervisor: Dr László Dorgai

Bay Zoltán Foundation for Applied Research

Institute for Biotechnology

2001

Contents

1. Introduction

Viruses infecting cultivated plants cause serious losses every year, therefore significant effort is made to control them. Since there is no economically feasible cure for plant virus diseases, the main focus of virus control is on the prevention of infection and the breeding of virus-resistant cultivars. The use of virus-free propagation materials, the screening of plant materials for the presence of the virus and the elimination of the infected plants are the tools of choice.

For taking effective measures, the knowledge of viruses, their propagation strategies and epidemiological properties are pivotal, along with the availability of specific, sensitive and fast detection methods. The present thesis describes the design and development of novel diagnostic tools for the detection of certain economically important viral pests by the use of nucleic acid amplification, which provide the most sensitive and specific detection methods available nowadays.

1.1. Short history of plant virology, plant virus diagnosis and viral taxonomy

The science of plant virology, and actually that of virology, is hardly older than 100 years, if we calculate it from the famous publication of M. V. Beijerinck about *Tobacco mosaic virus* (TMV), which he called '*Contagium vivum fluidum*' (1898). The name summarizes what he could know about these creatures: a contagious disease, which could be transmitted by a very small portion of the sap of a diseased plant. The newly infected plant developed similar symptoms, and could serve as a source of infection. He concluded that it must be able to multiply, thus it was living. Nevertheless, it was smaller than all the disease-causing microorganisms known in that age, since it could pass through a bacterial filter made of unglazed porcelain. The same discovery was published by Ivanosky in 1892, however, he was searching for a different explanation, about bacterial spores of very small size.

On the basis of the criteria described by Beijerinck, several presumed viral diseases of plants were identified at the beginning of the 20th century. However, only their infectivity, the caused symptoms and their biological properties could be characterized; the causal agents themselves remained out of reach for long time.

From historical records, certain cases of ancient viral infections could be identified in retrospective. The most famous one is, perhaps, the discovery of *Tulip breaking potyvirus*, which causes color breaking of tulip petals (McKay and Warner, 1933). In 1576, only 16 years after the introduction of tulips from the Middle East, a new variation of the flower, with petals of peculiar patterns, were found. The bulbs of these flowers were extremely expensive, until the growers found that the characteristic features could be transmitted by grafting. But this happened only decades later.

In 1930, the size of viruses was determined to range between 15 and 300 nm, as measured by passage through collodion filters. The scientists faced the enigma of how the whole machinery of a living organism could be packed into an entity hardly bigger than a protein molecule. In 1935, Stanley succeeded in crystallizing TMV, and the crystallized virus retained infectivity. Actually, it was found to be still infectious when tested 25 years later (Stanley and Walens, 1961). TMV was an ideal study object, since it is extremely resistant, withstands even heating to 95 °C. The plant viruses were found very diverse in these, so-called, physicochemical properties. In 1937, the presence of phosphorus was demonstrated in viruses (Bawden and Pirie), and finally they were recognized as nucleoprotein particles. Kausche, Pfankuch and Ruska visualized first the elongated particles of TMV by the newly invented electron microscope (Kausche et al., 1939). This technique had enormous potential in virus research, ranging from the visualization and the identification of viruses as the causal agents of diseases to the study of host cell-virus interactions.

The advent of serological techniques and that of molecular biology brought about a completely new era in virology, just like in almost every field of biology. Serological methods, i.e. ELISA (Enzyme-linked immunosorbent assay), still constitute the main diagnostic techniques in routine analyses, besides biological testing, which identifies the viruses on the basis of the caused symptoms on sensitive indicator plants. The combination of serology and electron microscopy resulted in powerful techniques, like decoration electron microscopy with immunogold-labeling. Molecular biological methods enabled the determination of the nucleic acid sequence and the gene content of viral genomes, their replication strategy, and provided specific and sensitive diagnostic tools. These technological advances enabled the scientists to collect a great amount of knowledge about viruses, which allowed their classification and required the reevaluation of the earlier concepts.

The first descriptive taxonomic systems for viruses relied on biological and physicochemical properties, like resistance to heat and chemical treatments (Johnson, 1927). In 1959, a morphology-based classification system was proposed for the elongated plant viruses (Brandes and Wetter). Interestingly, these features showed good correlation with biological properties, such as virus-vector specificity. In 1966, the predecessor of the International Committee on Taxonomy of Viruses (ICTV) was established, and since then they have been in charge of the regulation and standardization of the naming and classification of viruses. A universal taxonomic system was created with units of species, genera and families, based on genome organization, replication mechanism, particle morphology etc. Presently, more than 3600 virus species are recognized (van Regenmortel et al., 1999), but specialty groups keep track of more than 30 000 strains, substrains and pathotypes. In a recent report, ICTV proposed that the diversity of viruses infecting humans, domestic animals and cultivated plants has, most probably, already been mapped. This conclusion was made on the basis of the fact that very few viruses had been discovered in the

previous couple of years that did not fit into the existing taxa. The viruses of these few species, naturally, may represent only a small subset of the viruses hosted by the living organisms on Earth.

This is the present stage of knowledge (Bos, 1999; ICTV, http://www.ncbi.nlm.nih.gov/ICTV). However, scientists still have major challenges in the fields of virus taxonomy, identification and detection. The definitions of the taxa are difficult, mainly because of the polyphyletic origin of viruses (i.e. they do not have a common ancestor), the frequent occurrence of recombination and the gene transfer between host and virus. In 1991, ICTV accepted that: "A virus species is defined as a polythetic class of viruses that constitutes a replicating lineage and occupies a particular ecological niche (van Regenmortel, 1990)." Members of a polythetic class are defined by more than one properties, and no single property is essential or necessary. The problems of virus taxonomy are shared by researchers developing diagnostic methods for viruses: the difficulty of the definition of reliable and stabile features. In general, a complex approach, the detection of more than one properties is preferred. Finally, from a practical and economic point of view, the important features are virulence and epidemiological characteristics. These are often associated only with a strain or a pathotype of a virus species, and diagnostic tools are needed to separate these subgroups. Exploration of the genetic background of viral pathogenesis and the identification of pathogenicity-determining regions are pivotal, because they enable the detection of biologically meaningful properties in the otherwise fast-changing viruses.

New viruses and new pathotypes emerge from time to time. The viral objects of the present study, *Plum pox potyvirus* (PPV, Atanasoff, 1932) and the tuber necrotic pathotype of *Potato virus Y* (PVY^{NTN}, Beczner et al., 1984) appeared in the first and the second half of the 20^{th} century, respectively, as described in detail below. Their host plants, the stone-fruit trees and the members of the *Solanaceae* family (for example), had been cultivated for long time,

and their diseases were described long beforehand. Also, the spread of these viruses can be followed during the century on the basis of reports, showing that these cases represented genuine emergence.

1.2. The *Potyviridae* family and the *Potyvirus* genus

The viral objects of this study, PPV and PVY, both belong to the *Potyvirus* genus of the *Potyviridae* family. Actually, PVY is also their type member, and the taxonomic name was derived from the name of this species (*Potato virus Y*).

Potyviridae is probably the largest and most widespread plant virus family on Earth, counting more than 200 known definitive and possible members; its largest genus is the *Potyvirus*. They infect plants, usually only a narrow range of host species, and they are mostly transmitted by aphids. They are characterized by elongate, 680-900 nm long and 11-14 nm wide, flexuous particles, made up of approximately 2000 coat protein molecules (Fig. 1), and possess a single-stranded, positive sense RNA genome of 8.5-10 kb length, of which a single polyprotein is transcribed (Fig. 2).

A protein called VPg (Viral Protein genome-linked) is attached to the 5' end of the viral genome, and the genomic RNA carries a polyadenine tail. Virus replication occurs in the cytoplasm, in a membrane-associated manner. *Potyviruses* form characteristic inclusion bodies in the cytoplasm, the so-called 'pinwheels', and a different type of inclusion bodies in the nucleus. The viral polyprotein is processed by viral proteases into mature proteins. The functions of some of them have been elucidated, like RNA helicase (CI), VPg, protease (NIa), helper-component protease (HC-Pro), RNA-dependent RNA polymerase (NIb) and coat protein (CP). Recently, P1 and HC-Pro were associated with the inhibition of host RNA silencing, which is suspected to be a sequence-dependent defense mechanism of plants against RNA viruses (Ratcliff et al., 1997). The pathogenicity-determining region of PPV was found

Fig. 1

Electron microscopic picture of PVY particles.

(300,000x magnification)

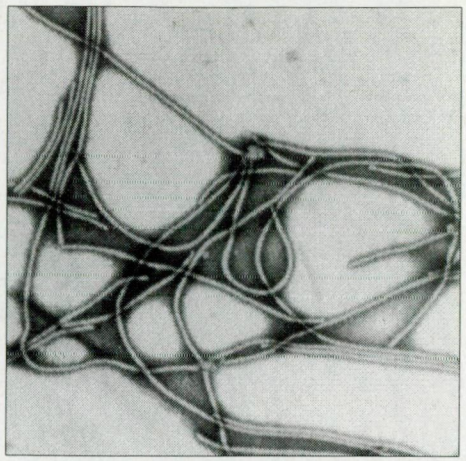

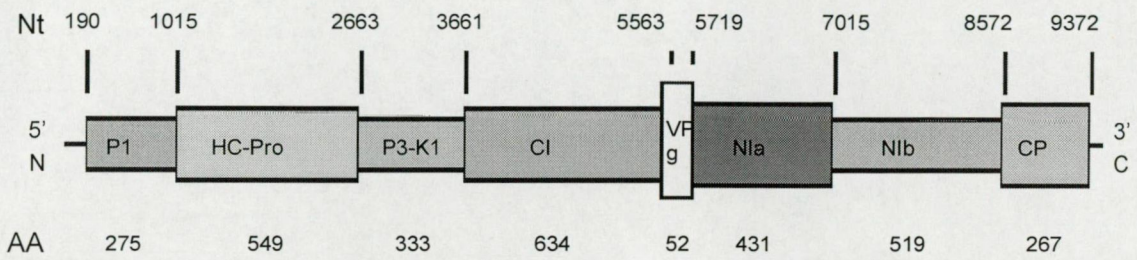

Fig. 2

Genome structure of viruses belonging to the *Potyvirus* genus (numbering is shown according to PVY, M95491).

Of the approximately 10 kb-long genomic RNA, a single polyprotein is transcribed, which is cleaved into functional proteins by viral proteases, mainly by NIa. The encoded proteins (for the explanation of the abbreviations see the text) are indicated by shaded boxes, and their lengths in amino acids are written below. The boundaries of the coding regions in the nucleotide sequence are shown in the top. (The figure was reproduced from unpublished results by courtesy of Dr C.D. Schoen.)

to locate in the P3-K1 coding region, however, no functions have been associated with it to date (Saenz et al., 2000).

1.3. *Plum pox virus* (PPV)

Plum pox is considered to be the most severe viral disease of plums, apricots and peaches, and is of great economic importance in many European countries (Németh and Kölber, 1994). Yield losses and overall economic losses have been catastrophic to plum and peach growers in the affected countries: all the infected trees have been removed and replaced with resistant varieties or with other crops. It also infects and causes disease in walnuts,

almonds, cherries and sweet cherries, and cause latent infections in stone-fruit weeds, like blackthorn, which may serve as reservoirs for the virus. PPV is spread by aphids in a non-persistent manner, but the introduction of infected propagation material is considered to be the most important means of long distance spread.

PPV was identified first on plums in 1917, and on apricots in 1933 in Bulgaria (Atanasoff, 1932; 1935). The virus gradually spread to Eastern Europe, and later to the whole continent. In Hungary it was found first on apricot in 1948 (Szirmai, 1948), and on peach in 1963, which was the first description of the occurrence of PPV on this host plant (Németh).

Two main serotypes, (Dideron, PPV-D) and (Markus, PPV-M), were distinguished by polyclonal antibodies (Kerlan and Dunez, 1976), which also differ in biological properties: the PPV-M isolates are more readily spread by aphids, and cause more severe symptoms on peach. In 1980, PPV was reported from Egypt, and the isolates were found to belong to a distinct serotype, which was designated El Amar (PPV-EA, Dunez, 1988). In the nineties, the virus spread all over the world: its presence was reported from India, Chile and very recently from the United States and Canada. In Moldavia, a new strain of PPV was identified, which could infect and cause disease on cherry trees (PPV-C, Nemchinov et al., 1996). The genomes of isolates belonging to the different groups were partially or completely sequenced.

PPV infection can be reliably diagnosed by biological tests, which consists in grafting on woody indicator plants (woody-indexing, Németh and Kölber, 1981). This method, however, is laborious and time-consuming. Polyclonal and monoclonal antibodies were generated for the generic (Cambra et al., 1994) and strain-specific detection of PPV (Kerlan and Dunez, 1979; Cambra et al., 1994; Boscia et al., 1997; Myrta et al., 1998a, 1998b, 2001), and the localization of the epitopes recognized by monoclonal antibodies was also attempted (Shukla et al., 1988). Sensitive PPV detection was achieved by the means of PCR (polymerase chain reaction), (Korschineck, et al., 1991; Levy and Hadidi, 1994). To

differentiate between the strains, group-specific oligonucleotide primers were applied (Candresse et al., 1995; Olmos et al., 1997), or PCR was coupled to serological (PCR-ELISA, Poggi-Pollini et al., 1997) or DNA analytical techniques (RFLP, restriction fragment length polymorphism, Wetzel et al., 1991; Hammond et al., 1998). To make PCR more suitable for routine testing, it was combined with high-throughput sample preparation procedures, such as, capturing by antibodies (IC-PCR, Wetzel et al., 1992), or squashing the plant material, or the insect, which may serve as virus vector, on a Whatman paper (print capture PCR, Olmos et al., 1996). The uneven distribution of the virus within the plant and the low virus titer outside the active growth period pose serious problems in PPV detection. During spring, all the methods provide sufficient sensitivity. In other seasons, however, the higher sensitivity of PCR or that of nested PCR is preferred (López-Moya et al., 2000).

To prevent the virus-caused loss, breeding for resistant cultivars presents an alternative approach to the systematic application of the above-described screening methods and the strict quarantine measures. Conventional breeding techniques did not prove adequate, because of the scarcity of resistant cultivars and the polygenic nature of the resistance traits (Dosba et al., 1992; Badenes et al., 1996). As a model system, transgenic *Nicotiana* plants carrying parts of the PPV genome coding for different proteins were generated, and they were found to display varying degrees of resistance (Ravelonandro et al., 1993; Regner et al., 1992; Palkovics et al., 1995). The experiments with woody plants were also encouraging: the transgenic *Prunus domestica* and *Prunus armeniaca* plants showed significantly higher resistance than the control trees (da Camara Machado et al., 1995; Ravelonandro et al., 1997).

1.4. *Potato virus Y* (PVY)

PVY infects a wide range of plants from 69 genera in 27 families (Edwardson and Christie, 1991), and causes severe economic losses, mainly in potato, pepper, tomato and tobacco crops. The virus was first described by Smith in 1931, as one of the agents that may

cause the yellows disease of potato, hence the name, *Potato virus Y*. The identified virus belonged to the group that is called now the common strain (PVY^O = ordinary), which is widespread all over the world (Le Romancer et al., 1994). Since then several variants of the virus have been isolated from different host plants.

The PVY viruses isolated from potato were grouped into three strains according to biological properties. PVY^O causes systemic crinkling and leaf drop on potato. The necrotic strain of PVY (PVY^N), which appeared in the fifties (Munro, 1955), is characterized by 'veinal necrosis' and leaf death on tobacco, while on potato, it causes only very mild mottling or no symptom at all. That is why, in the beginning, PVY^N infection remained unnoticed and could spread in an uncontrolled way for a long time. The virus is transported to the tubers, and on replanting, it causes secondary infections with generally more severe symptoms. Viruses of the PVY^C strain cause hypersensitive reaction in potato cultivars carrying the Nc resistance gene, in other respect they are similar to PVY^O (De Bokx and Huttinga, 1981). PVY strains could be differentiated by biological tests and by the use of polyclonal and monoclonal antisera. The serological and biological grouping, however, did not correlate perfectly (Chachulska et al., 1997).

In 1984, Beczner and colleagues described the potato tuber necrotic ringspot disease (PTNRD), and identified PVY as the causal agent. These isolates were found to belong to the PVY^N strain on the basis of serological reactions and the symptoms on tobacco, but the severe necrotic ringspots on the tubers clearly distinguished them, and they were designated PVY^{NTN} (necrotic, tuber necrosis). The tuber necrotic isolates were also associated with resistance breaking: they could infect and cause disease in potato cultivars that were immune to PVY or possessed high levels of field resistance (van den Heuvel et al., 1994). Since the first description, PVY^{NTN} has been detected in several European countries, as well as in Lebanon, Israel, California and Japan.

The definition of PVY^{NTN} is not unambiguous. The severity of the tuber symptoms varies with potato cultivars, virus isolates and environmental conditions, such as temperature and humidity (Le Romancer et al., 1994). Moreover, certain PVY^{N} isolates were also reported to cause moderate or poor tuber necrotic symptoms in some potato cultivars, mainly under green house conditions (Kerlan and Tribodet, 1996). In sum, continuity could be observed in the appearance and the severity of the symptoms, which made the definition of the pathotype difficult. It was proposed that the PVY^{NTN} designation should be reserved only for the isolates that cause tuber necrotic symptoms under field conditions.

Viruses belonging in the different subgroups of PVY were associated with differing etiology. Therefore, diagnostic tools were needed to detect the different strains and to separate the tuber necrotic isolates. Serological assays are available for strain-specific detection, however, the tuber necrotic isolates cannot be separated via this method from other PVY^{N} viruses. The biological test for PVY^{NTN}, i.e. the monitoring of tuber necrotic symptoms in susceptible potato cultivars, is time-consuming and laborious, and not entirely reliable for the above-mentioned reasons. RFLP and group-specific PCR assays were developed for the detection of PVY^{NTN} (Glais et al., 1996; Weilguny and Singh, 1998), but as more sequence data became available, the targeted nucleic acid motifs, which were located in the P1 coding region, were also found in isolates that were not tuber necrotic. A commercial RT-PCR assay for the differentiation of PVY strains and the PVY^{NTN} isolates was recently introduced to the market, but the exact diagnostic regions have not been disclosed.

The genome regions of PVY responsible for the distinct biological properties of the strains, and for the appearance of tuber necrotic symptoms have not been identified to date. It was proposed that the genetic determinant of the 'tobacco veinal necrosis' phenotype is most probably located outside the 5' and 3' terminal portions of the genome, excluding thus the non-translated parts and the P1 and CP coding regions (Chachulska et al., 1997). Revers et al.

revealed a correlation between the tuber necrotic pathotype and a gene rearrangement within the CP coding region (1996).

Naturally occurring resistant cultivars exist against the majority of PVY isolates, and they mostly replaced the previously popular, but sensitive ones. PVY^{NTN} was reported to break the resistance of the above-mentioned cultivars, and triggered another cultivar change.

The generation of resistant, transgenic tobacco and potato plants was attempted. CP-transgenic tobacco plants showed high resistance, but the experiments with potato have been less successful to date (Han et al., 1999). Recently, a different transgenic strategy, targeting potyviral polyprotein processing, was reported. Tobacco plants carrying cysteine proteinase inhibitor genes were generated, and they were found to be resistant to PVY and TEV (*Tobacco etch virus*), two economically important *Potyviruses* (Gutierrez-Campos et al., 1999).

1.5. Nucleic acid amplification methods and their application in diagnostic technology

Nucleic acid amplification, or rather replication, has been 'known and practiced' by all living organisms and viruses for ages; nevertheless, the idea and the *in vitro* realization of the large-scale amplification of a specific nucleic acid sequence was a milestone in several branches of biological and medical sciences. Since the invention of the first, and most widespread nucleic acid amplification method, the polymerase chain reaction (PCR, Mullis et al., 1986), it has become indispensable both in the academic and in the applied scientific research, as well as in routine diagnostic laboratories.

PCR 'copies' the way double-stranded DNA (dsDNA) is replicated in nature. Oligonucleotide primers bind to their complementary, so-called, target sequences, which are located in opposing positions on the two strands, and a DNA polymerase elongates them, synthesizing the template-complementary strands. By applying successive cycles of heat-

denaturation, primer annealing and elongation, a dsDNA product of defined length is amplified in a theoretically exponential rate.

Beside PCR, other nucleic acid amplification methods were also devised. Some of them 'applied' the DNA or RNA replication mechanisms of living organisms or viruses, like nucleic acid sequence-based amplification (NASBA, Compton, 1991; Kievits et al., 1991) and ligase chain reaction (LCR, Barany, 1991), or were original inventions like strand displacement amplification (SDA, Walker et al., 1992).

Development of nucleic acid databases and the accumulation of annotated nucleic acid sequences contributed substantially to the success and widespread application of the amplification methods, mainly to that of PCR. Assays were developed for the detection of various pathogenic agents: viruses, bacteria, fungi or gene rearrangements and point mutations. Novel pathogens were isolated and identified on the basis of conserved amino acid or nucleic acid patterns.

The main shortcoming of nucleic acid amplification-based methods, hampering their application in routine screenings, is the evaluation process, which usually involves the separation of the amplified product by gel-electroforesis, and detection with the help of nucleic acid intercalating dyes and UV illumination. This post-amplification processing makes the assays laborious and greatly increases the risk of the contamination of workspace with the amplicon molecule, leading to false positive results. To overcome these problems homogeneous (i.e. not needing product separation), real-time and closed-tube assays were developed, in which the amplified product could be detected in parallel with the reaction, and without opening the reaction vessel.

Another major improvement was the simplification of sample preparation. Several kits and procedures were developed for the fast and reliable nucleic acid extraction from various sources, and for the removal of inhibitory substances. Alternatively, protein-bound targets,

e.g. viral particles, can be selectively captured by antibodies attached to the inner surface of the reaction vessels, and thus can directly serve as input for an amplification reaction (immunocapture PCR, IC-PCR).

The current trend is further automation for high-throughput screening. Sample preparation is often coupled to amplification and detection, resulting in one single diagnostic procedure and an instrument for it. For on-field analyses, handheld, cost-effective, fully automated diagnostic devices were manufactured (Jordan, 2000). The process of assay development is also becoming standardized, and thereby is getting easier. Standard oligonucleotide and probe sets were developed, e.g. the Zip codes (Cheng et al., 2000), which are attached to target-specific oligonucleotides, and positive reactions can be detected in a universal way. A diversification of the applied amplification methods can also be observed (review: Schweitzer and Kingsmore, 2001): for different purposes, different approaches may be optimal. For point mutation detection, LCR, SDA, SNE (single nucleotide extension) and PCR with molecular beacons have been successfully used, while for the isolation of novel sequences, on the basis of conserved motifs, degenerated PCR, CodeHop PCR (Rose et al., 1998) or NASBA might be applied. Amplification techniques were combined with other technologies, like microarrays (review: Kurian et al., 1999) and FACS (fluorescence-activated cell sorter) analysis (Iannone et al., 2000), both for target and signal amplification, which opens up new vistas and ensures their further development.

1.6. Polymerase chain reaction

The story of the invention and the development of PCR has been described in detail in many books. Therefore, only the aspects concerning the studies presented are mentioned in this section.

The variations and applications of PCR are innumerous. Its unparalleled sensitivity and specificity made it the method of choice for many diagnostic applications. It is able to

amplify detectable amount of nucleic acid product from 10^2-10^4 target molecules. By applying a second amplification reaction with an internal oligonucleotide primer pair (nested reaction), it is possible to reach the theoretical detection threshold of 10^0 copies of template molecule.

The specificity of PCR is scalable: from a single nucleotide difference to the presence of a loosely-defined, conserved amino acid pattern, which may signify the members of a protein family, may equally well be detected. To design assays with exactly the required specificity, experimental and theoretical rules were described. The mismatch tolerance of oligonucleotide primers can be increased, i.e. the binding specificity decreased, by using a mixture of different oligonucleotides instead of only one species, which is called a degenerate primer, or by the incorporation of universal nucleotides, which interact with all the four bases with approximately the same stability. Beside universal nucleotides, like inosine, nitropyrolle or nitroindol (Loakes et al., 1995), pyrimidine and purine base analogues were also described (P and K analogues, respectively; Lin and Borwn, 1989; Brown and Lin, 1991).

For the isolation and identification of polymorphic sequences PCR was combined with digestion of the amplified product or the template by restriction enzymes, resulting in the RFLP (restriction fragment length polymorphism) and AFLP (amplified fragment length polymorphism) methods, respectively. During RFLP analysis, which was used in the course of the present study, the amplified product is digested by different restriction enzymes, and the number and the sizes of the restriction fragments are analyzed by gel-electrophoresis. In AFLP, universal adaptors are ligated to the digested complex target nucleic acids, and the resulting fragments are amplified using universal oligonucleotide primers that bind to the adaptors.

PCR, the primary template of which is DNA, was extended for the detection of RNA molecules: RNA is reverse transcribed into cDNA, which may serve as a template molecule in

the reaction. The method of combined reverse transcription and amplification is called RT-PCR.

For diagnostic procedures, it was very important that several amplifications could be carried out side by side in one reaction vessel, using the same pool of reagents (multiplex reaction). The possibilities of multiplexing and the specific design principles were investigated by Wang et al., who developed procedures to detect 46 single nucleotide polymorphisms (SNPs) in one reaction (1998).

PCR is compatible with several product analysis methods, such as gel-electrophoresis, colorimetric (PCR-ELISA), and fluorescent detection.

1.7. Nucleic acid sequence-based amplification (NASBA)

NASBA, and the related TAS (Transcription-based amplification system, Kwoh et al., 1989) and 3SR (Self-sustained sequence replication, Gingeras et al., 1990) methods, are RNA amplification procedures, designed on the basis of the retroviral life cycle. In NASBA, as a result of the concurrent activity of three enzymes (T7 RNA polymerase, reverse transcriptase and RNase H) complementary RNA is amplified from a ssRNA template in an isothermal reaction (Fig. 3).

The sensitivity of NASBA was shown to be equal or superior to that of PCR (Lunel et al., 1999). It is especially suited for the detection of messenger RNAs, because dsDNA does not, or may only in very high concentration, serve as its template, thus the incidental genomic DNA contamination in the sample does not interfere (Heim et al., 1998). NASBA was successfully applied for mRNA quantification (Smits et al., 1995). It is very convenient for the detection of RNA viruses too, because the viral genomic RNA can directly serve as a template molecule. Since it is an isothermal reaction, there is no need for specific instrumentation.

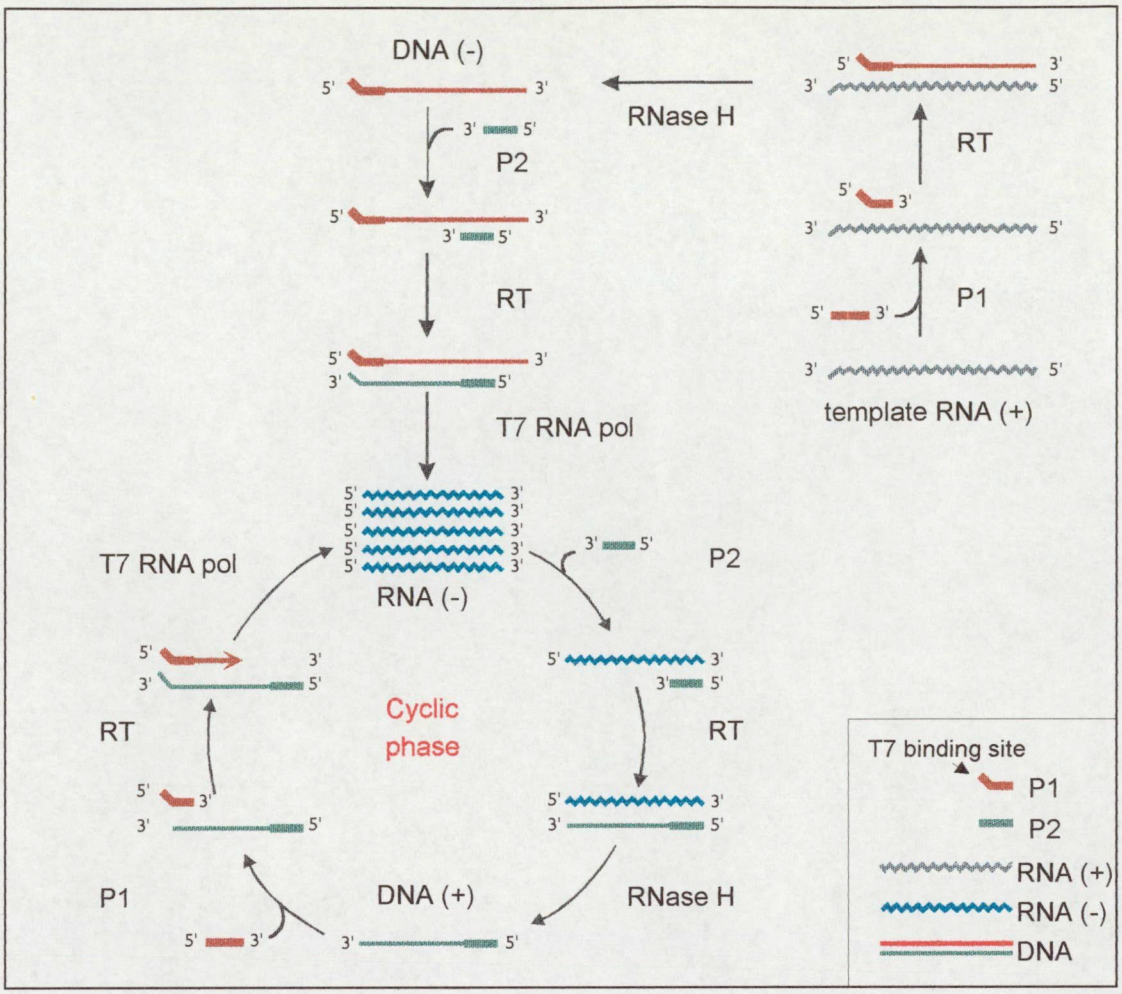

Fig. 3

Scheme of NASBA amplification.

Target RNA is reverse transcribed into ssDNA by AMV reverse transcriptase (RT-ase) and a T7 RNA polymerase recognition site, as part of the reverse oligonucleotide primer (P1), is introduced into the nascent cDNA. RNase H degrades RNA from the heteroduplex, thereby enabling the binding of the forward oligonucleotide primer (P2), and the synthesis of the complementary strand by RT-ase. T7 RNA polymerase binds to its double stranded recognition site, and synthesizes several copies of negative sense RNA molecules, which is the main product of the reaction. This step constitutes also the entry into the cyclic phase. P2 binds to the RNA, and it is elongated by RT-ase. RNase H degrades the RNA component of the heteroduplex, and allows the binding of P1. RT-ase synthesizes the second strand of the dsDNA molecule, and completes the T7 recognition site of the template strand.

Figure was reproduced from unpublished results by courtesy of Dr. C.D. Schoen

The amplified product is usually detected by Northern hybridization, after gel-electrophoretic separation and blotting. A homogeneous, real-time version of NASBA, called

AmpliDet RNA (Amplification and Detection of RNA), was also developed (Leone et al., 1998).

NASBA is a fast and sensitive method for the detection of RNA molecules; nevertheless it is less flexible than PCR. It has a size limit of a few hundreds of nucleotides for efficient amplification, and the components of the reaction mixture are fixed; the composition cannot be optimized further. NASBA was successfully applied for the high-throughput detection and quantification of HIV and other RNA viruses (van Gemen et al., 1993).

1.8. Real-time monitoring of nucleic acid amplification

To eliminate the shortcomings associated with nucleic acid amplification-based methods, such as labor-intensive post-amplification processing, low throughput and risk of carryover contamination, novel product analysis technologies were devised.

Homogeneous assays were first developed for PCR: the monitoring of product amplification was achieved by adding the intercalating dye ethidium bromide to the reaction mixture, the fluorescence of which increases upon binding to dsDNA (Higuchi et al., 1993). Evaluation was carried out either after the completion of the assay, or in real time, by monitoring the emitted fluorescence in defined intervals during the assay. Real-time PCR not only allowed fast evaluation, but also enabled more precise target nucleic acid molecule quantification. The number of cycles needed before fluorescence rose above the background level was found to be linearly dependent upon target concentration in a range of six orders of magnitude. Product analysis based on intercalating dyes, however, did not ensure that the detected DNA would be the specific product; any amplification byproduct could result in a positive signal.

Real time detection was also achieved by using sequence-specific fluorescent probes (Fig. 4). Taqman probes, also called hydrolysis probes, are oligonucleotides carrying a

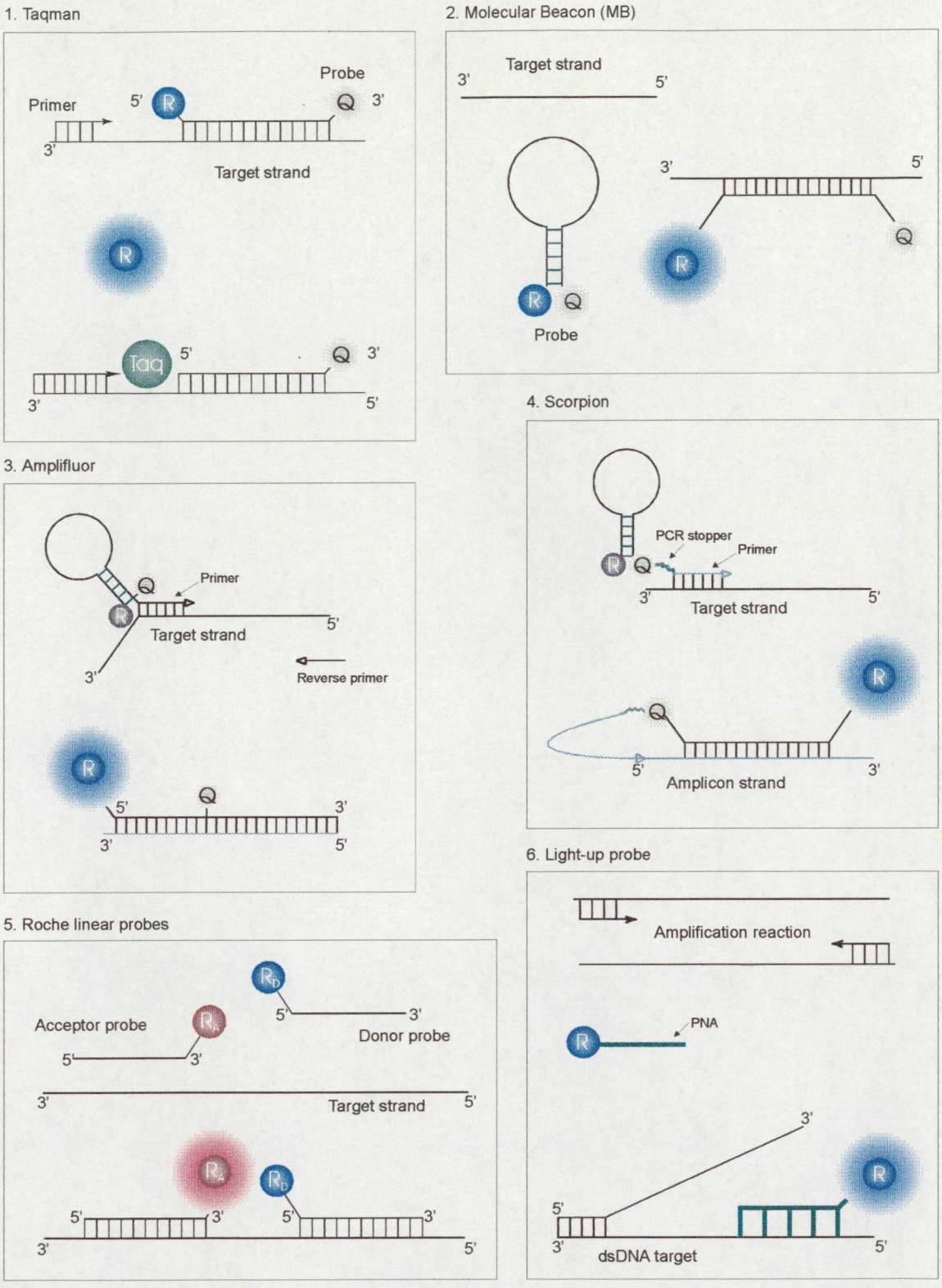

Fig. 4

Various strategies for real-time, homogeneous, fluorescent detection of nucleic acid amplification products. (Meaning of the signs: R = reporter dye; R_A = acceptor reporter dye; R_D = donor reporter dye; Q = fluorescence quencher group; PNA = peptide nucleic acid; Taq = Taq polymerase) For details, see the text.

fluorescent group on one end and a quencher group on the other (Livak et al., 1995). The light emitted by the fluorophore upon excitation is absorbed by the quencher molecule, i.e. fluorescence resonance energy transfer (FRET) occurs. PCR product detection by Taqman utilizes the 5'-3' exonuclease activity of Taq polymerase (Holland et al., 1991). The probe binds to its complementary sequence on the template strand in the annealing phase, and, during elongation, the enzyme cleaves the fluorophore off from the probe. Fluorescence emitted by the free fluorophore signals the accumulation of the specific amplification product. Recently, non-fluorescent, universal quencher groups were described for Taqman, which greatly increased the possibility of multiplexing. Lee et al. used six differently labeled probes in one assay, although the evaluation process needed substantially more complex analysis (1999).

Molecular beacons (MB, Tyagi and Kramer, 1996) provide another means for real-time detection; they are compatible not only with PCR amplification, but also with NASBA. MBs possess a target-complementary loop sequence flanked by inverted repeats of five to seven nucleotides. A fluorophore dye is attached to the 5' end, and a quencher group to the 3' end of the probe. In the absence of target molecule, the probe assumes a stem-and-loop structure bringing the fluorophore and the quencher into close proximity. Upon excitation, direct energy transfer occurs between the two groups and the reporter fluorescence is quenched. When the MB binds to its target sequence, the rigidity of the forming nucleic acid duplex forces the stem structure open, the fluorophore and the quencher groups are separated, and the reporter dye emits fluorescence. Versatile MBs, with fluorophores spanning the visible spectrum and possessing DABCYL as a universal, non-fluorescent quencher, were used successfully in several applications. MBs were also applied as probes on microarrays (Steemers et al., 2000), which eliminated the need for target nucleic acid labeling and the removal of unbound molecules, which required extensive washing steps.

The fluorescent hairpin probe structure was incorporated into a PCR oligonucleotide primer, thereby increasing the efficiency and the speed of hybridization. The hairpin portion of these, so-called, Amplifluor probes forms part of the primer sequence; thus the hybridization of the primer forces the fluorophore and the quencher apart (Nazarenko et al., 1997). The fluorescence of the probe is independent of the specificity of the amplified product.

Scorpions also contain a PCR primer and a hairpin probe portion within one oligonucleotide, however, the primer and the probe sequences are completely separated, and the loop region of the probe is complementary to a region of the amplicon adjacent to the primer (Whitcombe et al., 1999). Therefore, Scorpions confer an additional level of specificity for the assay. A 'PCR stopper' sequence is placed between the hairpin and the primer portions, the function of which is to block the polymerase 'reading through' into the probe part, which would result in a false positive signal.

Hybridization probes, called Roche linear probes, consist of two separate oligonucleotides, both carrying a fluorophore (Lay and Wittwer, 1997). They hybridize to the amplicon side by side, with a spacing of only one to five nucleotides. The upstream probe possesses a fluorophore, usually fluorescein, at its 3' end, the emitted light of which may excitate the other fluorophore, (e.g. LC-Red640), which is attached to the 5' end of the downstream probe, i.e. FRET may occur. The probes bind to the accumulating amplicon DNA strands in the annealing phase, and the progress of the reaction can be followed by measuring the fluorescence of the second dye upon excitation of the first one.

DNA binding enhances significantly the fluorescent abilities of asymmetric cyanine dyes, like thiazole orange (TO). This peculiar property of the dye was exploited for the real-time monitoring of amplification reactions; TO-coupled peptide nucleic acid (PNA) probes,

called Light-up probes, may increase their fluorescent ability by a factor of fifty upon target binding (Svanvik et al., 2000).

Although all the above-described probes were developed for real-time monitoring of amplification reactions in homogeneous formats, their fields of application, to some extent, differ. Taqman probes are ideal for the evaluation of PCR assays, both in real time and post-amplification, because they generate permanent fluorescence increase. Point mutations may be detected by Taqman probes, although their ability of discrimination is limited, because a relatively strong probe-amplicon interaction is needed for efficient cleavage, which, as a consequence, is only mildly affected by a single mismatch (Täpp et al., 2000). MBs, on the contrary, were described to possess increased specificity as compared to linear probes and readily detect SNPs (Tyagi et al., 1998; Bonnet et al., 1999; Täpp et al., 2000). Their fluorescent signal, however, should be measured in real-time, in the annealing phase of PCR, because at end point detection dsDNA strand reannealing outcompetes probe binding. For the same reason, the length of the detectable PCR product is limited. Unlike Taqman, it can be applied in NASBA reaction or on microarrays. Scorpion probes are similar to MBs in the range of application, although they cannot be used in NASBA. In PCR, however, the unimolecular nature of the probe-target interaction confers greater specificity and ensures stronger signal (Thelwell et al., 2000). Hybridization probes provide convenient means for mutation analysis, mainly because of the in-built function of Roche LightCycler instruments to determine the melting temperature of the probe-amplicon duplex. They can distinguish single mismatch differences, in most cases not only from the perfectly matching target, but also one type of mismatch from another type (Ahsen et al., 1999). The development of Light-up probes is still at an early phase, but they have some promising, distinct features. The use of PNA ensures stronger binding and the possibility of end-point detection, because it is not outcompeted by the complementary DNA strand. In the meanwhile, it retains point-mutation

specificity, since a relatively short PNA suffices, in the duplex of which a single mismatch results in significant destabilization.

1.9. Design of nucleic acid amplification-based assays

The development of nucleic acid amplification-based diagnostic methods includes careful selection of the target region, the primer and probe hybridization sites, and optimization of the assay conditions. Target region selection is generally preceded by extensive sequence analysis, in the course of which all the known target and non-target, but similar sequences are compared. Multiple sequence alignments help to identify the conserved and the variable regions, and they also may serve as input for clustering and phylogenetic programs to determine the relationships among the sequences. The diagnostic region is selected to be group- or subgroup-specific, according to the purpose of the assay.

The sequences of the oligonucleotide primers and probes are chosen, within the confinement of the selected target region, to ensure specificity and sensitivity. The oligonucleotide primers and probes are expected to hybridize exclusively to the target sequence: under the conditions of the assay they are not supposed to bind to any other, potential binding site on the template nucleic acid, or on themselves. The 3' end of an oligonucleotide primer is further checked to avoid any complementarity of significant length (>5-7 nucleotides), because it might lead to elongation by the polymerase and the formation of byproducts. Thus the main task of primer and probe design is to predict the strength of an oligonucleotide's binding to the target and non-target, but similar sequences with reasonable precision, under the conditions of the assay.

1.10. Prediction of nucleic acid duplex stability

Nucleic acid duplex formation can be characterized by the thermodynamic parameters of the transition: standard enthalpy (ΔH°), standard entropy (ΔS°) and standard free energy (ΔG°), the latter of which is closely related to the equilibrium constant.

$$\Delta G^\circ = - R * T * \ln(K) \qquad (1)$$

R universal gas constant (1.987 cal/K*mol)
T temperature (K)
K equilibrium constant of duplex formation

According to the nomenclature of thermodynamics, ΔG° would be designated free enthalpy. In the literature, however, the free energy term is applied for the description of nucleic acid duplex stability, and it is universally used in that context (see e.g. SantaLucia, 1998); therefore this term was used in this study too. For aqueous solutions, like the *in vitro* and *in vivo* environments of the objects studied by molecular biologists, the two measures (i.e. free enthalpy and free energy) are practically equal.

A related and widely used parameter is the melting temperature (T_m): the temperature at which half of the oligonucleotides bind to the target sequences, while the other half are unbound. T_m is a concentration- and symmetry-dependent parameter.

$$T_m[K] = \Delta H^\circ / (\Delta S^\circ + R * \ln C_T) \qquad (2)$$

$T_m[K]$ melting temperature in Kelvin
C_T strand concentration, if the oligonucleotides are self-complementary
strand concentration/4, if they are non-self-complementary, but the two types of oligonucleotides are at equal concentration
$C_A - C_B / 2$, if the hybridizing oligonucleotides are non-self-complementary, and they are present at different concentrations (C_A and C_B are the concentrations of the more concentrated and less concentrated strands, respectively)

Several methods and models were constructed to predict the binding characteristics of an oligonucleotide to its target sequence. The first approximation for T_m calculation for the duplexes formed by short oligonucleotides (<20 nucleotides) and their target sequences was given by Wallace.

$$T_m\ [°C] = 2 * (A + T) + 4 * (G + C) \quad (3)$$

A, T, G, C the number of A, T, G and C nucleotides in the oligonucleotide, respectively

It assumed a monovalent cation concentration of 0.9 M, typical of hybridization assays. For amplification reactions its usefulness is limited. Howley and colleagues provided a different formula, which was also based on the GC content of the sequence, but took into account the sequence length, and was applicable for various ionic conditions.

$$T_m\ [°C] = 81.5 + 0.41 * (\%GC) - 500 / L + 16.6 \log [M] \quad (4)$$

%GC	the ratio of G and C nucleotides in the sequence
L	length of the sequence in nucleotides
M	monovalent cation concentration (mol/l)

Later, the accumulating experimental evidences suggested that, beside nucleotide composition, other, sequence-dependent factors affect also strongly the T_m, and the applicability of this formula was restricted mostly for polynucleotides.

The nearest neighbor (NN) theory provided the first and still widely accepted model to take into account the sequence dependence of nucleic acid duplex stability (DeVoe and Tinoco, 1962; Crothers and Zimm, 1964). It assumed that, in addition to the hydrogen bonds between the bases, the most significant component of the free energy change accompanying duplex formation is the interaction between the adjacent bases (base stacking). Therefore, the contribution of a given base pair to the stability of the duplex depends on the identity and orientation of the neighboring bases. Thus not the single base pairs, but the dinucleotide pairs may be regarded as the units the free energy contribution of which are constant.

Ten NN dimer duplexes exist for DNA-DNA or RNA-RNA Watson-Crick homoduplexes, the $\Delta H°$, $\Delta S°$ and $\Delta G°$ contributions of which were determined experimentally (Xia et al., 1998). The values of NN parameters published by different research groups could be reconciled, with extrapolations, and the derived unified parameters were found valid for oligomer, polymer and dumbbell nucleic acids, too (SantaLucia, 1998). In addition, the NN parameters were measured for RNA-DNA helices (Sugimoto et al., 1995), and for DNA

duplexes containing single, internal mismatches (Allawi and SantaLucia, 1997, 1998a, 1998b, 1998c; Peyret et al., 1999). The validity of the NN theory was evidenced by comparing the predicted and measured values of the thermodynamic parameters, and also by comparing the stabilities of distinct oligonucleotide duplexes with identical NN dimers.

The thermodynamic measurements were carried out in solutions with compositions far different from the physiological salt concentrations, and at different temperatures. Therefore, correction factors were needed for valid calculations. The effect of changing salt concentration on nucleic acid melting was found not to depend on the nature of the nucleic acid duplex (i.e. DNA-DNA, RNA-RNA, DNA-RNA, Nakano et al., 1999), but for oligomers and polymers differed (SantaLucia, 1998).

$$\Delta G^{\circ}_{37(\text{oligomer, [Na+]})} = \Delta G^{\circ}_{37(\text{unified oligomer, 1 M NaCl})} - 0.114 * N * \ln [Na^{+}] \quad (5)$$

$$\Delta G^{\circ}_{37(\text{polimer, [Na+]})} = \Delta G^{\circ}_{37(\text{unified oligomer, 1 M NaCl})} - 0.175 * \ln [Na^{+}] - 0.20 \quad (6)$$

$\Delta G^{\circ}_{37(\text{unified oligomer, 1 M NaCl})}$	unified NN parameters (for DNA)
$\Delta G^{\circ}_{37(\text{oligomer, [Na+]})}$	ΔG°_{37} of an oligonucleotide at the given Na^{+} concentration (correction is basically identical for other monovalent cations except for Li^{+}, Nakano et al., 1999)
$\Delta G^{\circ}_{37(\text{polimer, [Na+]})}$	ΔG°_{37} of a polinucleotide at the given Na^{+} (monovalent cation) concentration
N	the total number of phosphates in the oligonucleotide duplex divided by two (approximately the oligonucleotide length)

The effect of bivalent cations depends greatly on the type of the ion. The stabilizing effect of Mg^{2+}, which is a frequent component of amplification reaction buffers, was found to be about 140 times larger than that of Na^{+} (Nakano, 1999).

ΔG° can be calculated from ΔH° and ΔS°, which are regarded as temperature-independent parameters, if not too large temperature extrapolation from 37 °C is needed.

$$\Delta G^{\circ} = \Delta H^{\circ} - T * \Delta S^{\circ} \quad (7)$$

T	temperature (K)

The NN theory was applied in various fields of molecular biology, such as probe design for Southern and Northern hybridizations (Albretsen et al., 1987), design of oligonucleotides for antisense inhibition of gene expression or to be used as primers for amplification reactions. Rychlik et al. proposed a formula, which contained the predicted

melting temperatures of the duplexes formed by the primers with the target sequence and that of the product, for the calculation of the optimal annealing temperature for PCR (1990).

$$T_a^{OPT} = 0.3 * T_m^{primer} + 0.7 * T_m^{product} - 14.9 \quad (8)$$

T_a^{OPT} optimal annealing temperature (°C)
T_m^{primer} T_m of the less stabile oligonucleotide primer (°C)
$T_m^{product}$ T_m of the PCR product polymer (°C)

The NN model was applied for the prediction of the free energy change of secondary structure transitions, and was implemented in softwares to predict the optimal folding of short DNA or RNA molecules, via free energy minimization (MFold, http://bioinfo.math.rpi.edu/~mfold/), and for the calculation of the stability of a given structure (efn2, http://bioinfo.math.rpi.edu/~mfold/rna/energy/form1.cgi). In addition to the free energy change resulting from the stacking of bases, energies for loop formation, terminal mismatch pairs, and coaxial stacking were also considered in the calculations (review: Zuker, 2000).

Nucleic acid interactions are very complex both *in vivo* and *in vitro*. To be able to take into account at least some aspects of this complexity, the calculations of the free energy change of duplex formation and that of secondary structure transitions were combined for the prediction of the free energy change accompanying the hybridization of structured probes to structured target molecules. The model described by Matthews et al. (1999) assumes that the secondary structures of the complementary regions of both the target and probe molecules have to unfold before the duplex could form, and, accordingly, the equilibrium constants of these transitions were incorporated to derive an 'overall' free energy change of the process.

$$\Delta G^{\circ}_{overall} = \Delta G^{\circ}_{duplex} + R * T * [\ln(K_{leff} + 1) + \ln(K_{target} + 1)] \quad (9)$$

$\Delta G^{\circ}_{duplex}$	free energy change associated with nucleic acid duplex formation
R	universal gas constant
T	temperature (K)
K_{leff}	effective equilibrium between the unfolded and both the unimolecularly and bimolecularly folded oligonucleotides (for its calculation an approximatory formula is given by Matthews et al)
K_{target}	equilibrium constant of the local disruption of the secondary structure of the target molecule in the probe-complementary region

The model was implemented in the OligoWalk program, which was applied, among other purposes, for predicting potential target regions for antisense inhibition of mRNAs molecules.

Bonnet et al. (1999) described the thermodynamic basis of the enhanced specificity of MB probes. They proposed that it is due to the beacon structure itself; furthermore, that every structurally constrained probe possesses enhanced specificity, because the structure stabilizes the unbound oligonucleotide. In the case of MBs, the strength of probe-target interaction is determined by the stability of the formed duplex and by the stability of the stem structure. Since the formation of the stem-and-loop structure of an MB and MB-target duplex interaction are mutually exclusive, a dynamic equilibrium exists between the two processes, which both can be characterized by their respective equilibrium constants.

$$BT \underset{K_{2\to1}}{\overset{K_{1\to2}}{\rightleftharpoons}} B_{closed} + T \underset{K_{3\to2}}{\overset{K_{2\to3}}{\rightleftharpoons}} B_{open} + T$$

B:	molecular beacon
T:	target molecule
$K_{1\to2}$:	dissociation constant of beacon-target complex (also named as K_d)
$K_{2\to1}$:	inverse of $K_{1\to2}$
$K_{2\to3}$:	equilibrium constant of beacon opening (also indicated as K_{MB})
$K_{3\to2}$:	inverse of $K_{2\to3}$

Formulas were presented to calculate the above-mentioned equilibrium constants from the measured fluorescence values at defined target molecule concentrations (Bonnet et al., 1999).

For the purposes of MB probe design, at present, mostly experimental rules are used. For the prediction of the most stabile structures of MB probes, MFold secondary structure prediction program for ssDNA is generally applied, while the melting temperature of the probe-target duplex is approximated by the GC rule (equation **(4)**). As a rule of thumb, it was proposed that the T_m of the stem-and-loop structure and that of the duplex both should be 7-10 °C higher than the temperature of detection (annealing temperature in the case of PCR). These principles have been very useful for MB probe design; however, the integration of the different thermodynamic models, like the prediction of the stability of secondary structure and nucleic acid duplex, for the prediction of MB behavior is still lacking.

2. Aims

The studies described in this thesis had practical and theoretical goals. We aimed to develop novel diagnostic tools for the generic, and strain-specific detection of two plant viruses, PPV and PVY, which might present improvements on the currently available methods. Both pathogens are of significant economic importance, and their spread should be strictly controlled. Despite the rigorous quarantine measures, the areas affected by them are still expanding.

In addition, we attempted to contribute to the theory of assay design: to characterize the behavior and the specificity of molecular beacon probes in AmpliDet RNA assay, by the application of thermodynamic models.

For PPV, presently, the routine screening of woody propagation and plant materials for international exchange is performed mainly by ELISA using monoclonal antibodies, which affords high-throughput, relatively sensitive detection and strain-identification. PCR-based methods are also applied, when a higher confidence of the virus-free state of stone-fruit tree siblings is required. The PCR assays developed provide either generic or strain-specific detection. These methods, however, can not be readily used for the simultaneous detection of PPV and the typing of all the four strains, since they make use of different parts of the viral genome, or require the application of different diagnostic technologies. Further, the differentiation of the two main strains of PPV (D and M) was based on detecting polymorphic nucleotides that do not result in amino acid change, i.e. they are silent mutations.

We aimed to develop a method that enables the sensitive and specific detection, and the subsequent typing of a PPV isolate belonging to any of the four strains. Assay development was preceded by extensive sequence analyses, and the diagnostic regions were selected on the basis of the location of strain-specific amino acid patterns, so that they could be expected to be associated with distinct biological, or serological properties.

Potato virus Y is a widespread pathogen that causes significant losses annually. Again, ensuring the virus-free state of the propagation material is the key to prevent the virus-caused losses. Characterization, strain identification and the differentiation of tuber necrotic isolates are pivotal, because the different viral subgroups are associated with different etiology. The currently used screening method involves germination of the stored tubers, and the resulting small plants are assayed via ELISA. The positive samples are further tested by strain-specific monoclonal antibodies. The separation of PVY^{NTN} isolates, however, is not feasible by serological methods, and the biological test is time-consuming and labor-intensive.

Therefore, our aim was to develop a sensitive, high-throughput assay for both the detection of PVY, and for the differentiation of its strains and the tuber necrotic isolates. The higher sensitivity of nucleic acid amplification-based methods could also make the germination of the tubers unnecessary. We have chosen AmpliDet RNA as an optimal diagnostic tool, which can directly amplify RNA and could enable the separation of the different viral types by the use of multi-color molecular beacons. Thus detection and typing can be carried out in a single reaction, in real time, reducing the cost, the labor required and the risk of carry-over contamination.

AmpliDet RNA assay is a particularly useful method for the specific and sensitive detection of RNA molecules. Its design principles, however, are still based on trial-and-error. The models widely used for the prediction of nucleic acid duplex stability are difficult to apply for AmpliDet RNA, because of the special composition of NASBA reaction mixture, and because the MB probe binds to an RNA molecule, which usually possesses strong secondary structure. The stem-and-loop structures of the MB probes themselves also have a significant effect on the stability of the interaction. The specificities of MBs in AmpliDet RNA have not been studied or published to date.

Thus, our aim was to characterize MB binding to target RNA molecules under the conditions of AmpliDet RNA assay, and to find and test methods that could predict the binding properties. For this purpose, we attempted to apply the thermodynamic description of MBs, the nearest neighbor model, and to test the validity of the presented approach by comparison to experimental data.

We also aimed to characterize the effect of different mismatches in the probe complementary region on the specificity of detection by MBs, and to test various nucleotide analogues for their ability to increase probe tolerance.

3. Materials and methods

3.1. Integrated RT-PCR/nested PCR diagnosis for differentiating between the subgroups of *Plum pox virus*

3.1.1. Virus isolates and cloned viral sequences

PPV-D originated from Dr. M. Barbra and was maintained on GF 305 peach indicator plants under greenhouse conditions. Plasmids carrying cloned cDNAs overlapping the coat protein (CP) coding region of PPV-M and PPV-C were kindly provided by Dr. L. Palkovics (Palkovics et al., 1993) and Dr. L. Nemchinov (Nemchinov et al., 1996), respectively. PPV-EA, in the form of symptomatic GF 305 leaves, was a gift from Dr. T. Candresse.

The PPV isolates analyzed in this study were from the strain collection of the Plant Health and Soil Conservation Station of the Ministry of Agriculture, Budapest, Hungary. The majority of them represented Hungarian isolates collected from symptomatic trees in 21 orchards, in distinct growing regions, between 1966 and 1995, and were maintained on GF 305 under field conditions. Seven isolates originated from Germany (SK21, SK28 and SK80), France (SK25 and SK26), the Czech Republic (SK1) and Slovakia (SK190), and were maintained on GF 305 under vector proof greenhouse conditions.

3.1.2. Multiple alignments of PPV sequences

The publicly available PPV CP sequences were compared at an amino acid and nucleic acid level by using the PILEUP program of the GCG Sequence Analysis Software Package (Devereux et al., 1984 and the Program Manual for the Wisconsin Package, Version 8, September 1994, Genetics Computer Group, 575 Science Drive, Madison, Wisconsin, USA 53711). Consensus sequence was generated and the differences were highlighted by the PRETTY program of the same package.

3.1.3. Design and synthesis of oligonucleotide primers for RT-PCR and PCR

Virus- or viral subgroup-specific regions were selected on the basis of the multiple sequence alignments, and PCR primers were synthesized accordingly. The melting temperature was determined and the lack of potential false priming sites or undesirable secondary structure was checked by the OLIGO 4.0. program (Rychlik et al., 1994).

The oligonucleotides (Table 1) were synthesized on a Cruachem model PS250 synthesizer, using phosphoramidite chemistry, and were purified by denaturing polyacrylamide gel-electrophoresis (10% 19:1 acrylamide:bisacrylamide, 7 M urea).

Name	Sequence
M3-5′	TCCAACRTTGTTRTRCACCA
M4-5′	TCCAAYRTAGTKGTSCATCA
M2-3′	CGYYTRACTCCTTCATACCA
M1-5′	GCAGCAACTAGCCCAATAMT
M5-3′	TGTTCCAAAAGTTTGCRRTTGAGGT
M6-5′	GYGGCAACRACTCAACCAG
M7-3′	CCTTCCTGYRTTCACCAAAGT
M8-5′	TAGTCACCACTACACAGCAG
M9-3′	AGGAGGTGTAGTAGTTGTTG
M10-5′	GGGAAATGATGACGACGTAACTCT
M11-3′	CAATTACCCCATACGAGAAT
H-3NCPPV*	GTAGTGGTCTCGGTATCTATCATA
C-3NCPPV*	GTCTCTTGCACAAGAACTATAACC

Table 1

Oligonucleotide primers for PPV detection and strain differentiation.

* PCR primers for the 3' non-coding region of PPV genome, developed by Levy and Hadidi (1994).

3.1.4. RNA extraction from fresh and lyophilized tissues of leaves of stone-fruit trees

Total RNA was extracted from 100 mg of fresh leaves or an equivalent amount of lyophilized leaves as described by Spiegel et al. (1996), with minor modifications. The tissue was pulverized in liquid nitrogen and mixed with 1 ml of homogenization buffer (200 mM Tris/HCl, pH 8.5; 1.5% SDS; 300 mM LiCl; 10 mM EDTA; 1% Na deoxycholate; 1% Nonidet P 40; 0.5% v/v mercaptoethanol added before use; all solutions were made with DEPC-treated water). The homogenate was centrifuged (all centrifugations were performed at 4 °C, 12 000 rpm, for 15 min) and the supernatant was mixed with an equal volume of 5 M potassium acetate, pH 6.0. After incubation for 15 min on ice, the suspension was centrifuged.

The supernatant was transferred to a new Eppendorf tube and the RNA was precipitated with an equal volume of isopropanol (1 h at -20 °C). The precipitate was collected by centrifugation and washed with 1 ml of 70% aqueous ethanol on ice. The pellet was dried under vacuum and dissolved in 30 µl of DEPC-treated sterile water.

3.1.5. Reverse transcription and PCR for PPV

cDNA synthesis was carried out in a reaction mixture containing 2 µl of freshly prepared RNA for template; 1 pmol of M2 or C-3NCPPV primer; 20 U of M-MuLV reverse transcriptase (Gibco, Fermentas); 100 µM of each dNTP; 1 mM DTT; 50 mM Tris/HCl, pH 8.3; 75 mM KCl and 6 mM $MgCl_2$ in a final volume of 25 µl. The reaction mixture was incubated at 37 °C for 1 h and stored at -20 °C.

PPV-specific products were amplified by PCR, using a PTC-100 thermal controller (MJ Research, Inc.) in a 25 µl volume, containing 5 µl of cDNA; 100 pmol of each general primer (M2 and M3/M4); 100 µM of each dNTP; 1 U of Taq polymerase; 10 mM Tris/HCl, pH 9.0; 50 mM KCl; 1 mM $MgCl_2$ and 0.1% Triton X-100. Denaturation at 93 °C for 3 min was followed by 30 cycles of 30 sec at 93 °C, 30 sec at 55 °C and 1 min at 72 °C, with a final extension step at 72 °C for 5 min. Conditions for the amplification of strain-specific products were the same, except that 100 pmol of specific primers and 1 µl of the 1000-fold diluted first PCR reaction mixture for template were used.

PCR products or restriction fragments were separated by electrophoresis on a 2% agarose gel and visualized by ethidium bromide staining. The images were documented with a gel analysis system (GDS-7600, UVP). RsaI was purchased from Fermentas, while Taq DNA polymerase was from Zenon Biotechnology Ltd., Szeged, Hungary; these enzymes were used as recommended by the manufacturers. All other reagents were purchased from commercial sources and were used without further manipulation.

3.1.6. DASI-ELISA for PPV strain differentiation

PPV strains were identified using strain-specific monoclonal antibodies (MAbs); namely, MAbAL specific to PPV-M (Boscia et al., 1997), MAbEA24 specific to PPV-EA (Myrta et al., 1998b), MAbAC and TUV specific to PPV-C (Myrta et al., 2001), MAb4DG5 specific to PPV-D, and the universal MAb5B (Cambra et al., 1994). Infected GF305 leaves were ground in PBS-Tween 20 extraction buffer (1/10 w/v) and two plate wells were filled with plant sap from each sample. ELISA reactions were read with a Titertek Multiskan photometer at 405 nm. Positive samples were those that gave a reading (average of two wells) at least three times higher than that for the healthy control in 1 h.

3.2. Development of a multiplex AmpliDet RNA assay for the simultaneous detection and typing of PVY isolates

3.2.1. Virus isolates

The PVY isolates used in the study are listed in Table 2 (pp. 62). Twelve isolates originated from the Plant Research International BV collection (Nos. 1-12). Sixteen isolates (Nos. 13-28) were kindly provided by Dr S. L. Nielsen; these represented Danish isolates mostly, but also contained PVY isolates from Lebanon, Romania and Hungary. PVY^{O} (U09509) was a gift from Dr R. P. Singh. The isolates were transferred to and maintained on *Nicotiana tabacum* plants. A collection of 18 PVY^{NTN} isolates, maintained on *in vitro* potato plant cultures, were kindly provided by Dr I. Wolf (Nos. 30-47). Biological characterization of the isolates was carried out previously (Singh and Singh, 1996; Wolf and Horváth, 2001; Nielsen, personal communication).

3.2.2. Comparative and phylogenetic analyses of PVY sequences

Full-length CP coding nucleotide sequences of 39 PVY isolates and that of *Pepper mottle virus* (PMV) were retrieved from GenBank and were aligned by CLUSTAL W

(Thompson et al., 1994). The sequences of PVY viruses isolated from non-potato hosts were excluded from this analysis, unless they were biologically characterized and classified into PVY^{NTN} or into one or other of the 3 strains. All the preliminary multiple sequence alignments were also performed by using CLUSTAL W.

Phylogenetic analyses were carried out on two shorter sections of the alignment: the 5' 72 nucleotides and the 3' 100 nucleotides, by using the PHYLIP package 3.5 (Felsenstein, 1993). The corresponding regions of PMV CP coding sequence were used as outgroup. Pairwise distances were calculated by means of DNADIST, using the bootstrap option with 100 replicates. Clustering was performed from the distance matrices by NEIGHBOR. Consensus trees were generated by CONSENSE, and were visualized by TREEVIEW (Page, 1996).

Bootscanning (Salminen et al., 1995), as implemented in the SimPlot program (© Stuart C. Ray), was performed to identify the chimerical PVY CP coding sequences. The potentially parental, i.e. non-recombinant, sequences were defined as the consensus of those PVY^{N}, PVY^{O} and PVY^{C} sequences that were clustered into the same group on the basis of the 5' and 3' part of the CP coding region. A 200 nucleotide-long window was slid with steps of 20 nucleotides along the alignment of the test sequence with the potentially parental sequences, and the program carried out phylogenetic analysis on these alignment 'sections'.

3.2.3. Design of oligonucleotide primers for NASBA

Target sequences for 2 reverse (P1), and 3 forward (P2) PVY-specific oligonucleotide primers flanking the diagnostic region were selected. Their performance in NASBA was tested in all possible combinations, using serial dilution of RNAs, representing the 4 PVY viral types, as template. The amplicon RNAs were detected with a generic, biotin-labeled probe by Northern hybridization. Primer combination P1A-3' + P2D-5' (Table 3) was found to be the most effective and was selected for use in the later experiments.

3.2.4. Molecular beacon design

The strength of the interaction between the RNA amplicon and the DNA MB probe was predicted by using the OligoWalk program (Mathews et al., 1999). Formation of the required stem-and-loop structure of the MBs and its stability were predicted by the MFold program for ssDNA (SantaLucia, 1998). For the sequences of the MBs see Table 3.

Name	Sequence
P1A-3′	AATTCTAATACGACTCACTATAGGGGAAAAGTCGAGGTTGGGCTGA
P2D-5′	TCTCAGATGTTGCAGAAGCGTA
PVY-T7-forward-5′	AATTCTAATACGACTCACTATATAGGGGGCTTATGGTTTGGTGCAT
RNA-3′	GTACAGGAAAAGCCAAAATACTTA
PVY-5′	GCTATCACGTCCAAAATGAGAATG
PVY-3′	ATCCTCGGTGGTGTGCCTCT
SEQ-5′	TATCACGTCCAAAATGAGAATGCC
SEQ-3′	GGTGGTGTGCCTCTCTGTGT
P-PVY	Biotin-CACGAACACCAGTGAGGGCTAG
MB-N1	Texas Red-GCAACC TGGAAGTTTGGCTCGSTATG GGTTGC-D
MB-N2	HEX-CGGTC CTAGAGAGGCACACATTCAAATG GGACCG-D
MB-O1	TAMRA-GCAGCA GGTPTAGCGCGPTATGCCTTTG CTGC-D
MB-O2	FAM-CGACGT TGAGGTCACATCACGAACAC ACGTCG-D

Table 3

PVY-, or PVY subgroup-specific oligonucleotide primers, probes and molecular beacons.

The stem sequences of MBs are underlined, while the target complementary regions are separated by spaces.

P stands for universal pyrimidine, S indicates a degenerate position of G and C, and D designates DABCYL, the non-fluorescent quencher group. The MBs and oligonucleotides were purchased from Isogen Bioscience BV, The Netherlands.

3.2.5. RNA extraction from potato leaf and tuber tissue, and cDNA synthesis from PVY genomic RNA

Total RNA was extracted from 100 mg of tobacco or potato leaf, or potato tuber tissue, using the RNeasy Plant Mini Kit (Qiagen) according to the manufacturer's instructions.

RNA was denatured in the presence of 0.5 μM oligo dT oligonucleotide primer, 1.67 x Taqman buffer A (Applied Biosystems), 6.67 mM $MgCl_2$ and 4 U RNA Guard (Amersham Pharmacia Biotech) in 12 μl final volume for 5 min at 65 °C. After cooling at 25 °C for 15 min, 2 U MuLV reverse transcriptase (Applied Biosystems), 4 U RNA Guard and dNTP were added to 300 nM final concentration, each in 8 μl volume. Complementary DNA synthesis was carried out for 100 min at 37 °C, followed by an inactivation step at 95 °C for 5 min.

3.2.6. Synthesis of in vitro RNA

In vitro transcribed, positive-sense PVY RNA was used as template in NASBA for the determination of assay sensitivity, which was synthesized according to the following protocol.

In a PCR reaction, a 557 nucleotide-long region of the 3' part of the CP gene was amplified with PVY-T7-5' and RNA-3' oligonucleotide primers, using PVY cDNA as template (see section *3.2.5*) in a 50 µl reaction mixture containing 1 x GeneAmp PCR buffer, 2 mM $MgCl_2$, 300 nM dNTP each, 0.1 µM primers, 2 µl cDNA and 1.25 U AmpliTaqGold polymerase. After initial denaturation and activation at 95 °C for 10 min, the following cycle was repeated 30 times: 0.5 min at 93 °C, 0.5 min at 55 °C and 1 min at 72 °C. At the end of the reaction, a final extension step at 72 °C for 10 min was included. All the reagents were purchased from Applied Biosystems.

The PCR product was purified with the High Pure PCR Product Purification Kit from Roche and eluted in 50 µl sterile, DEPC-treated water.

RNA was transcribed in a reaction mixture containing 1 x T7 RNA polymerase transcription buffer, 0.5 mM NTP each, 100 mM DTT, 10 U RNA Guard, 150 U T7 RNA polymerase and 5 µl of the purified PCR product for 2 h at 37 °C. The reagents were purchased from Amersham Pharmacia Biotech. DNA template was degraded via digestion by 10 U DNase I for 30 min at 37 °C, and the synthesized RNA was purified by using the RNeasy Mini Kit from Qiagen. The size of the transcribed RNA was checked by gel-electrophoresis; the purity and the concentration were determined by measuring the UV absorption at 260 and 280 nm on a Beckman spectrophotometer.

3.2.7. NASBA amplification

A solution containing 4 µl 5x NASBA-buffer (200 mM Tris-HCl, pH 8.5, 60 mM $MgCl_2$, 350 mM KCl, 2.5 mM DTT, 5 mM of each dNTP, 10 mM each of ATP, UTP and

CTP, 7.5 mM GTP and 2.5 mM ITP), 4 µl 5x primer mix (75% DMSO and 1 µM of each primer) and 2 µl of RNase-free H_2O was prepared. When NASBA was performed in the presence of MBs (0.05 µM MB-N1, 0.02 µM MB-N2, 0.05 µM MB-O1 and 0.02 µM MB-O2), water was replaced by the MB mix. Five µl RNA extract or water (negative control) was added and the samples were denatured at 65 °C for 5 min. After incubation at 41 °C for 5 min, 5 µl enzyme mix (375 mM sorbitol, 2.1 µg BSA, 0.08 U RNase H, 32 U T7 RNA polymerase and 6.4 U AMV-reverse transcriptase) was added to each tube. After five min equilibration at 41 °C, the samples were transferred to a Fluoroskan FL fluorometer, to monitor the amplification in real time, and were incubated at 41 °C for 1.5 h. The reagents were provided by Organon Teknika, The Netherlands.

3.2.8. Detection of NASBA amplicon RNA by Northern hybridization and enhanced chemiluminescence (ECL)

NASBA products were analyzed by electrophoresis on a 1% pronarose gel containing 0.5 µg/ml EtBr. Gels were run at 10 V/cm for 20 min in 1x TAE buffer, and were blotted onto a Z-probe nylon membrane in 0.3 M NaCl and 30 mM Na-citrate (2x SSC) solution for 20 min. Nucleic acids were cross-linked to the membrane by UV exposure at 365 nm for 2 min. The filter was hybridized with the biotinylated P-PVY probe (Table 3) in a final concentration of 1.5 nM at 50 °C for 60 min, in the presence of 5x SSC, 7% SDS, 20 mM Na-phosphate, pH 6.7 and 10x Denhardt's solution. The filter was washed twice with 3x SSC, 1% SDS at 50 °C for 5 min, and once with 0.1% SDS and 2x SSPE (20 mM Na_2HPO_4, 0.36 M NaCl and 2 mM EDTA) at room temperature for 10 min. The blot was then incubated for 30 min with 2 µl streptavidin/peroxidase conjugate in 5x SSPE and 0.5% SDS, followed by two washes with 2x SSPE, 0.1% SDS for 1 min and one for 10 min. Subsequently, the blot was washed twice with 2x SSPE for 2 min, followed by an incubation in substrate solution (ECL detection reagent, Amersham Pharmacia Biotech) for 60 sec, and exposed to X-ray films.

3.2.9. Fluorescence measurement and correction for overlapping spectra

Fluorescence was measured on a Fluoroskan FL instrument. FAM, HEX, TAMRA and Texas Red fluorophores were excitated at 485, 530, 544 and 584 nm and the emitted light was measured at 538, 555, 590 and 612 nm, respectively. The signals were corrected for the overlap of excitation and emission spectra.

3.3. Design of molecular beacons for use in AmpliDet RNA assay

3.3.1. Nucleic acids representing viral, bacterial or fungal sequences

Batches of cDNAs representing sequences of *Arabis mosaic virus* (ArMV, the most similar sequence in the databank: X81814), *Apple stem pitting virus* (ASPV, D21829) and the *Tox5* mRNA of *Fusarium poae* (Fus, U15658) was provided by Michel M. Klerks. Genomic DNA for *Ralstonia solanacearum* (Rs, AB024607) was a gift from Dr Jan van der Wolf, while cDNAs of *Potato virus Y* CP coding regions (PVY^N, U91747; PVY^{NTN}, M95491; PVY^O, D12539) were provided by Dr Cor D. Schoen.

3.3.2. Molecular beacons and oligonucleotides

MB probes ArMV, ASPV and Fus were from Michel M. Klerks while MBs Cms1, Cms2 (specific for *Clavibacter michiganensis sepedonicus*, U09764) and Rs were provided by Dr Jan van der Wolf (the sequences of the MBs are shown in Table 4, pp. 70). They were designed to detect the respective viral, bacterial or fungal nucleic acids (*2.3.1.*). MB Na is specific for PVY^N and PVY^{NTN}, while MB Nb for PVY^N. MBs Oa and Ob recognize sequences of PVY^O. All the other MB probes with label 'O' detect both PVY^O and PVY^{NTN}. Oligonucleotides used for mutagenesis and PCR are shown in Table 5. The oligonucleotide primers and MB probes were designed as described previously, and were provided by Dr Cor D. Schoen, Dr Jan van der Wolf, Michel M. Klerks and Isogene B.V., The Netherlands.

Name	Sequence
R1-U-5'	TTTATGAGGACACATCACGAACAC
R1-C-5'	TTTATGAGGGCACATCACGAACAC
R1-G-5'	TTTATGAGGCCACATCACGAACAC
R1-U-3'	GTGATGTGTCCTCATAAAAGTCAA
R1-C-3'	GTGATGTGCCCTCATAAAAGTCAA
R1-G-3'	GTGATGTGGCCTCATAAAAGTCAA
R2-U-5'	TTTATGAGGTCAAATCACGAACAC
R2-C-5'	TTTATGAGGTCAGATCACGAACAC
R2-A-5'	TTTATGAGGTCATATCACGAACAC
R2-U-3'	GTGATTTGACCTCATAAAAGTCAA
R2-C-3'	GTGATCTGACCTCATAAAAGTCAA
R2-A-3'	GTGATATGACCTCATAAAAGTCAA
ArMV-P1-3'	*AATTCTAATACGACTCACTATAGGG*AAGGGCTACATATATGCACTTTA
ArMV-P2-5'	GTCTCTCAAGTATCTGACAA
ASPV-P1-3'	*AATTCTAATACGACTCACTATAGGG*AGGACTTTGAGTTTGCAGCATGA
ASPV-P2-5'	GCAGATGTTGGAGCCTCAGA
Fus-P1-3'	*AATTCTAATACGACTCACTATAGGG*GAATTCCTTTGTAGAATGACATGA
Fus-P2-5'	ATGTTGGATTGAGCAGTACA
Rs-P1-3'	*AATTCTAATACGACTCACTATAGGG*AGAGGCCTTGCGGTCCCCCACT
Rs-P2-5'	TGGCGGCATGCCTTACACA

Table 5

Oligonucleotides used in this study. Sense primers have the suffix 5', while the antisense ones the suffix 3'. The oligonucleotide primers used for mutagenesis were labeled with the name of the RNA target for the generation of which they were applied. The nucleotides to be substituted are underlined. Reverse oligonucleotide primers for NASBA were named P1, while the forward ones P2. The target sequence is also indicated in the naming of the primers. The sequences corresponding to T7 polymerase recognition sites are shown in italics.

3.3.3. 'Overlap' oligonucleotide mutagenesis

Site-directed oligonucleotide mutagenesis was essentially carried out as described by Ho et al. A 557 nucleotide-long region of the 3' part of the PVY^{NTN} CP coding region was amplified in two overlapping fragments by Pfu polymerase (Promega), according to the manufacturer's instructions. The primers were PVY-T7-5' (Table 3) and one of the reverse mutagenesis primers, and RNA-3' (Table 3) in pair with the corresponding forward mutagenesis primer. The amplified fragments were purified using the High Pure PCR Product Purification Kit from Roche.

A second round of amplification was carried out using 5 µl of the 100-times diluted purified products of the appropriate pairs of PCR reactions, as templates, with the two outer oligonucleotide primers (PVY-T7-5' and RNA-3'), by Pfu polymerase. The products were

purified, and cloned into EcoRV-digested pBC-SK vector. The presence of the introduced mutations was verified by sequencing.

3.3.4. In vitro RNA transcription

In vitro transcribed RNA was used for assessing the signals of MBs with mismatching RNA targets, and for producing homogeneous and pure RNA solution for the determination of the stability of MB-RNA interactions. In each case, template DNA for RNA synthesis was amplified in PCR with the respective oligonucleotide primers designed for NASBA (Table 5), using the appropriate template nucleic acid (*3.3.1.*). For the amplification of PVY sequences P1A-3' and P2D-5' were used (Table 3). The templates for the transcription of RNAs with substitutions in the MB complementary-region were amplified from plasmids containing the mutagenized fragments (*3.3.2.*) with P1A-3' and P2D-5'.

In vitro RNA synthesis and the determination of RNA concentration were performed as described in section *3.2.6.*

3.3.5. Thermal denaturation profiles of MBs in the absence and the presence of target RNA

MB melting curves were recorded essentially as described by Bonnet et al. (1999). The fluorescence of 50 nM molecular beacon was monitored in a solution containing 50 mM Tris-HCl, pH 8.5, 70 mM KCl, 0.5 mM DTT, 375 mM sorbitol and 0.7 mM $MgCl_2$ (NASBA-like solution), in the absence or the presence of 300 nM target RNA molecules in 20 µl volume, as a function of temperature. Tris-HCl stock solution (1 M, pH 8.5) was prepared with DEPC-treated water, under RNase-free conditions, and all the other solutions were treated with DEPC. The measurements were carried out using an Applied Biosystems Prism 7700 instrument, in black-colored 8-well strips (purchased from Nunc), to reduce light reflection. After 15 min equilibration at 80 °C, the temperature of the samples was reduced from 80 °C to 15 °C, with steps of 1 °C lasting for 5 min each, and then increased from 15 °C

to 80°C in the same rate, to check that no non-equilibrium hysteresis occurred. Fluorescence was measured in the last 30 sec of each step. The values measured during the first part of the experiment were used for calculation, because after longer periods some photo-bleaching could be observed, reducing the signal at higher temperatures. Each melting curve was measured in three parallel samples, for which the calculations were performed separately, and the resulting equilibrium constants were averaged.

The measured fluorescence was corrected for the temperature-dependence of FAM or TET, and was normalized for the maximum emitted light (fluorescence of an MB measured at 80 °C, i.e. in heat-denatured state, was taken as 1.00), as described by Bonnet et al.

To determine the effect of nucleotides (12 mM) and proteins (2.1 μg BSA and enzymes) present in NASBA reaction mixture, the melting behavior of MBs was monitored in their presence, and absence, in a solution containing all the other components of the reaction mixture. To simulate the experienced shift in melting, MB melting properties were measured in solutions with various Mg^{2+} concentration, and were compared to those experienced in NASBA mixture.

The factors characterizing the DMSO- and sorbitol-dependence of MB melting were determined in NASBA-like solution, except for that it contained varying concentration of DMSO (0; 5; 10; 12.5; 15; 17.5; 20 v/v %) or sorbitol (0; 100; 200, 250; 300; 350; 400; 450; 500 mM).

3.3.6. Calculation of K_{MB}, K_d and T_m

The equilibrium constants of MB opening and duplex dissociation at the temperature of the assay (i.e. 41 °C) were calculated according to the formulas, provided by Bonnet et al.

$$K_{MB,41} = (F_{41} - \beta) / (\gamma - F_{41}) \quad (10)$$

$K_{MB,41}$ Equilibrium constant of MB opening at 41 °C
F_{41} Corrected and normalized fluorescence signal at 41 °C
β Fluorescence of MBs in a closed state, as measured at 15 °C
γ Fluorescence of the MB in random coil state (determined at 80 °C, thus it is 1.00, by definition)

$$K_{d,41} = [(\alpha - F_{41}) * T_0] / [(F_{41} - \beta) + (F_{41} - \gamma) * K_{MB,41}] \quad (11)$$

$K_{d,41}$ Equilibrium constant of MB-RNA duplex dissociation at 41 °C
α Fluorescence of MBs in a target-bound state. It was approximated as 1.00.
T_0 Target molecule concentration

The melting temperature of an MB was determined as the temperature where half the MBs are closed and the other half are in random-coil state.

$$F_{(Tm)} - \beta / 2 = \gamma / 2 \quad (12a)$$
$$T_m: \quad \text{where } F = 0.5 + \beta / 2 \quad (12b)$$

$F_{(Tm)}$ Corrected and normalized fluorescence at the melting point
T_m Melting temperature

Calculations for the prediction of RNA-DNA heteroduplex stability on the basis of NN theory, corrections for the presence of additives (DMSO and sorbitol) and for difference in salt concentrations, were performed by using a C program (Szemes, unpublished results). All other calculations were carried out by macros in Excel.

3.3.7. Evaluation of the specificity of MBs with templates containing single mutations in AmpliDet RNA assay

NASBA was carried out with 10^5 molecules of template RNA, in the presence of 50 nM MB, as described previously *(3.2.7.)*. The fluorescence of MBs in the amplification reaction with the perfectly matching template (Table 6: R0) was taken as 1.00 and the signals with the mutant RNAs (Table 6: R1 and R2 sets of RNA) were evaluated in comparison.

4. Results

4.1. Integrated RT-PCR/nested PCR diagnosis for differentiating between the subgroups of *Plum pox virus*

4.1.1. Design of the assay

The two major strains of PPV, Dideron (D) and Marcus (M), were first described on the basis of serological properties (Kerlan and Dunez, 1979). The separateness of these groups was reinforced by biological and epidemiological characteristics. Since the El Amar (EA) and the Sour Cherry (C) strains were also reported to be serologically distinct, the coat protein (CP) coding region appeared suitable for the differentiation of the PPV strains. We attempted to identify the amino acid motifs that might be associated with the distinct serological properties, and to assign the underlying nucleic acid patterns as diagnostic regions.

The major antigenic determinants are located in the N and C-terminal ends of the coat protein, which protrude from the capsid (Shukla et al., 1988). The majority of the strain-specific epitopes were proposed to locate in the variable N-terminal region (Candresse et al., 1998). In search of strain-specific motifs, a multiple sequence alignment of 24 full-length and 2 partial PPV CP sequences, publicly available in GenBank, was carried out. The CP sequences of viruses that had not been characterized serologically were included in the PPV-D or M groups according to the presence or absence of the RsaI restriction site used to separate these strains by RFLP (Wetzel et al., 1991). As expected, the majority of the sequence differences were found in the amino-terminal regions of the CPs, spanning approximately the first 100 amino acids. The differences often occurred in clusters, characteristic for the PPV-D and M strains, respectively (Fig. 5). The biologically not characterized sequences fitted nicely into the PPV-D and M groups, showing high similarity

Fig. 5

Alignment of the N-terminal part of the PPV CP sequences; numbering is indicated relative to the start of the CP region. The sequences were grouped according to the strains. The consensus is shown in the first line and for the individual sequences only the differing amino acids are indicated; periods stand for deletions or unknown sequences. The positions of the generic primers are shown by shaded boxes, and those of the strain-specific primers by open boxes. The completely different amino acid pattern of X81080, overlapping the position of the 3' generic primer, results from a frameshift mutation; at a nucleic acid level it is similar to other PPV sequences

to them along the whole sequence. The primary structures of the PPV-C and EA CP sequences differed substantially from each other and also from those of the other two groups.

Regions of group-specific differences between the PPV-D and M types could be selected, just like unique sequence motifs for the PPV-EA and PPV-C strains (boxed in Fig. 5). Oligonucleotides for PCR primers were designed accordingly, on the basis of the underlining nucleic acid patterns (M1-5', M5-3' for PPV-D, M6-5', M7-3' for PPV-M, M8-5', M9-3' for PPV-EA and M10-5' and M11-3' for PPV-C. For the sequences see Table 1). When necessary, the oligonucleotides were degenerated so as to be complementary to all known PPV CP sequences of the respective strain.

Flanking the region of divergence, conserved sequences were searched for as target sites for primers for generic PPV detection. The position of the 5' generic primer was selected immediately upstream of the codon of the first CP amino acid (indicated by a shaded box in Fig. 5). This region displays moderate polymorphism at a nucleic acid level for the four PPV types. Two sets of degenerated oligonucleotides were therefore designed: one specific for the PPV-D and M types (M3-5'), while the other for the PPV-EA and C types (M4-5'). In the PCR reactions a 1:1 mixture of the two sets was used. The 3' generic primer (M2-3', its position is shown by a shaded box in Fig. 5) was also mildly degenerated to compensate for the known variations.

4.1.2. Specificity of the primers

The abilities of the primers to detect the presence of PPV and to differentiate between the four strains were tested. RNAs prepared from PPV-EA and PPV-D-infected plant samples and plasmids carrying cloned cDNAs overlapping the CP region of the PPV-M and PPV-C types were used as templates. The products amplified by the generic primers had the expected size (Fig. 6). The four nested PCR carried out on the diluted amplicons of the first reaction

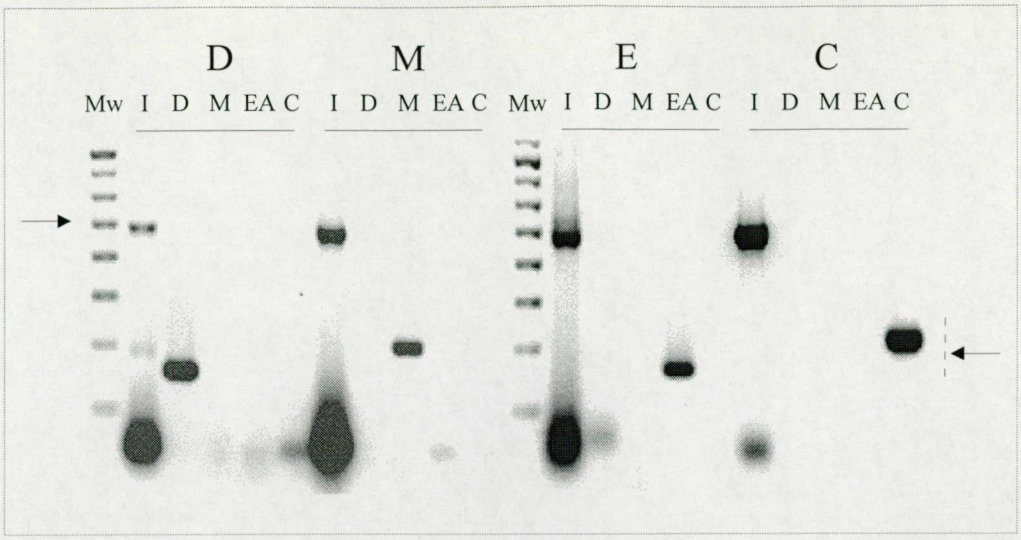

Fig. 6

Detection and typing of PPV. Generic PCR detection (I) was carried out with templates representing PPV-D, PPV-M, PPV-EA and PPV-C strains, followed by four strain-specific nested reactions. The types of the templates are shown on the top, while the strain-specific nested reactions are indicated above the lines. The arrows on the left and on the right point to the expected products of the generic and strain-specific PCR reactions, respectively.

resulted in strain-specific products with no detectable cross-reaction. These results demonstrated that the integrated RT-PCR system performed well in a model situation.

In order to test the specificity and sensitivity of the diagnostic procedure under field conditions, we prepared RNAs from 40 independent plant samples exhibiting symptoms of PPV infection. Two sets of PCR reactions were carried out in parallel. In the first set, the newly developed primers were used. The second set served as a control, in which PPV was detected by primers designed for the 3' non-coding region (C-3NCPPV and H-3NCPPV), as described by Levy and Hadidi (1994).

The presence of the virus was detected in 33 of the 40 samples. Among the 33 positives, 16 generated detectable products in both sets of primary PCR reactions. In the remaining 17 samples, PPV was detected only with the differentiating nested PCR reactions. The 7 samples that failed to produce any PPV-specific PCR products with our primers also gave negative results with the control primer pair. Of the positives, 18 isolates were characterized as PPV-M and 7 as PPV-D type with no ambiguity. Eight samples produced

both PPV-D and M-characteristic PCR products; coincidentally, one of them was always a dominant component. PPV-EA and PPV-C strains were not detected in this set of samples.

4.1.3. Correlation between PCR, RFLP and serological typing

The method developed was validated by comparing the results of the integrated RT-PCR system to those of serological and RsaI-RFLP typing. Ninety-two samples, of which 85 isolates were collected in Hungary and 7 in other countries, were analyzed. Two overlapping subsets of this collection were also characterized by RsaI-RFLP and by ELISA with strain-specific monoclonal antibodies.

The results are summarized in Table 7. PCR detected 52 PPV-M and 20 PPV-D single and 14 D/M, 5 M/C and 1 D/M/C mixed infections. The serological analysis indicated 68 isolates belonging to PPV-M and 21 to PPV-D serotypes, among the 89 isolates tested. No PPV-C or PPV-EA, or any mixed infection was detected by ELISA. The results of PCR and those of serological typing were identical in 68 cases (76.4%), all of them representing single PPV-D or M infections. Consistent results were obtained for 18 samples (20.2%), i.e. ELISA detected one of the two or three PPV strains indicated by PCR. In a single case (isolate SK185; 1.1%), the results of the two methods were contradictory. This sample was characterized by PCR as a PPV-D strain, while ELISA indicated a PPV-M type. The result of RFLP typing supported that of PCR. Forty-six of the 92 samples were analyzed by RFLP. In 42 cases (91.3%), the results of PCR and RFLP typing were identical, including 40 single PPV-M or PPV-D infections and 2 M/D mixed infections. The remaining four analyses (8.7%) gave consistent results. The overall correlations with the two independent diagnostic approaches were excellent: 100% for PCR/RFLP and 98.9% for PCR/ELISA.

isolate code	source species	year of isolation	PCR typing	RsaI RFLP typing	ELISA typing	isolate code	source species	year of isolation	PCR typing	RsaI RFLP typing	ELISA typing
SK1*	plum	1972	M	M	M	SK77	plum	1974	M/(C)	M	M
SK2	plum	1974	M	nt	M	SK80*	plum	1980	(D)/M	nt	M
SK3	peach	1974	M	nt	M	SK82	plum	1973	M	nt	M
SK4	plum	1974	M	nt	M	SK83	myrobalan	1979	(D)/M	nt	M
SK6	apricot	1966	(D)/M	M	M	SK84	myrobalan	1979	M	M	M
SK12	plum	1973	M	M	M	SK91	apricot	1982	(D)/M	nt	M
SK13	plum	1973	M	nt	M	SK181	peach	1986	(D)/M	nt	M
SK18	Prunus sp.	1970	M	nt	M	SK185	peach	1986	D	D	M
SK21*	plum	1971	M	nt	M	SK186	peach	1986	M/(C)	M	M
SK22	peach	1972	M	nt	M	SK188	peach	1986	(D)/M	nt	M
SK23	apricot	1972	M	nt	M	SK190*	plum	1991	D	nt	D
SK25*	apricot	1973	M	nt	M	SK191	plum	1991	M	M	M
SK26*	apricot	1973	(D)/M	nt	M	SK192	apricot	1993	M	M	M
SK28*	plum	1971	D/M	nt	M	SK193	peach	1993	D	D	D
SK33	plum	1986	M	M	M	SK194	peach	1993	(D)/M	Nt	M
SK35	plum	1986	M	nt	M	SK195	peach	1991	D	D	D
SK36	plum	1973	M	M	M	SK196	peach	1991	(D)/M	D/M	nt
SK37	plum	1986	M	M	nt	SK197	peach	1991	(D)/M	D/M	D
SK40	peach	1973	M	M	M	SK198	peach	1991	M	nt	M
SK41	apricot	1971	M	M	M	SK199	peach	1991	M	M	M
SK42	plum	1986	M	M	M	SK201	peach	1991	D	D	D
SK43	apricot	1968	M	M	M	SK203	myrobalan	1991	D	Nt	D
SK44	apricot	1968	M	M	M	SK204	almond	1991	M	M	M
SK45	plum	1986	M	M	M	SK205	wild apricot	1991	M	M	M
SK46	plum	1986	M	M	M	SK206	peach	1991	M	M	M
SK47	plum	1986	M	nt	M	SK207	almond	1991	M	M	M
SK48	greengage	1974	M	nt	M	SK208	apricot	1991	M	M	nt
SK50	plum	1986	M	nt	M	SK209	peach	1991	D/M	Nt	D
SK52	apricot	1978	M/C	nt	M	SK210	peach	1991	D	Nt	D
SK53	apricot	1978	M	nt	M	SK211	peach	1991	D	Nt	D
SK54	peach	1976	(D)/M	nt	M	SK212	apricot	1991	D	Nt	D
SK55	peach	1976	M	nt	M	SK233	peach	1992	D	D	D
SK56	peach	1976	M/C	nt	M	SK236	peach	1992	D	D	D
SK58	peach	1976	M/(C)	M	M	SK237	peach	1994	M	Nt	M
SK59	peach	1976	M	M	M	SK238	peach	1994	D	Nt	D
SK60	plum	1986	M	M	M	SK239	peach	1994	D	D	D
SK61	peach	1975	M	M	M	SK240	peach	1994	D	Nt	D
SK64	apricot	1979	(D)/M/C	nt	M	SK241	peach	1994	D	D	D
SK63	myrobalan	1978	M	M	M	SK242	plum	1991	D	Nt	D
SK65	plum	1986	M	M	M	SK243	peach	1995	D	Nt	D
SK67	plum	1986	D/(M)	nt	M	SK244	peach	1995	D/M	M	M
SK68	plum	1986	M	M	M	SK245	plum	1995	M	nt	M
SK70	plum	1982	M	nt	M	SK246	plum	1995	M	nt	M
SK72	plum	1978	M	M	M	SK247	apricot	1995	D	D	D
SK74	plum	1979	M	M	M	SK248	plum	1995	D	nt	D
SK76	plum	1974	M	M	M	SK249	wild almond	1995	D	nt	D

Table 7

PCR, RFLP and ELISA typing of PPV isolates. (*) Not Hungarian isolates.

4.2. Development of a multiplex AmpliDet RNA assay for the simultaneous detection and typing of PVY isolates

4.2.1. Identification of nucleic acid sequence motifs suitable for differentiation of PVY isolates

Genomic region(s) associated with the distinct etiological properties of the PVY strains or of the tuber necrotic isolates have not been identified to date. For group-specific detection, therefore, unique sequence motifs were searched along the whole viral genome. PVY sequences available in public databases were retrieved and were compared both at an amino acid and at a nucleic acid level. The sequences of PVY viruses isolated from non-potato hosts were excluded from the analysis, unless they were biologically characterized and classificd into the PVY^{N}, PVY^{O}, PVY^{C} or the PVY^{NTN} type. Nine full-length, among them one PVY^{NTN}, and numerous partial sequences were aligned. Strain-specific sequence motifs were observed in several genomic regions (data not shown); for the tuber necrotic isolates, however, apart from variations of a few nucleotides, no characteristic region could be identified. The evaluation of the significance and uniqueness of these small polimorphisms was difficult due to the low number of PVY^{NTN} sequences.

Within the CP gene, a rearrangement correlating with the tuber necrotic pathotype was reported previously (Revers et al., 1996). The PVY^{NTN} CP coding sequences were found to be chimerical: the 5' part shows high similarity to PVY^{N}, while the 3' end to PVY^{O} sequences, which could have arisen in consequence of a recombination event between a PVY^{N} and a PVY^{O} genome. This genome region, therefore, appeared promising for diagnostic purposes.

To explore this possibility and to compare biological and sequence-based classification, the PVY CP coding regions were clustered based on similarity. Since several rearrangements were reported within this genome region (Revers et al., 1996), phylogenetic

analysis of the full-length sequences was inappropriate. Instead, we performed clusterings based on shorter sequence stretches at the 5' (72 nucleotides) and 3' (100 nucleotides) ends of the CP region, and attempted to identify the parental, non-recombinant sequences and the corresponding sequence clusters (Fig. 7). By the analysis of the 5' CP region, three groups were identified, mostly corresponding to the $PVY^{NTN/N}$, PVY^{O} and PVY^{C} types. The 3' tree contained two clusters: one corresponding to the PVY^{N} strain and a large group containing the PVY^{O}, PVY^{NTN} and PVY^{C} isolates. As expected, the PVY^{NTN} sequences were grouped into different clusters depending on which part of the CP coding sequence was analyzed. Two PVY^{N} (U06789, S74813) and one biologically not characterized isolate (X68223) were also located in different clusters in the two trees, indicating their recombinant nature. Two additional PVY^{N} sequences (PVY^{N}-Wi, Z70238; and PVY^{N}-Fr, X12456) clustered with PVY^{O} in both analyses, which is not surprising, since they had already been reported to possess CPs characteristic for PVY^{O} (Chachulska et al., 1997).

To locate the presumed recombination sites the chimerical and the irregular isolates were analyzed by bootscanning, which, given a set of potential parental sequences, indicates probable rearrangements in the test sequence. In our analysis, the parental, non-recombinant strains were defined as the consensus of the regular PVY^{N}, PVY^{O} and PVY^{C} sequences, i.e. which clustered to the group of their strains based on both the 5' and 3' parts.

Bootscanning analysis was performed with every PVY CP coding sequence. Each PVY^{NTN} sequence possessed a single rearrangement within the analyzed region (an example is shown in Fig. 8), located in the same position. The biologically not characterized, recombinant isolate (X68223) contained the same rearrangement, suggesting that it belongs to the PVY^{NTN} group, which is possible, considering that it originated from Hungary, where the prevalence of this pathotype was reported (Wolf and Horváth, 2001).

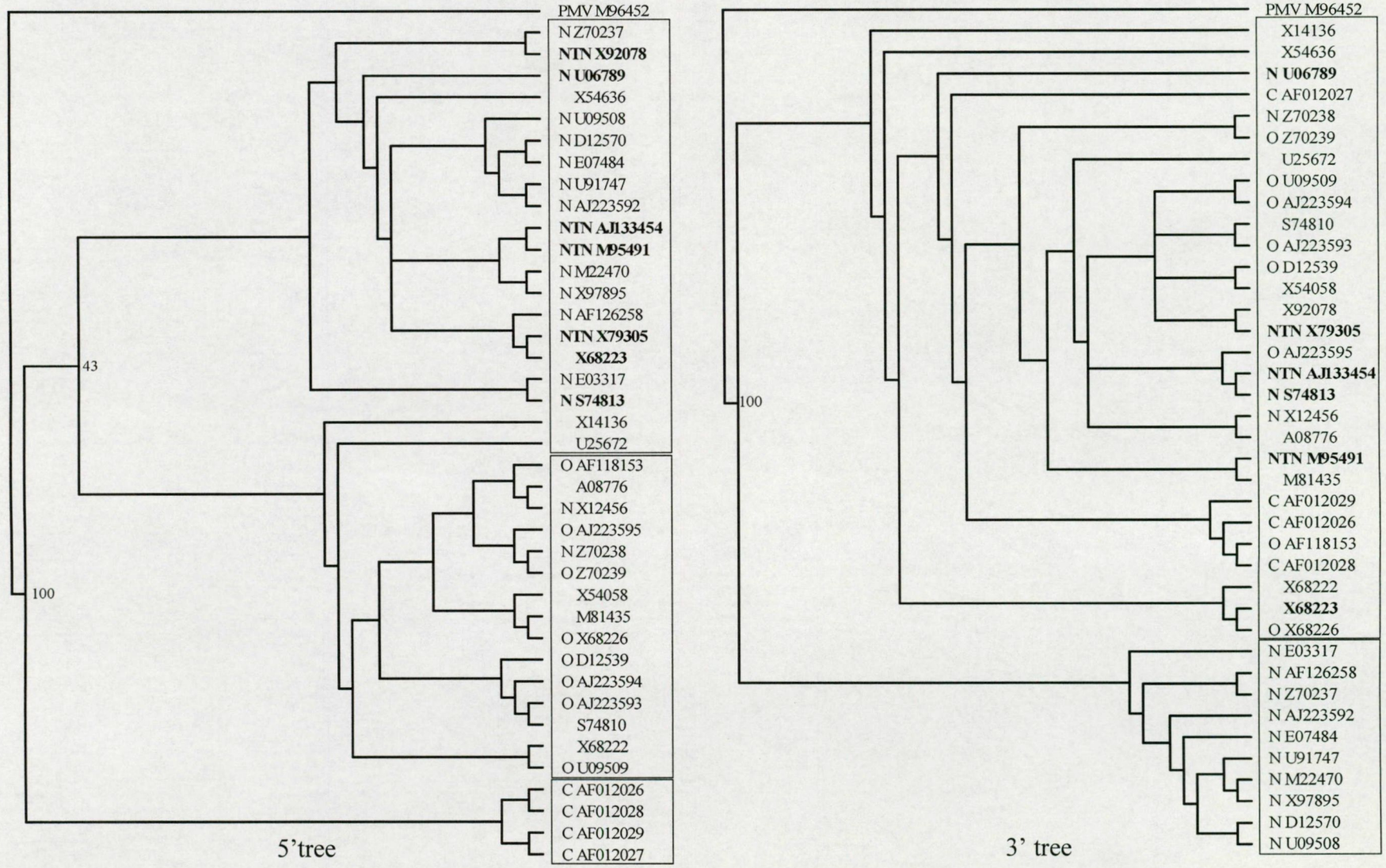

Fig. 7

Phylogenetic trees depicting the relationships of the 5' 72 and 3' 100 nucleotide-long regions of the PVY coat protein coding sequences, respectively. The corresponding region of *Pepper mottle virus* (PMV) was used as outgroup in the analyses. The main clusters are boxed, and the bootstrap values showing the significance of their separation are indicated. The sequences that were placed into different clusters in the two analyses are shown in bold.

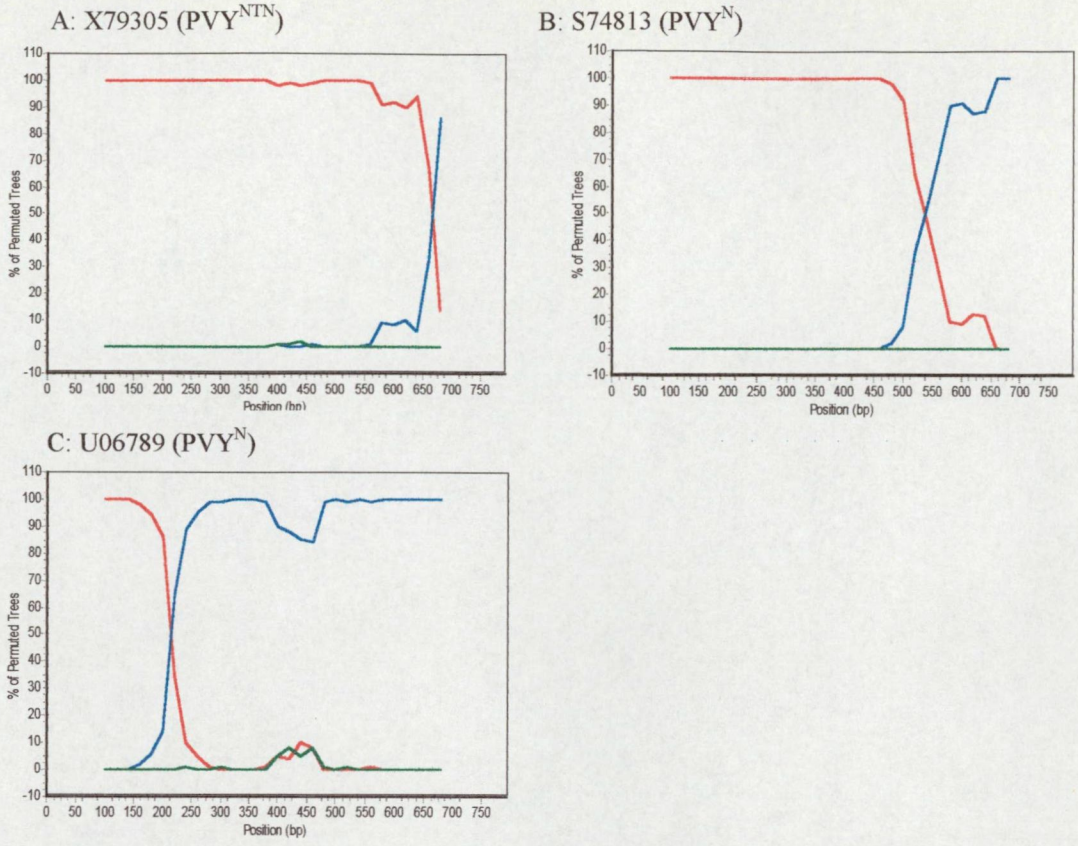

Fig. 8

Analysis of recombinant PVY sequences by bootscanning. The sequence to be tested was aligned with the potential parental sequences, i.e. the consensus sequences of the three strains. Phylogenetic trees were constructed for 200 nucleotide-long sections of the alignment, and this 'window' was slid along the sequences. For each position, 100 bootsrapped samples were generated and the percentage of the cases the analyzed sequence stretch clustered together with a strain was plotted in function of the position: red stands for PVY^N, blue for PVY^O and green for PVY^C. The analysis of a typical PVY^{NTN} isolate (X79305), and those of two 'irregular' PVY^N viruses (S74813 and U06789) are shown.

The other two recombinant isolates underwent a rearrangement in different regions (Fig. 8B and C). Taken together, three main clusters of PVY CP coding sequences were identified, mostly corresponding to the PVY^N, PVY^O and PVY^C biological strains. PVY^{NTN} isolates were found to be chimerical by bootscanning analysis too, and the rearrangement correlated perfectly with the tuber necrotic pathotype. Therefore, this genome region appeared suitable for the specific detection of PVY^{NTN} and for PVY strain differentiation.

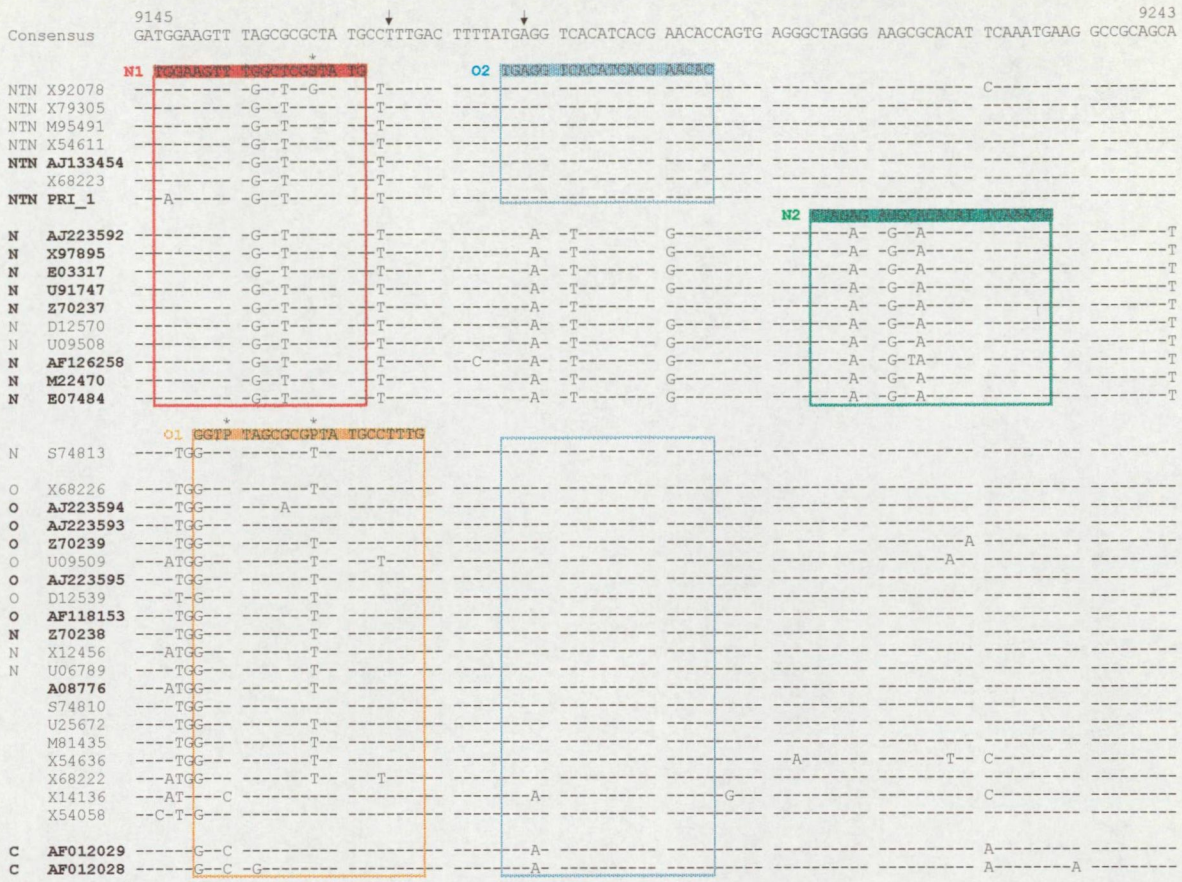

Fig. 9

Alignment of the PVY CP coding nucleotide sequences, showing the region used for strain discrimination. PVY-Hu (M95491) was used as a reference for numbering. The sequences not clustered by Revers et al. (1996) are shown in bold. The consensus sequence is given in the top line, while for the other sequences only the differing nucleotides are indicated. The biological strain classification, when available, is shown in front of the sequences. The diagnostic rearrangement within the PVY^{NTN} CP coding region is located between the positions 9168 and 9183, indicated by arrows. The positions of the MBs are boxed and the sequences of MB-N1, MB-N2, MB-O1 and MB-O2 are highlighted in red, green, orange and blue, respectively. The universal pyrimidines (P) in the sequence of MB-O1 and the degenerate position (S = G and C) in MB-N1 are indicated by asterisks. The MBs bind to NASBA amplicon RNAs, which are complementary to the genomic RNA shown in the picture.

4.2.2. Design of the assay

PVY^{N} and $PVY^{O/C}$ cluster-specific sequence motifs were selected at both sides of the presumed recombination site (Fig. 9), which could serve as target areas for the strain-specific MBs. The beacons were named MB-N1, MB-N2, MB-O1 and MB-O2, according to specificity and position. Flanking this diagnostic region, conserved sequences were selected as binding sites for PVY-specific NASBA primers. With the MB probes, three groups of

A

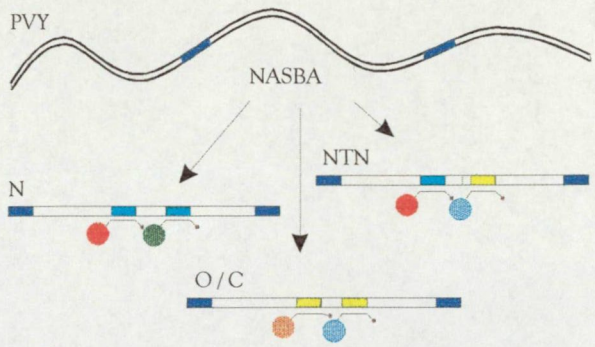

B

	Single infection			Mixed infection		
	NTN	N	O/C	N + NTN	NTN+ O/C	N + O/C
MB-N1	+	+	-	+	+	+
MB-N2	-	+	-	+	-	+
MB-O1	-	-	+	-	+	+
MB-O2	+	-	+	+	+	+

Fig. 10

A: Scheme of the AmpliDet RNA assay. In a generic NASBA, a region of the CP coding sequence is amplified for all PVY isolates. With four MBs, three PVY clusters can be identified: the PVY^{NTN} isolates are detected via MB-N1 (Texas Red, red) and MB-O2 (FAM ,blue), PVY^{N} via MB-N1 and MB-N2 (HEX, green), while the $PVY^{O/C}$ cluster via MB-O1 (TAMRA, orange) and MB-O2. The PVY^{N} and $PVY^{O/C}$-specific motifs are shown by green and yellow rectangles, respectively.

B: Diagnosis of single and mixed infections of PVY isolates.

isolates can be detected: one containing all the PVY^{NTN} isolates (by MB-N1 and MB-O2), one with PVY^{N} isolates (by MB-N1 and MB-N2) and a third one with isolates of PVY^{O} and PVY^{C} (by MB-O1 and MB-O2), as shown in Fig. 10A. The use of four MBs was necessitated by the fact that mixed infections of PVY strains may occur. Since MB-N2 and MB-O1 are unique for the PVY^{N} and $PVY^{O/C}$ strains, respectively, a mixed PVY^{N} and PVY^{O} infection can be identified correctly and is not mistaken for PVY^{NTN} (Fig. 10B).

PVY isolates are numerous and they possess some sequence heterogeneity in the MB target areas, even within the cluster. The aim was to design MBs that would be specific to their cognate target molecule, but could tolerate a mismatch between the probe and the respective amplicon RNA. Therefore, the MBs were selected to contain a minimum of three discriminatory nucleotides for differentiation between the viral types, and to possess a loop length ranging from 20 to 23 nucleotides.

To tolerate known sequence polymorphisms present in the MB binding site, the nucleotide compositions of two MBs were modified. The target area of MB-O1 was the most divergent, therefore two universal pyrimidine analogues (P) were incorporated to compensate

for C/T polymorphisms in two positions. The P analogues form base pairs with the corresponding A and G nucleotides in the NASBA amplicon RNA, which is complementary to the PVY genomic RNA. MB-N1 was degenerated in one position. The hybridizing parts of the other MBs were identical to the consensus sequence of the respective cluster.

The assay was developed for use on a fluorometer with variable wavelength light source, which enables the application of a wide range of fluorescent dyes. To be able to fully discriminate among the signals of the different MBs, fluorophores with excitation and emission maxima well spaced in the spectrum were required. Accordingly, FAM, HEX, TAMRA and Texas Red were selected as labels for the MBs.

4.2.3. Performance of the assay

The specificity of the MBs for the different PVY clusters was determined using RNAs of well-defined representatives of each strain, and that of the tuber necrotic isolates, as template. Each MB was found to be perfectly specific and gave signal only with its cognate target(s) (Fig. 11A).

The MBs were also tested for mismatch tolerance with isolates containing single or multiple nucleotide polymorphisms in the target regions: a PVY^{O} isolate (U09509) had a nucleotide substitution in the MB-O1 hybridization site, PRI_1 (PVY^{NTN}) had a variable nucleotide in the MB-N1 target area, while 53-38 (PVY^{C}) had one in the MB-O1 and one in the MB-O2 binding site too (unpublished results; for the sequences see Fig. 9). The MBs tolerated the mismatches in all cases but one, and gave specific but reduced signals with these polymorphic isolates (Fig. 11B). The single exception was the binding of MB-O1 to PVY^{C} (53-38), in which case an A/G change in the MB target region within the NASBA amplicon RNA was not tolerated.

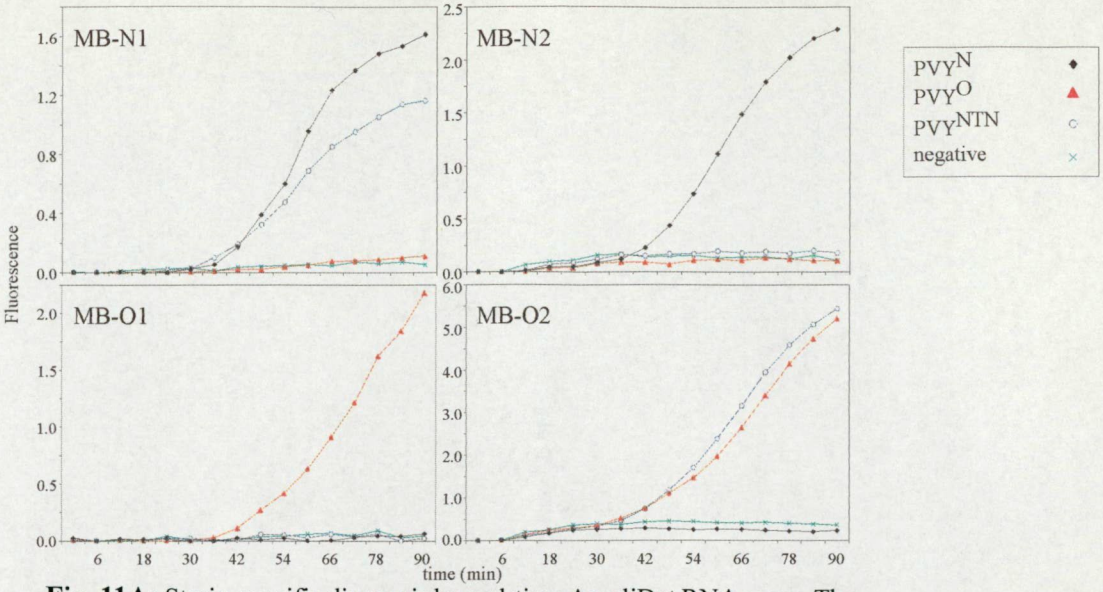

Fig. 11A: Strain-specific diagnosis by real-time AmpliDet RNA assay. The signals of each MB are shown in a separate panel.

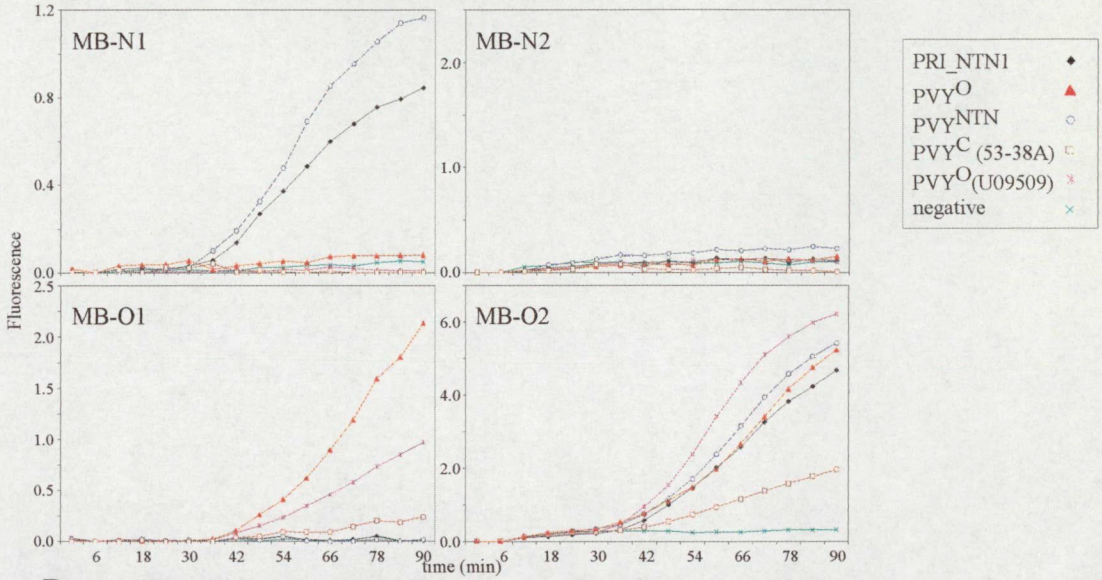

B: AmpliDet RNA assay with PVY isolates containing a mutation in one or other of the MB target areas: PRI_NTN1 (mutant in the target region of MB-N1), U09509 (MB-O1) and 53-38 (MB-O1 and MB-O2). The signals with non-mutant PVY^{NTN} and PVY^{O} isolates are included for comparison.

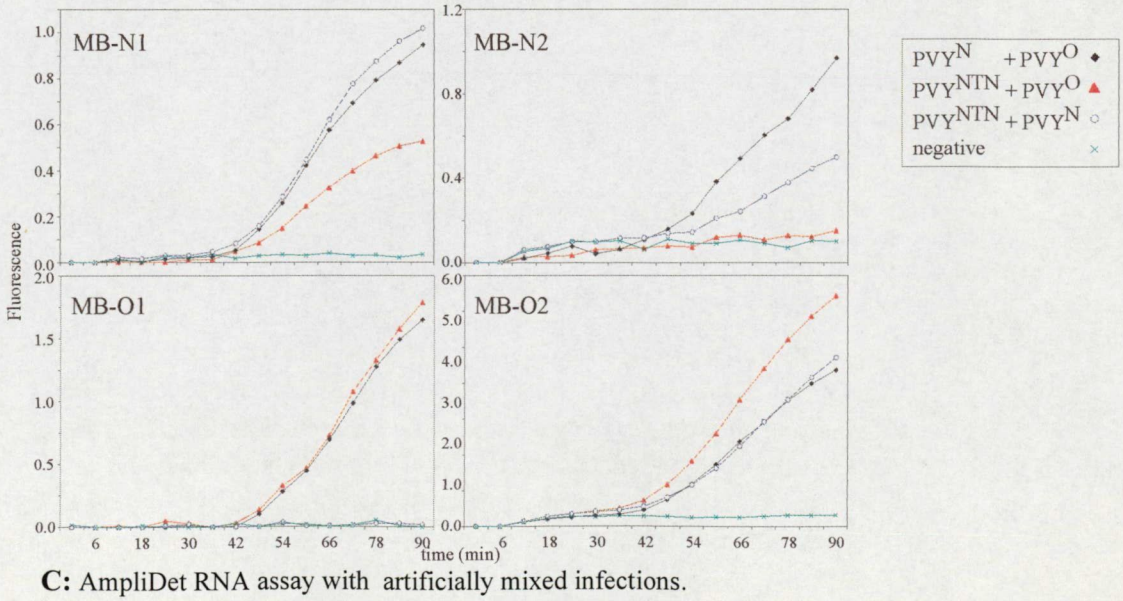

C: AmpliDet RNA assay with artificially mixed infections.

The detectability of mixed infections was also tested. The signals of assays performed on artificial mixtures of RNA samples are shown in Fig. 11C. Mixtures of PVY^{NTN} with either PVY^{O} or PVY^{N} could be diagnosed unambiguously and correctly. A PVY^{N}/PVY^{O} mixed infection, as expected, resulted in positive signals with all MBs. Although it does not rule out the presence of PVY^{NTN} being present as a third infecting virus, such double or triple infections are expected to be rare and demand additional examination.

The sensitivity of NASBA was determined without MBs, and also in the presence of one and four MBs, to establish how the binding of the probes affects the sensitivity. The detection threshold was determined by using a serial dilution of *in vitro* transcribed RNA as template, representing PVY^{NTN}, PVY^{N} and PVY^{O} sequences. In the absence of MBs and in the presence of one MB, the sensitivity of the assay was 10^{1} copies of RNA per reaction (Fig. 12), suggesting that the amplification power of NASBA was not hindered significantly by the hybridization of an MB in the concentration range used. When all four MBs were present, the sensitivity was lowered by one order of magnitude to 10^{2} copies of RNA per reaction.

4.2.4. Validation of the assay

The performance and reliability of the assay were assessed by analyzing 47 PVY isolates originating from 6 countries (Table 2). First, a set of biologically characterized isolates were tested (Table 2 Nos.: 1-29). The results of AmpliDet RNA were identical or consistent ($PVY^{O/C}$ diagnosis in the case of a PVY^{O} or a PVY^{C} infection) with those of biological strain determination in all cases but one. Nine PVY^{NTN}, 9 PVY^{N}, 8 PVY^{O} and 2 PVY^{C} viruses, representing isolates from 6 countries were diagnosed correctly. The single exception (isolate 53-47) gave signals characteristic of PVY^{N}, but was previously described as PVY^{NTN} (Nielsen, personal communication).

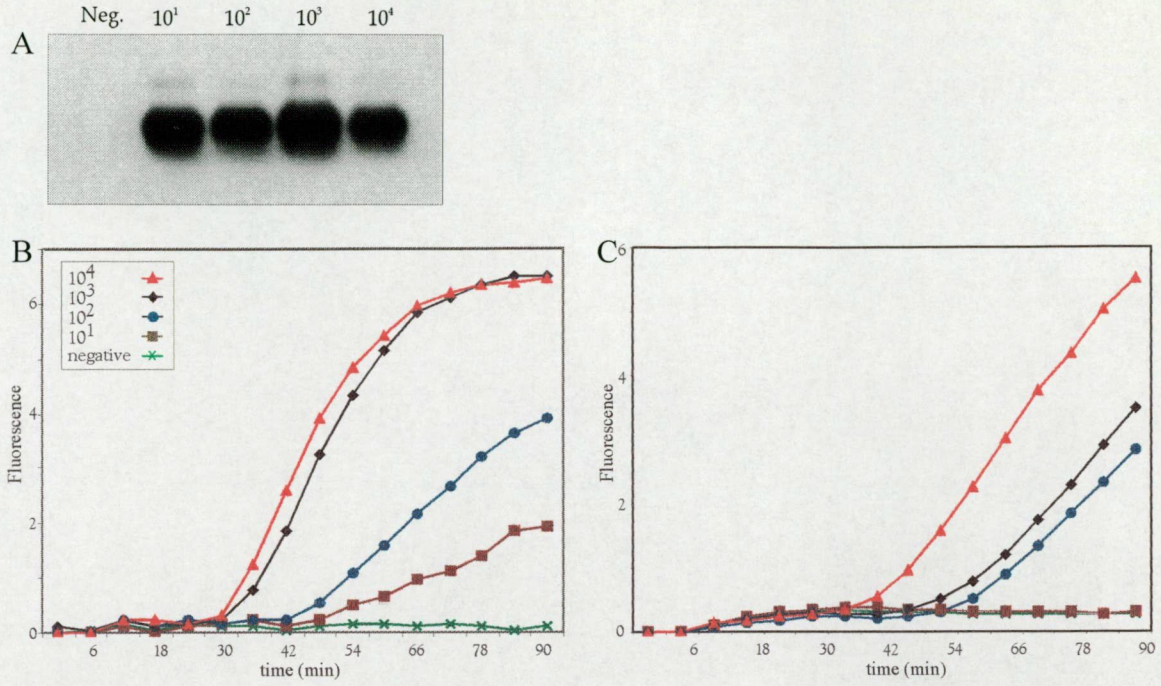

Fig. 12

Sensitivity of PVY-specific NASBA reaction and AmpliDet RNA assay with 10^1, 10^2, 10^3 and 10^4 copies of *in vitro* transcribed RNA (see section *2.2.6.*).

A: Northern hybridization of NASBA reaction products.

B: Sensitivity of AmpliDet RNA assay in the presence of one MB (MB-O2).

C: Sensitivity of the assay with four MBs, where two MBs hybridize to the amplified RNA molecules.

No.	Isolate code	Origin	Biol. strain	AmpliDet	No.	Isolate code	Origin	Biol. strain	AmpliDet
1	751	The Netherlands	NTN	NTN	25	53-31	Denmark	O	O/C
2	PRI_NTN1	The Netherlands	NTN	NTN	26	53-45	Denmark	O	O/C
3	Nicola 250	The Netherlands	NTN	NTN	27	53-38	Denmark	C	O/C
4	Kondor 417	The Netherlands	NTN	NTN	28	D-40	Denmark	C	O/C
5	Liseta 67	The Netherlands	NTN	NTN	29	U09509	Canada	O	O/C
6	Premiere100	The Netherlands	NTN	NTN	30	KE 1	Hungary	NTN	NTN
7	601	The Netherlands	N	N	31	KE 3	Hungary	NTN	NTN
8	602	The Netherlands	N	N	32	KE 9	Hungary	NTN	NTN
9	603	The Netherlands	N	N	33	KE 17	Hungary	NTN	NTN
10	604	The Netherlands	N	N	34	KE 20	Hungary	NTN	NTN
11	606	The Netherlands	N	N	35	KA 2	Hungary	NTN	NTN
12	607	The Netherlands	N	N	36	KA 3	Hungary	NTN	NTN
13	53-46	Denmark	NTN	NTN	37	KA 5	Hungary	NTN	NTN
14	53-47	Denmark	NTN	N	38	KA 6	Hungary	NTN	NTN
15	NTN-Attica	Hungary	NTN	NTN	39	KA 8	Hungary	NTN	NTN
16	NTN-Lb	Lebanon	NTN	NTN	40	KA 9	Hungary	NTN	NTN
17	NTN-R	Romania	NTN	NTN	41	D 1	Hungary	NTN	NTN
18	53-17	Denmark	N	N	42	D 2	Hungary	NTN	NTN
19	53-24	Denmark	N	N	43	D 3	Hungary	NTN	NTN
20	53-25	Denmark	N	N	44	D 5	Hungary	NTN	NTN
21	53-15	Denmark	O	O/C	45	D 6	Hungary	NTN	NTN
22	53-16	Denmark	O	O/C	46	D 9	Hungary	NTN	NTN
23	53-28	Denmark	O	O/C	47	D 10	Hungary	NTN	NTN
24	53-19	Denmark	O	O/C					

Table 2

Comparison of the results of AmpliDet RNA typing with those of biological characterization.

Eighteen isolates collected from independent PVY outbreaks in Hungary were also analyzed. On the basis of symptoms in susceptible potato cultivars Vital and Murillo they were classified as PVY^{NTN} (Wolf and Horváth, 2001). All these isolates were successfully detected and were correctly identified by AmpliDet RNA assay as PVY^{NTN}.

Taken together, the AmpliDet RNA assay gave correct strain identifications in 46 cases: 27 PVY^{NTN}, 9 PVY^{N}, 8 PVY^{O} and 2 PVY^{C} isolates were successfully identified.

4.3. Design of molecular beacons for use in AmpliDet RNA assay

4.3.1. MB characterization, design principles and the applied prediction models

The most important properties characterizing MBs for target molecule detection are specificity, signal intensity and background fluorescence. Specificity means the ability of a probe to discriminate perfectly complementary target molecules from those containing one or more nucleotide substitutions. Different levels of specificity may be desirable for different diagnostic purposes: the detection of SNPs requires highly specific MBs, while assays for bacterial or viral pathogens should be more tolerant, in order to detect more divergent isolates too. Signal intensity characterizes the fluorescence increase of the probe in the presence of target molecules (it can be determined under defined conditions, and can be expressed as percentage of maximum fluorescence). Background fluorescence results from a small portion of probes that are in open conformation at the temperature of the assay, and is measured in the absence of target.

MB probes can be assessed in quantitative terms via these properties, and their abilities for real-time detection can be compared. For optimal MB performance, signal intensity should be close to 100%, i.e. almost all the MBs should be in a target-bound state in the presence of excess target, while the background signal should be low. The required degree of specificity depends on the type of the assay; preferably it should be designable.

Bonnet et al. presented a joint equilibrium model of MB-target interaction (1999), and provided an experimental approach to determine the equilibrium constant of MB opening (K_{MB}), and that of the dissociation of probe-target duplex to closed MB and free target molecule (K_d). Obviously, these constants are in close relationships with the above-described properties: background fluorescence is related to K_{MB}, while signal strength to K_d. The free energies of the transitions can be deduced from the equilibrium constants (equations **(10)** and **(11)** in section *3.3.6.*).

We attempted to create and validate a model for MB design for AmpliDet RNA assay, i.e. to predict the free energy change accompanying MB stem-and-loop structure formation, and that of MB-RNA amplicon hybridization, under NASBA conditions. For this purpose, we applied the model described by Matthews et al. (1999) for the prediction of the strength of interaction between structured probes and structured target molecules. The formula presented (equation **(9)** in *1.10.*) was simplified. First, the bimolecular interaction of the probes was neglected, since the MBs in the absence of target molecules, because of kinetic reasons, participate mainly in the unimolecular reaction of beacon structure formation. Thus, K_{leff} could be substituted by K_{MB}, and, as a consequence, an approximation step in the calculation of K_{leff} was eliminated.

$$\Delta G^{\circ}_{overall} = \Delta G^{\circ}_{duplex} + RT * [\ln(K_{MB}+1) + \ln(K_{target}+1)] \qquad (13)$$

$\Delta G^{\circ}_{overall}$:	overall free energy change of probe-target binding
$\Delta G^{\circ}_{duplex}$:	free energy change of nucleic acid duplex formation
K_{MB}:	equilibrium constant of MB opening.
K_{target}:	equilibrium constant of target secondary structure formation at the site of hybridization
T:	temperature (K).
R:	universal gas constant

The free energy gain of nucleic acid duplex formation ($\Delta G^{\circ}_{duplex}$) was calculated using the NN model with RNA-DNA heteroduplex parameters. The most stabile secondary structure and the corresponding free energy change associated with beacon structure formation (ΔG°_{MB}) were predicted by the use of the Zucker algorithm, as implemented in the

MFold program for ssDNA. The structure of the RNA target molecule in the RNA-MB complex, and in unbound form, i.e. in the presence and absence of MBs, can be predicted by MFold for ssRNA. The equilibrium constants in equation **(13)** were calculated from the respective predicted free energy values:

$$K_c = e^{-\Delta G^\circ_c / RT} \qquad (14)$$

K_c: Equilibrium constant of one of the component processes (K_{target} or K_{MB})
ΔG°_c: Free energy change of the component processes (ΔG°_{target} or ΔG°_{MB})

The thermodynamic parameters applied were determined in solutions with compositions largely different from that of NASBA reaction mixture. Therefore, for valid predictions, extrapolations were needed for the discrepancy in temperature and cation concentration. These factors, as parameters, were taken into account in a calculation by MFold for ssDNA. Also, correction factors were available for duplex stability calculations at various ion concentrations (equation **(5)**), and ΔG°_{duplex} at different temperatures could be derived from ΔH° and ΔS° (equation **(7)**). However, to our knowledge, no extrapolation is available for the calculation of ssRNA secondary structure stability for ionic concentration or temperature.

Since all the components of equation **(13)** ought to be extrapolated to the same conditions, two calculation methods were plausible. First, if all the components are taken into account, no correction is feasible. (Practically, a monovalent cation concentration of 0.9-1 M is assumed, the common medium for thermodynamic measurements, and a temperature of 37 °C.) Second, if the disruption of target molecule secondary structure in the probe complementary region is neglected, extrapolations for both the difference in ion concentration and temperature can be made. (Certainly, target secondary structure can, and should be considered at the design of an assay.) The simplified formula of equation **(13)** according to the latter calculation method:

$$\Delta G^\circ_{overall} = \Delta G^\circ_{duplex} + RT * [\ln(K_{MB}+1)] \qquad (15)$$

For the analyzed MB set (Table 4) calculations were carried out according to both formulas, and, after comparison to experimentally determined stability values, the method providing a better approximation was chosen.

4.3.2. Prediction and measurement of MB melting properties under NASBA-like conditions

Beside the difference in ion concentration and temperature, NASBA reaction mixture constitutes a unique environment for nucleic acid interactions in several other respects too. It contains a large amount of dimethylsuplhoxide (DMSO, 15%), sorbitol (375 mM), nucleotides (12 mM) and proteins (2.1 μg BSA and enzymes). DMSO and sorbitol were reported to lower the melting temperature (Musielski et al., 1981; Wang et al., 1993). We determined their effect for MB melting behavior experimentally, and correction formulas were derived.

MB melting curves were recorded in solutions containing various amount of DMSO. As expected, the MBs showed sigmoid curves, and the steepness of their slopes was found to be independent of DMSO concentration. However, DMSO caused a shift in the temperature range of the melting transition (Fig. 13A). By plotting the T_m of an MB as a function of DMSO concentration, the shift was found to be linearly dependent on concentration (Fig. 13B). The slope of the fitted linear was similar for the 10 MBs tested: 0.512 °C per % DMSO on average (standard deviation: 0.04145, data not shown), which is similar to results determined in a different system (Musielski et al., 1981). The influence of sorbitol on melting was also measured, and was found to be linear in the examined concentration range (0.003 °C per mM sorbitol, data not shown). Extrapolations for the presence of these two additives were incorporated into one correction formula.

$$\mathbf{T_m = T_{m\,(0\%DMSO,\ no\ sorbitol)} - 0.512 * D - 0.003 * B} \qquad \textbf{(16 a)}$$

T_m:	melting temperature (°C)
$T_{m\,(0\%DMSO,\ no\ sorbitol)}$:	T_m in assay solution without DMSO or sorbitol
D:	DMSO concentration (volume %)
B:	sorbitol concentration (mM)

Fig. 13A

Melting curves of MB-Nb in solutions containing 0-20 volume % DMSO. Fluorescent signals were normalized for maximum fluorescence measured at 80 °C.

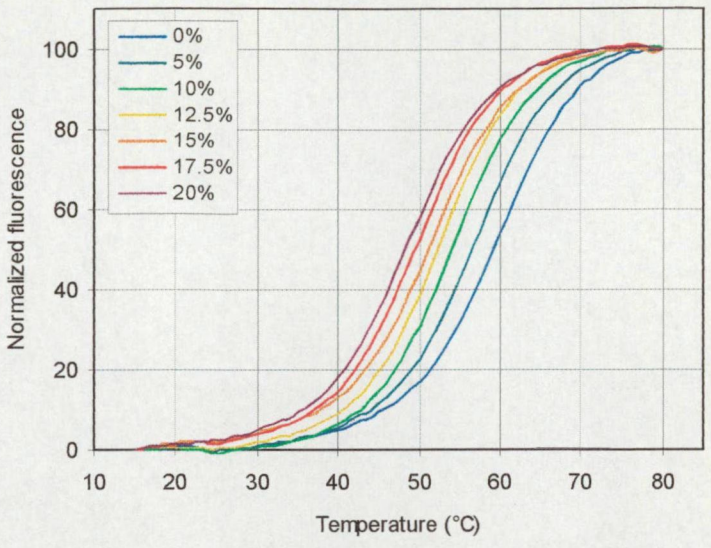

Fig. 13B

Dependence of the melting temperature (T_m) of MB-Nb on DMSO concentration.

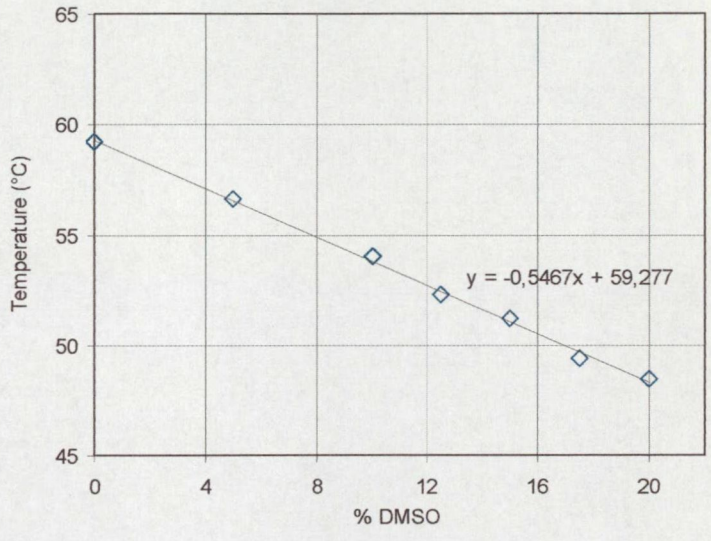

Fig. 14

Melting curves of MBO20b in NASBA reaction mix, and in solutions containing all the components of the reaction mix, except for the nucleotides and proteins.

Sample A contained 12 mM Mg^{2+}, which is the concentration present in the reaction mix, while sample B had only 0.7 mM. The latter concentration was found to simulate well the the effect of NASBA reaction mix on MB melting.

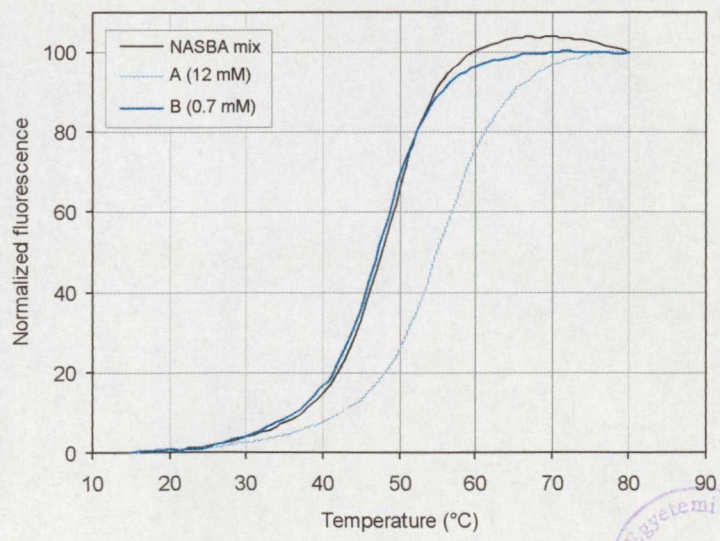

For the conditions of NASBA amplification:

$$T_{m\ (15\ \%\ DMSO,\ 375\ mM\ sorbitol)} = T_{m\ (0\ \%\ DMSO,\ no\ sorbitol)} - 8.805\ °C \qquad \textbf{(16 b)}$$

Since the slopes of the melting curves were found to be independent of DMSO concentration, the above-described formula provides a good approximation for other parts of the melting curve too. Notably, the normalized fluorescence of an MB in a solution containing DMSO and sorbitol can be extrapolated from that measured in the absence of these additives.

$$F_{(MB,T,\ 15\ \%\ DMSO,\ 375\ mM\ sorbitol)} = F_{(MB,\ T-8.805,\ 0\ \%\ DMSO,\ no\ sorbitol)} \qquad \textbf{(16 c)}$$

Normalized fluorescence is directly related to the K_{MB} (equation **(10)**), and thus to the free energy change associated with the transition.

$$\Delta G^{o}_{(T,\ 15\ \%\ DMSO,\ 375\ mM\ sorbitol)} = \Delta G^{o}_{(T+8.805,\ 0\ \%\ DMSO,\ no\ sorbitol)} \qquad \textbf{(16 d)}$$

The influence of nucleotides and proteins present in NASBA reaction mix was also evaluated. They were found to cause a substantial shift in the melting transition, similarly to the effect of DMSO, and this shift could be simulated well by reducing the Mg^{2+} concentration to 0.7 mM (Fig. 14). Since nucleotides were reported to chelate Mg^{2+} ions, and thereby reduce its effective concentration, it is plausible that this might have causal relationship with the experienced shift. The subsequent melting experiments were carried out in that solution containing reduced Mg^{2+} concentration, in the absence of nucleotides or proteins (NASBA-like conditions).

Taken together, MB melting under the conditions of AmpliDet RNA assay could be well simulated by extrapolation for DMSO and sorbitol, and by reducing the Mg^{2+} concentration to make up for the presence of nucleotides and proteins.

4.3.3. Experimental determination and prediction of melting temperature and the stability of the stem-and-loop structure for MBs

The T_m-s of MBs were determined as the temperature where half of the MBs were open, deduced from the normalized fluorescence signal. The equilibrium constants of the melting transitions were measured essentially as described by Bonnet et al., and the respective free energy values were calculated according to equation **(1)**.

The most stabile secondary structure of the MBs, their free energy values and melting temperatures were predicted by MFold, the parameters of which were set to simulate NASBA-like conditions. The effect of potassium ions was treated as equivalent to that of sodium ions (Rychlik et al., 1990). The parameters for MFold were: 70 mM Na^+, 0.7 mM Mg^{2+}, T = 50 °C (the corrected value of T would be equal to 49.805 according to formula **(16 b)**, which was rounded to 50, because only integers were allowed as input).

The predicted and experimentally determined T_m and $\Delta G°_{41}$ values ($\Delta G°$ of MB structure at 41 °C, which is the temperature of NASBA) were compared and plotted for 16 MBs (Table 4, Figs. 15A and B). Melting temperatures could be predicted with an average error of 2.842 °C, while $\Delta G°_{41}$ with 0.452 kcal/mol. Interestingly, the prediction of MBs with 4GC stems (possessing a 6-nucleotides-long stem sequence containing of 4 G/C and 2 A/T nucleotides) was much more accurate (average error for T_m: 1.785 °C, for $\Delta G°_{41}$ 0.208 kcal/mol) than those with 5GC stem (5 G/C and 1 A/T; average error for T_m: 4.201 °C and for $\Delta G°_{41}$ 0.766 kcal/mol). Actually, the values measured for MBs with 5GC stems were not more scattered than those for probes with 4GC stems; rather the free energies of the former were predicted systematically to be higher, especially for the most stabile MBs. The effect of loop length on beacon stability and melting temperature can also be observed: both of them decrease, although not in a linear fashion. For example, a difference of 3.3 °C and 0.675

No.	Name	Sequence	T_m(p)	T_m(e)	$\triangle G_{41}°$(p)	$\triangle G_{41}°$(e)
1	Na	GCAACC GGAAGTTTGGCTCGCTATG GGTTGC	49.76	48.0	-1,02	-0,96
2	Nb	CGTCCA CTAGAGAGGCACACATTCA TGGACG	48.96	45.0	-0,93	-0,89
3	Oa	GCTCTG TATGGTTTAATTCGAAATCTGC AGAGC	45.16	45.0	-0,42	-0,65
4	Ob	GCAGCA GTTTAGCGCGTTATGCCTTTG CTGC	50.86	51.0	-1,24	-1,59
5	Fus	CGACGT GATGGAGAACTGGATGGT ACGTCG	49.96	45.8	-1,06	-0,67
6	ArMV	GCAGGT GATGGAACTCATAAGGTGTA CCTGC	49.06	51.6	-0,92	-0,75
7	ASPV	GCTCCA ACGCAAAGCATGTCTGGAAC TGGAGC	46.26	44.0	-0,53	-0,49
8	O20b	CGACGT TGAGGTCACATCACGAACAC ACGTCG	47.96	48.0	-0,79	-1,00
9	O19b	CGAGC TGAGGTCACATCACGAACA AGCTCG	49.66	50.7	-1,01	-1,39
10	Cms2	CCGTGC ATGTGCGCCCCCCAAG CACGG	60.16	55.06	-2,54	-1,83
11	Cms1	GCCAGG AACGTGCAGAGATGTGCGCCCC TGGC	57.46	51.0	-3,67	-1,41
12	Rs	CCAGGC AAAGACTAGCTAATA GCCTGG	59.06	51.5	-2,16	-1,36
13	O19	CGGAGC ATGAGGTCACATCACGAAC GCTCCG	55.46	52.8	-1,78	-1,62
14	O21	CGGAGC ATGAGGTCACATCACGAACAC GCTCCG	53.96	50.3	-1,57	-0,83
15	O22	CGGAGC ATGAGGTCACATCACGAACACC GCTCCG	53.26	50.0	-1,47	-1,02
16	O25	CGGAGC TATGAGGTCACATCACGAACACCAG GCTCCG	50.16	49.5	-1,13	-0,86

Table 4

Comparison of the predicted and the experimentally determined melting temperatures and free energy values of MB secondary structures. Within the MB sequences, the hybridizing parts are separated by spaces, while the stem portions are indicated by underlines. Except for the TET-labeled ArMV, all the MBs carried FAM as a fluorophore. In each case, DABCYL was applied as a quencher, attached to the 3' end of the probe.

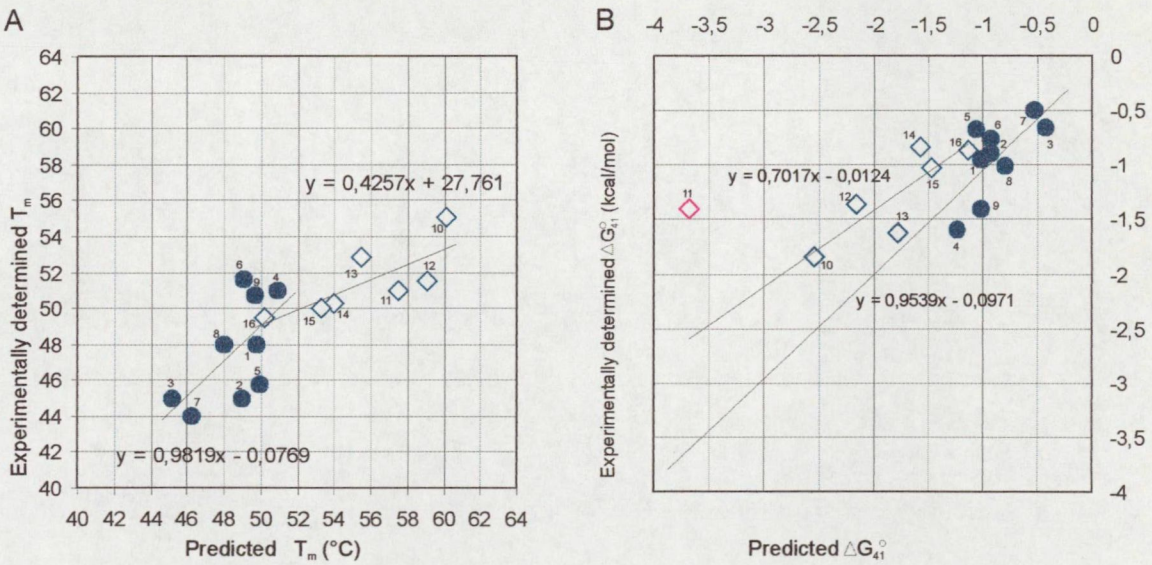

Fig. 15

Comparison of the predicted and experimentally determined melting temperatures (**A**) and free energy changes associated with beacon structure formation (**B**). The numbers identify the MBs according to Table 4. The T_m and $\triangle G°_{41}$ values of MBs with 4GC stems are shown by filled circles, while those with 5GC stems by open rhombi. The pink rhombus shows an MB with largely deviating free energy values, which was not taken into account for the calculation of the trendline.

kcal/mol was measured between the T_m and the $\Delta G°_{41}$ of MBs O19 and O25, respectively, which possessed the same stem structure and had overlapping hybridizing parts.

4.3.4. Prediction and experimental determination of the stability of MB-target interaction

The free energy change accompanying MB-RNA target association was approximated according to formulas **(13)** and **(15)**. K_{MB} was calculated from the free energy values predicted by MFold, as described in the previous section. The free energy gain from duplex formation was approximated by the NN model by applying formulas **(7)** and **(5)** for extrapolations for temperature and monovalent cation concentration, respectively. The effect of Mg^{2+} ions on duplex stability was stated to be 140 times stronger than that of Na^+ ions (Nakano et al., 1999), and it was taken into account accordingly. The influence of DMSO and sorbitol on nucleic acid duplex stability was assumed to be similar to the effect determined for MB melting, and the same correction formula **(16 d)** was applied.

The binding constants of MB-RNA interactions were determined in the presence of six-fold target molecule excess, as described by Bonnet et al. The length of target RNA molecules ranged from 174 to 252 nucleotides, representing NASBA amplicons, so that the binding properties of MBs in a real assay could be well simulated. The measured values represented overall free energy values, since we determined the equilibrium constant of the binding of closed MBs to structured target molecules.

The experimentally determined free energy values were compared to those calculated according to equations **(13)** and **(15)**. The latter formula gave substantially better correlation, which is shown in Table 8 and Fig. 16A (the results according to formula **(13)** are not shown). The predicted values and the experimental data were in good agreement, with 1.16 kcal/mol average discrepancy, excluding the four extreme data points. These latter were neglected, because their measured fluorescence signals were very close to the limits of the method applied, not enabling reliable calculation. However, they represented good, working MBs,

No.	Name	$\triangle G^{\circ}_{o,41}(p)$	$\triangle G^{\circ}_{o,41}(e)$
1	Na	-11,92	-10,36
2	Nb	-9,33	-9,93
3	Oa	-8,08	-8,55
4	Ob	-14,55	-11,98
5	Fus	-9,05	-9,62
6	ArMV	-8,62	-9,54
7	ASPV	-9,92	-9,83
8	O20b	-9,02	-10,76
9	O19b	-8,27	-10,01
12	Rs	-0,47	-7,44
13	O19	-7,23	-9,24
14	O21	-8,71	-10,67
15	O22	-11,07	-12,09
16	O25	-12,55	-11,39

Table 8

Comparison of the predicted and measured overall free energy values associated with the hybridization of closed MB probes to perfectly matching RNA target molecules (expressed in kcal/mol).

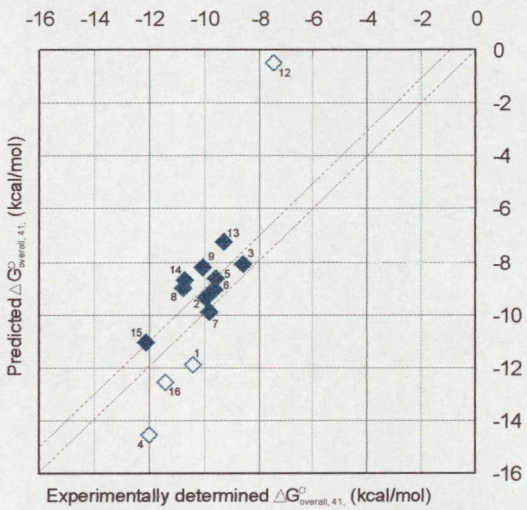

Fig. 16

Predicted and experimentally determined overall free energy change values of MB - target RNA interaction. The data points indicated by filled rhombi were used for the evaluation of the prediction method. (for details see the text). The line above the theoretical diagonal indicates a minor, systematic over-prediction, which might be taken into account in calculations.

therefore they were included in the figure. The predicted free energies appeared to be systematically higher than the experimentally determined values. If a shift of 0.95 kcal/mol is considered, as shown on Fig. 16, the average error becomes only 0.605 kcal/mol between the measured and 'corrected' data sets.

4.3.5. Specificity of MBs in AmpliDet RNA assay

Specificity indicates the degree to which a probe can interact with targets containing minor differences, like single nucleotide substitutions, in the probe-complementary regions. Different mismatching nucleotide pairs were reported to destabilize nucleic acid duplexes to different degrees. The NN model was found valid for DNA-DNA duplexes containing single, internal mismatches, and their parameters were determined. The validity of the NN theory for mismatching duplexes together with the results reported by Bonnet and colleagues indicate that

the effect of the location of the mismatch is negligible on duplex destabilization, provided that it is not in ultimate or penultimate position. Nevertheless, to characterize beacon specificity with each type of mismatch, a great number of mutant target RNA molecules would have had to be synthesized. Since it was not practically feasible, we decided to determine the range of this destabilizing effect, by the characterization of mismatch types that are expected to belong to the most stabile and to the least stabile ones, respectively, as deduced from DNA-DNA mismatch NN parameters. Accordingly, dT-rG, dG-rU and dG-rG pairs are expected to be relatively stabile, since they can form hydrogen bonds with each other (Allawi and SantaLucia, 1997). In general, a GC rich environment also has a stabilizing effect. In contrast, mismatch pairs formed by cytosine with another cytosine or other nucleotides belong to the least stabile type (see the NN parameters for mismatching duplexes).

To characterize the specificity of MBs in AmpliDet RNA assay, a test system with a set of MBs and with three sets of complementary RNA molecules (R0, R1 and R2 sets) was created, as shown in Table 6. Six MBs with hybridizing regions of 19-25 nucleotides were synthesized. Four of them had identical, 5GC stem sequences, while the other two possessed 4GC stems. Their specificities were evaluated with a perfectly matching target, and two sets of target RNA molecules differing only in a single nucleotide within the target regions of the MBs (Table 9).

The beacons with loop length of 19 nucleotides (O19 and O19b) were found to be point mutation specific with all the tested mismatching targets (Fig. 17A and Table 9). MBs with loop lengths of 20 (O20b) and 21 (O21) nucleotides tolerated the mismatches that had been predicted to be stabile, however, their signals in AmpliDet RNA with template RNAs of the R2 set, as could be expected, were close to that of the negative control (Fig. 17B). The two longest MBs (O22 and O25) tolerated all the tested single mismatches, although to

Name	Sequence
MB O19b	5′ FAM-CGAGC TGAGGTCACATCACGAACA AGCTCG-D 3′
MB O20b	5′ FAM-CGACGT TGAGGTCACATCACGAACAC ACGTCG-D 3′
MB O19	5′ FAM-CGGAGC ATGAGGTCACATCACGAAC GCTCCG-D 3′
MB O21	5′ FAM-CGGAGC ATGAGGTCACATCACGAACAC GCTCCG-D 3′
MB O21-P	5′ FAM-CGGAGC ATGAGGTCAPATCACGAACAC GCTCCG-D 3′
MB O21-I	5′ FAM-CGGAGC ATGAGGTCAKATCACGAACAC GCTCCG-D 3′
MB O21-K	5′ FAM-CGGAGC ATGAGGTCAIATCACGAACAC GCTCCG-D 3′
MB O22	5′ FAM-CGGAGC ATGAGGTCACATCACGAACACC GCTCCG-D 3′
MB O22-P	5′ FAM-CGGAGC ATGAGGTCAPATCACGAACACC GCTCCG-D 3′
MB O22-I	5′ FAM-CGGAGC ATGAGGTCAKATCACGAACACC GCTCCG-D 3′
MB O22-K	5′ FAM-CGGAGC ATGAGGTCAIATCACGAACACC GCTCCG-D 3′
MB O25	5′ FAM-CGGAGC TATGAGGTCACATCACGAACACCAG GCTCCG-D 3′
R0	3′.GAAAACUGAAAAUACUCCAGUGUAGUGCUUGUGGUCACUCCCGAU.5′
R1-U	3′.GAAAACUGAAAAUACUCCUGUGUAGUGCUUGUGGUCACUCCCGAU.5′
R1-G	3′.GAAAACUGAAAAUACUCCGGUGUAGUGCUUGUGGUCACUCCCGAU.5′
R1-C	3′.GAAAACUGAAAAUACUCCCGUGUAGUGCUUGUGGUCACUCCCGAU.5′
R2-A	3′.GAAAACUGAAAAUACUCCAGUAUAGUGCUUGUGGUCACUCCCGAU.5′
R2-U	3′.GAAAACUGAAAAUACUCCAGUUUAGUGCUUGUGGUCACUCCCGAU.5′
R2-C	3′.GAAAACUGAAAAUACUCCAGUCUAGUGCUUGUGGUCACUCCCGAU.5′

Table 6

MB set with a perfectly matching target molecule (R0) and two sets of RNA molecules (R1 and R2), containing a substitution in the MB target region (shown in red). The hybridizing sequences of the MBs are separated by spaces from the rest of the MB sequence. The stem structures are indicated by underlines. All the MBs carried FAM as a fluorescent moiety and DABCYL (D) as a quencher. The MBs had overlapping hybridizing sequences of differing lengths from 19 to 25 nucleotides. Two of them possessed 4GC stems, while four MBs had identical, 5GC stem sequences.

The complementary RNA molecules were 212 nucleotides-long; the region of 60-104 nucleotides is shown, from the 3' end to the 5' to indicate the MB-complementary region.

The R1 RNA molecules could form relatively stabile mismatching duplexes with MBs, because the variable position was in a GC rich environment. Furthermore, the guanine of R1-G could form base pairs with the corresponding T of the MBs. The variable position in the R2 set was in an AU rich neighborhood. In the corresponding position of the MBs, a cytosine was located, which had been stated to form the least stabile mismatches in the case of DNA-DNA duplexes. Thus the MBs were expected to bind with significantly less stability to the members of the R2 RNA set.

The nucleotide analogues were incorporated into the MBs in a position complementary to the variable nucleotide of the R2 RNA set (shown in blue, for the abbreviations see the text).

MB/template	R0	R1-U	R1-G	R1-C	R2-U	R2-A	R2-C
O19	++	-	-	-	-	-	-
O19b	+++	-	-	-	-	-	-
O20b	+++	++	+++	+	-	-	-
O21	+++	++	++	+	-	+/-	-
O21-I	-	nt	nt	nt	-	-	-
O21-K	-	nt	nt	nt	-	-	-
O21-P	+++	nt	nt	nt	+/-	+++	+
O22	+++	+++	+++	+++	++	+++	+
O22-I	-	nt	nt	nt	-	-	-
O22-K	-	nt	nt	nt	-	-	-
O22-P	+++	nt	nt	nt	+	+++	++
O25	+++	+++	+++	+++	++	+++	+

Table 9

Mismatch tolerance vs. point mutation specificity of MBs in an AmpliDet RNA assay. NASBA was carried out with constant amount of template molecules (the RNA used as template is shown in the head of the columns), in the presence of one or other member of the MB set (rows). Signal strength was evaluated as the ratio of MB fluorescence with the perfectly matching template. For O19, even the signal with R0 was evaluated as moderately strong, because it was significantly lower than the fluorescence of any of the other MBs with R0. For the analogue-containing MBs, the fluorescence of the corresponding probe without analogue was considered as 1.

- No signal (< 0.2)

+/- Very weak signal (0.2 – 0.3)

\+ Weak signal (0.3 – 0.5)

++ Moderately strong signal (0.5 – 0.7)

+++ Strong signal (0.7 <)

nt Not tested (The analogues were incorporated into a position complementary to the variable nucleotide of the R2 RNA set. Thus, with the members of the R1 mutant set the analogue-containing MBs would possess an additional mismatch, the effect of which was not tested.)

Fig. 17

Real time monitoring of MB signals with perfectly matching and mismatching target RNA molecules in AmpliDet RNA reaction. The signals are shown as the ratio of the fluorescence of the MB with R0. For the sequences, see the text.

A: MB O19b, a point mutation specific MB

B: MB O21 tolerates only the expected relatively stabile mismatches.

C: MB O22: a mismatch tolerant MB

Fig.18

Signals of a universal pyrimidine-containing MB (MB O21-P).

The signals of MB O21 with the members of the R2 RNA set, and with the perfectly matching target (R0) are also shown, and the latter was used for normalizaton (= 1).

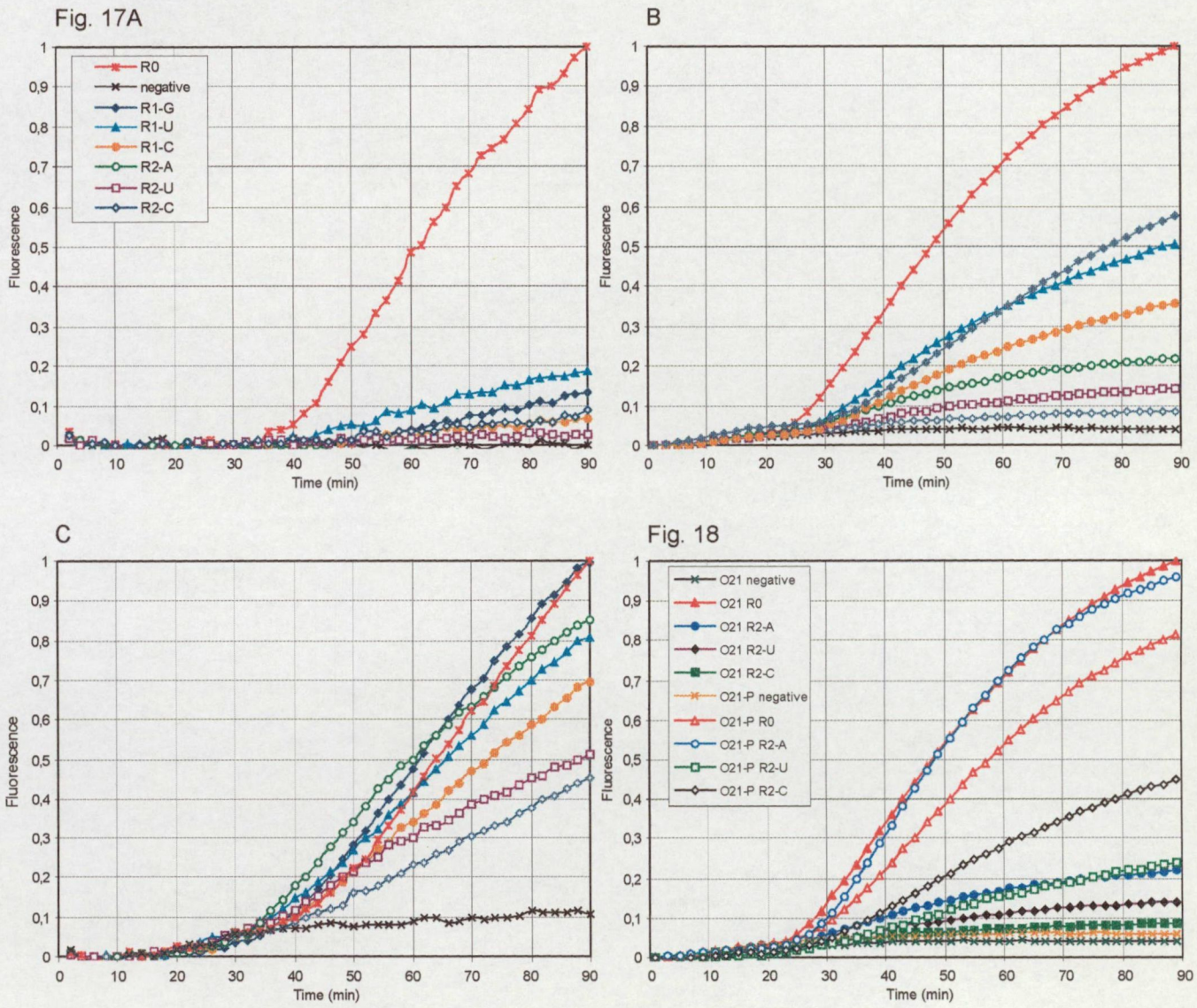

different degrees (Fig. 17C). Mutations, especially the strongly destabilizing ones, resulted in a reduced signal in both cases. Interestingly, R2-A proved to be a relatively good target, which could not be predicted on the basis of the mismatch NN parameters.

The mismatch tolerance of nucleic acid probes can be increased by the incorporation of nucleotide analogues opposite to the polymorphic position in the target molecule. We tested inosine (I), universal pyrimidine (P) and universal purine (K) nucleotide analogues for this purpose. The analogues were incorporated into MBs O21 and O22, opposite to the variable position of the R2 RNA set, which contained the more destabilizing substitutions. The I and K analogues did not increase significantly the mismatch tolerance of MBs (Table 8). Universal pyrimidine, however, greatly enhanced the stability of MB binding to the mismatching target RNAs: both dP-rA and dP-rG interactions were significantly more stabile than dC-rA (Fig. 18). The signals of P-containing MBs (O21-P and O22-P) with target RNAs having either A or G in the variable position (R2-A and R0) were high, comparable to that of the analogue-less MB with the perfectly matching target (Table 8).

4. Discussion

Plant viruses are deleterious, highly adaptive and fast-changing pathogens. The diagnostic processes and the control measures should likewise be fast, adaptive and flexible. The viral objects of this study, *Plum pox virus* and *Potato virus Y*, are among the most wide-spread and harmful viral pests: they are quarantine pathogens, and the effected areas are still expanding.

Biological sciences, among them molecular biology, provided many efficient tools for experts in the field of plant protection; in fact, entire interdisciplinary fields were established. The aim of the studies presented in this thesis was to design and develop novel nucleic acid amplification-based diagnostic methods for the above-mentioned plant viruses. In addition, we attempted to establish design principles for molecular beacon probes for AmpliDet RNA assay, which might be of help in the process of assay design.

The assays developed are complex diagnostic procedures, serving for both the detection and typing of the targeted viruses. The viral subgroups were defined mostly on the basis of biological (in case of PVY), or serological and biological properties (for PPV), previously. Since the pathogenicity-determining genomic regions have not been identified for any of the targeted viral types to date, extensive sequence analyses were performed for the selection of potential diagnostic regions.

In assay design, we followed similar strategies in both cases. Generic (i.e. virus-specific) amplification was achieved via virus-specific oligonucleotide primers binding to conserved regions, and the type of the detected isolate was identified via subgroup-specific oligonucleotide primers or probes.

In the case of PPV, the presumed location of the antigenic determinants was taken into account, since the strains were defined, at least partially, on the basis of distinct serological properties, and most of the strain-specific epitopes were mapped to the 5' portion of the CP

coding region. Therefore, our nucleic acid sequence-based assay was also targeted to this part of the genome; more precisely, to the nucleic acid sequences corresponding to the identified strain-specific amino acid patterns. The conserved parts of the CP coding region allowed the selection of PPV-specific sequences for generic detection.

In the case of PVY, a rearrangement within the CP coding region was associated with the tuber necrotic isolates. Further, the strains were reported to be serologically distinct, although they did not separate perfectly. To assess the potential diagnostic value of the CP coding region, and to explore the sequence-based relationships between different PVY isolates, the publicly available sequences were compared. Phylogenetic analyses were carried out on shorter alignment sections. The area of the presumed recombination point was selected as diagnostic region, enabling the separation of the chimerical PVY^{NTN} isolates, and the viruses belonging to the two main clusters, mostly corresponding to the PVY^{N} and $PVY^{O/C}$ biological strains. The exceptions were few PVY^{N} isolates that had CP sequences similar to PVY^{O}. These viruses, however, would also be diagnosed as PVY^{O} by other assays detecting specific features of the coat protein, like serological methods and the recently developed RT-PCR method (Walsh et al., 2001).

For the development of the above-mentioned assays, two nucleic acid amplification methods were applied: integrated RT-PCR/nested PCR (for PPV) and multiplex AmpliDet RNA (for PVY). Both methods provide high specificity, and their sensitivity approaches the theoretical limit. They are complex diagnostic techniques, suitable for detection and differentiation, and amenable for high-throughput screening. For PPV, the presence of the virus can be detected, and the strain of the infecting isolate can be identified in two rounds of PCR. The application of nested reactions for strain-specific diagnosis increases the sensitivity of the assay. Via the AmpliDet RNA assay developed, cluster-specific PVY detection can be achieved in a single, closed-tube reaction, within 2 hours. The application of homogeneous

detection reduces the risk of carry-over contamination and eliminates the labor-intensive post-amplification analysis.

The specificity of the oligonucleotide primers designed for the detection of PPV strains was demonstrated by using biologically and serologically characterized viral isolates, or cloned cDNAs, as template. Under these conditions, the primers were found to be perfectly specific for their cognate target sequences.

The performance of the assay was assessed by the simultaneous detection and differentiation of numerous PPV isolates, collected mainly in Hungary, by three different methods: two overlapping subsets of the 92 isolates tested were also typed by ELISA and RsaI-RFLP. In 76.4% of the cases, ELISA and PCR provided identical results, while in 20.2%, ELISA detected one of the strains indicated by PCR (consistent result). The two methods gave contradictory strain identification only in the case of one isolate; in this exceptional case the independent RFLP analysis supported the result of PCR. Typing by our method and by RFLP showed excellent correlation: diagnoses in the case of 91.3% of the samples were identical, while in the remaining cases consistent. The good overall correlations between the three independent diagnostic approaches suggest that the selected patterns were suitable as diagnostic regions for strain-specific detection, and that the sequences available in the databank represented well the molecular variability of the CP coding region of PPV, at least that of the sequences of isolates originating from Europe and Egypt. Consistent results, in each case, meant that ELISA (or RFLP) detected only one of the strains indicated by PCR. It is very unlikely that the product accumulation in more than one nested reactions was due to the relaxed specificity of the differentiating primers, since they worked with great specificity with well-characterized samples. Also, 75% of the field samples gave a single, characteristic PCR product in only one of the nested reactions, with no background. It is more likely that

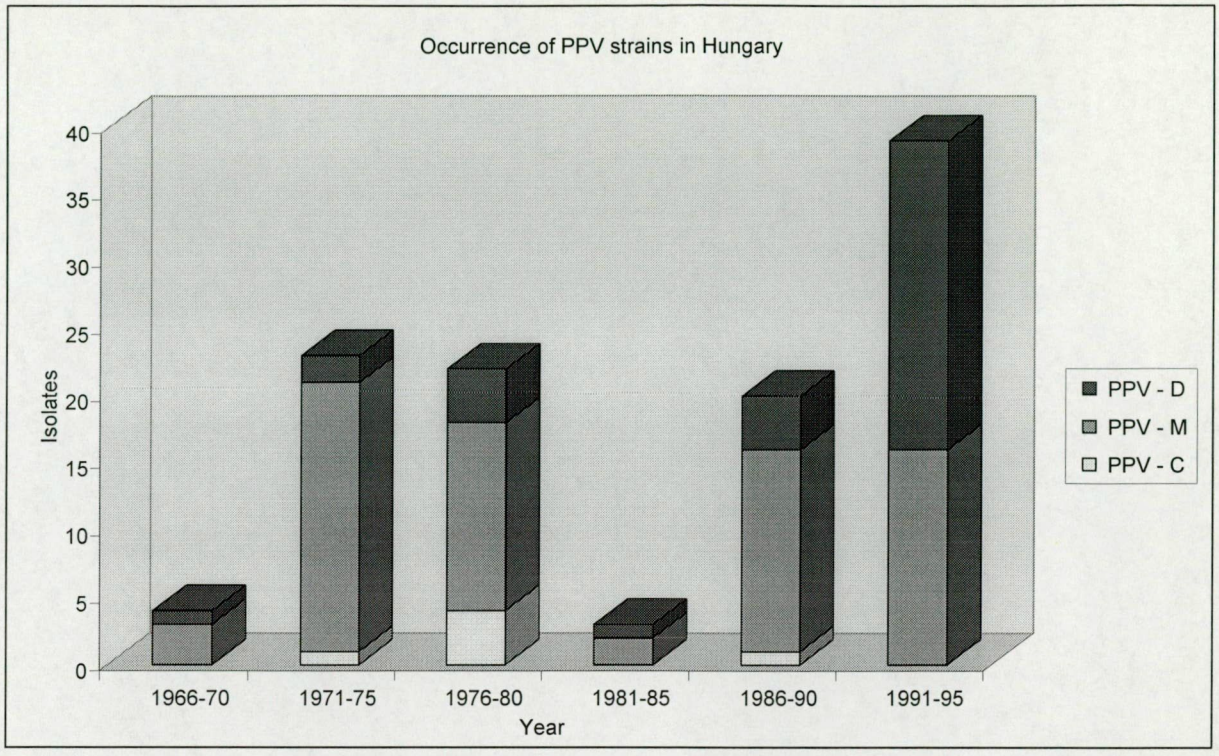

Fig. 19

Occurrence of different PPV strains among the isolates collected in Hungary from 1966 until 1995, as identified by the integrated RT-PCR/nested PCR method, either as a single infecting virus or as a component of a mixed infection. The columns represent summations of the occurrences for 5-year periods.

these cases represent mixed infections, which might have been missed by ELISA (or RFLP) because of the lower sensitivity of these methods.

An unexpected outcome was the observation of a surprisingly high incidence of the PPV-D strain in Hungary (Fig. 19). A striking feature was the temporal distribution of the numbers of PPV-D viruses collected. It was detected in 9 of 50 isolates collected up to 1986, by PCR (18%), only one of which contained this type as a single infecting virus. ELISA did not indicate the presence of PPV-D in this subset of isolates, which is, perhaps, not surprising since most of these isolates had PPV-M as a major and PPV-D as a minor component, as indicated by the relative amounts of the PCR products.

Among the 35 isolates collected between 1991 and 1995, PPV-D was detected in 23 cases by PCR (65.7%) and in 20 cases by ELISA. This huge increase in the incidence of PPV-D coincides with the political and economic changes in Hungary, and suggests that PPV-D

was 'imported' into Hungary by uncontrolled propagating materials in this period, during which plant sanitary regulations were not enforced as strictly as previously. The results are in good agreement with earlier reports of an increasing PPV-D incidence in Hungary among isolates collected after 1995 (Pribék and Gáborjányi, 1997; Pribék et al., 1998).

The AmpliDet RNA assay developed for the detection and typing of PVY consists in a generic NASBA amplification followed by strain-specific identification by 4 MBs: 2 MBs recognize PVY^{N}, and two $PVY^{O/C}$-specific sequences, while the chimerical PVY^{NTN} isolates are signaled by a PVY^{N}- and a $PVY^{O/C}$-specific probe. Assay performance was evaluated by using RNAs of biologically characterized viruses as templates. The method was found to be perfectly specific for the targeted PVY clusters; the MBs gave signals only with their respective target molecules. Artificially mixed infections could also be diagnosed successfully.

The PVY genome contains several variable positions within the MB target regions. In the course of MB design, different strategies were followed to make the probes tolerant to the known sequence polymorphisms: MB-N1 was degenerated in one position, and two universal pyrimidine (P) nucleotides were incorporated into MB-O1. The mismatch tolerance of the MBs was tested by using isolates containing a mutation in the target regions. All mismatches but one were tolerated, and the presence of the substitution was indicated by reduced signals. The one exception was an A/G transition affecting the hybridization site of MB-O1, which contained two P analogues. Universal pyrimidines were earlier reported to bind less efficiently to guanines than to adenines (Hill et al., 1998) and, incidentally, the amplicon of the mutant isolate contained guanines as hybridizing counterparts to P in both positions. We assume that this additional destabilizing of the probe-target duplex contributed to the lack of MB binding in this case. As a result, some PVY^{C} isolates do not give a signal with MB-O1; they are detected solely via MB-O2. In fact, the signals of PVY^{C} isolates are quite

characteristic: a reduced MB-O2 signal with or without MB-O1. Since the probes were shown to produce positive, but reduced signals with isolates containing a single mismatch, the use of MBs not only enables the detection of the viral types, but would also indicate polymorphisms in the MB target regions, which span approximately 40 nucleotides.

The combination of generic oligonucleotide primers and group-specific MBs offers a convenient means of multiplex detection. The number of MBs used in a single assay is primarily limited by the ability to distinguish between the fluorescent signals of the different dyes. In the assay developed 4 MBs were used and their signals could be distinguished perfectly. Two MBs bound to each amplicon RNA, and it was found that the assay retained sufficient sensitivity for diagnostic purposes, although the sensitivity of NASBA was lowered.

The assay was validated by testing 47 PVY isolates originating from 6 countries. With the exception of one isolate, all were detected successfully, among them 27 PVY^{NTN}, 9 PVY^{N}, 8 PVY^{O} and 2 PVY^{C} viruses. The exceptional isolate (53-47) belonged in the PVY^{NTN} group and gave signals characteristic of PVY^{N}.

Since the completion of the experimental phase of the present study, a number of PVY CP coding sequences, representing isolates from various countries, have been submitted to GenBank. The analysis of these sequences indicated that the assay developed would correctly identify the newly described PVY^{N}, PVY^{O} and PVY^{C} isolates. Some PVY^{NTN} isolates, however, did not contain the characteristic rearrangement targeted, thus they would be mis-typed. These isolates had distinct geographical distribution, originating from North America, Northern-Europe and Japan. It is noticeable that the exceptional PVY^{NTN} isolate that failed to give an NTN-specific signal in our assay originated also from Northern-Europe (Denmark). The polymorphism of tuber necrotic isolates is not without an example: the distinct biological features and nucleic acid patterns in the P1 coding region of North American PVY^{NTN} viruses

were also reported (McDonald and Singh, 1996; Weilguny and Singh, 1998). Therefore, we suggest that the chimerical nature of the PVY^{NTN} CP merely correlates, but does not have a causal relationship with the phenotype. Nevertheless, the diagnostic procedure described would identify most of the PVY^{NTN} viruses, mainly the ones originating from Europe.

Any diagnosis is only as good as the information on the basis of which it was designed. Our knowledge about the molecular variability of these viruses, and the consequences of the sequence polymorphisms for their biological and epidemiological properties is far from complete. Nevertheless, the assays developed provide sensitive and specific tools for large-scale virus detection and typing, keeping in mind that the biological and molecular properties might not correlate perfectly. These assays serve not only as tools for routine screenings, but also for extensive epidemiological analyses, which may help to characterize better these viruses, and their subgroups, and to improve our knowledge about them by identifying exceptional, divergent isolates.

The third study described in this thesis deals with the characterization of MB probe behavior in AmpliDet RNA assay. We attempted to establish and validate a prediction method for MB design, which could be reliably used for practical purposes. The study focused on nucleic acid interactions under the conditions of AmpliDet RNA assay, which is unique due to the preset composition of the reaction mixture, and because of the special properties of RNA-DNA heteroduplex formation. It was necessitated because the melting behavior of oligonucleotides under the conditions of NASBA was not well characterized.

Beacon properties important for target molecule detection, such as signal strength and background fluorescence, are directly related to the equilibrium constants of MB-RNA binding, and to that of the opening of the stem-and-loop structure, respectively. In this study, these equilibrium constants and the corresponding free energy values of the transitions were predicted and determined experimentally for a set of MBs and their target RNA molecules.

The validity of the proposed prediction methods was evaluated by comparing the predicted and measured values.

MB structure, its melting temperature and the associated free energy changes were predicted by using the MFold program for ssDNA. The stability of MB-RNA interaction was approximated by applying a modified version of the model proposed by Matthews et al. for the characterization of the binding of structured probes to structured target molecules. Since, in the case of MBs, bimolecular probe-probe interactions are not favored kinetically, the formula presented could be simplified, and thus an approximation in the calculation was eliminated. The component accounting for the structural changes of the target molecule was not taken into account, because no extrapolations were available for the difference in cation concentrations and temperature for ssRNA secondary structure prediction. Free energy change accompanying duplex formation was approximated using the NN model with parameters for RNA-DNA heteroduplex. The free energy changes of these transitions were extrapolated for the ion concentrations of NASBA reaction mix, and the temperature of the assay. The effects of the additives for which no correction were available were determined experimentally, and were taken into account accordingly.

The melting temperatures and the free energy changes of MB structure formation at 41 °C could be predicted with an average error of 2.842 °C and 0.452 kcal/mol, respectively. MBs with 6 nucleotide-long stems containing 4 or 5 GC-s performed equally well; the predictions were, however much more accurate for MBs with 4GC stems (average error for T_m 1.785 °C, for $\Delta G°_{41}$ 0.208 kcal/mol). As expected, MBs with 5GC stem sequences were generally more, while probes with longer loop sequence were less stabile. In general, the range of the free energy values of the stem-opening for good, working MBs (at least the range that we could explore) was found wide: from -0.53 to -1.83 kcal/mol, although the MBs with

ΔG°_{41} more than -1 kcal/mol had higher background fluorescence at 41 °C (> 15 %, unpublished results).

To characterize MB-target hybridization, the equilibrium constants of the binding of MBs to target RNAs were determined. The overall free energy changes could be well approximated, with an average error of 1.16 kcal/mol (about 10%). It can be regarded as a good prediction, provided the complexity of the experimental system. Further, the predictions of the components that contribute to the overall free energy change are associated with a certain limit of precision too. For example, the NN model with RNA-DNA parameters gave predictions for ΔG°_{37} within 6% error in a substantially less complex system (Sugimoto et al., 1995).

The free energy range of MB-target interactions of well-performing probes was found wide. The upper 'limit' seems to be around -8.5 kcal/mol, which characterized MBs with relatively weak signal. No conclusion concerning the lower limit can be made on the basis of our experiments. In general, the predicted free energy values were higher than the measured ones (by approximately 1 kcal/mol), which could be taken into account in assay design.

In this study, NASBA amplicon RNAs with lengths of a few hundred nucleotides were used as target molecules, so that the measured values would characterize well MB binding in an AmpliDet RNA assay. In such a complex system two-state transition, which is implicitly presumed in the usage of the NN theory, cannot be supposed. However, the NN model was successfully and extensively used in other complex systems, like for T_m calculation of oligonucleotide primers for PCR. Also, the NN theory could enable to take into account the specific features of RNA-DNA heteroduplexes.

To study the relationship between the stability of MB-RNA interaction and the specificity of an MB probe in AmpliDet RNA assay, an experimental system was created. To exclude potential variability deriving from the difference of secondary structure of the target

RNA molecule, or from that of the probe, a set of MBs with uniform hybridizing regions of increasing lengths were synthesized. Their specificities were evaluated in AmpliDet RNA assay using perfectly matching and mutant RNA molecules as template. Studies with DNA-DNA duplexes containing single mismatches demonstrated that, depending on the types of the mismatching bases, they may stabilize or destabilize the duplex to various degrees. Since a similar phenomenon can be reasonably expected for RNA-DNA heteroduplexes, two different mutant RNA sets were created: one is expected to represent the most stabile mismatches, and a second for the expectedly least stabile ones.

All the members of the MB set were found suitable for the detection of the complementary target, however they reacted very differently with the mismatching targets. As expected, the signals of MBs with the first mutant set were significantly higher than those with the second RNA set. An exception was found too: a heteroduplex with dC-rA mismatch resulted in a relatively strong binding.

The tolerance of MBs towards mismatches increased with the length of the hybridizing region. The shortest MBs (19 nucleotide target complementary region, $\Delta G°_{41,exp}$: -9.24 and -10.01 kcal/mol) 'rejected' all mutant targets, including the members of the first set. MBs with 20 and 21 nucleotide-long hybridizing regions ($\Delta G°_{41,exp}$: -10.76 and -10.67 kcal/mol) tolerated the mismatches with the first RNA set (which formed the more stabile mismatching pairs), but the molecules of the second set were not bound. MBs with hybridizing parts of 22 nucleotides or more ($\Delta G°_{41,exp}$: -12.09 and -11.39 kcal/mol) could tolerate all the mismatches tested. These experiments demonstrated that MB probes can detect readily relatively stabile mismatches in AmpliDet RNA assay, and that continuity exists between point mutation specificity and mismatch tolerance The free energy values characterizing the binding of the probes studied are indicative, although the examined set is too small and not representative for a generally reliable conclusion. Mismatches, even in the

case of relatively long MBs, may cause reduced signal. This phenomenon could be utilized for discriminating between target molecules with small polymorphisms, resulting in different mismatch types.

The possibility to increase the mismatch tolerance of MBs with base analogues was also examined. The analogues were incorporated into the probes in a position opposite to the variable nucleotide of the second mutant RNA set. Of the molecules tested, only universal pyrimidine (P) was found to increase significantly the tolerance of MBs: the pairing of P with both A and G allowed a signal strength comparable to that of an MB with the perfectly matching target. Interestingly, the pairing of P with the presumably non-cognate, pyrimidine nucleotides also confers greater stability, i.e. results in higher fluorescent signal. Although, it may well indicate only that C, the nucleotide substituted by P, forms the least stabile mismatch pairs.

Taken together, the comparison of predicted and experimentally determined melting temperatures and stability values showed that the presented approach provides reliable prediction for MBs in AmpliDet RNA assay, and within a reasonable limit of error. MB specificity, the tolerance or rejection of mutant target molecules, in function of hybridizing region length or the free energy change associated with the binding, was assessed. The incorporation of universal pyrimidine promises to be a good strategy to increase MB tolerance of a C/U polymorphism (which results in an A/G variation in the NASBA amplicon), the good performance of which was also demonstrated by MB-O1 (AmpliDet RNA assay for PVY typing), which contained two P analogues. Since all the experiments were carried out in NASBA-like, or NASBA reaction mixture, the results can be easily extrapolated and utilized for MB design for AmpliDet RNA assay.

Summary

Novel nucleic acid amplification-based diagnostic techniques were developed for the detection and characterization of two economically important plant viruses: *Plum pox virus* (PPV) and *Potato virus Y* (PVY). Both of them are deleterious and widespread pathogens, therefore plant propagation materials have to be routinely screened to ensure their virus-free state. The assays developed provide high specificity and sensitivity, and are suitable for high-throughput analysis. In addition, we have proposed a novel prediction principle and technique to assist the design of the molecular beacon probes (MB) to be used in AmpliDet RNA assay, based on thermodynamic models. The range of MB specificity under assay conditions was characterized.

For the simultaneous detection of PPV and the separation of its strains, (PPV-D, PPV-M, PPV-EA and PPV-C) an RT-PCR/nested PCR method was developed. Within the N-terminal portion of the coat protein (CP), which had been reported to carry the major antigenic determinants, amino acid patterns characteristic for each strain were identified. Strain-specific oligonucleotide primers were designed to hybridize to the corresponding nucleotide sequences, while conserved regions were selected for generic primers in the flanking areas. The oligonucleotides were degenerated, when necessary, so as to be complementary to all the known target molecules.

The assay developed consists in a PPV-specific RT-PCR reaction, followed by four nested reactions, one for each strain. The validity of the technique was tested using biologically characterized viruses, or their cloned cDNAs overlapping the CP region, as template. High specificity was observed with no detectable cross-reaction.

The sensitivity of the assay was evaluated by comparing the diagnoses of 40 field samples collected from symptomatic trees with the results of a generic PCR method detecting

specific patterns in the 3' non-coding region. The newly developed procedure proved to be more sensitive.

Ninety-two isolates were characterized via our method. The results were compared to the diagnoses obtained by ELISA and by the previously developed RsaI-RFLP assay, and very high correlations were observed. Our assay identified a significantly larger number of mixed infections, of which the other two methods usually indicated only one component. Since the high specificities of the primers were demonstrated, it can be supposed that this result shows the higher sensitivity of our method for mixed infections. The analysis revealed a surprisingly high incidence of PPV-D in Hungary, the appearance of which coincided with the economical and social changes after 1990.

A multiplex AmpliDet RNA assay was developed for the specific detection of PVY, and for the differentiation of the PVY^{N}, $PVY^{O/C}$ strains and the tuber necrotic isolates (PVY^{NTN}). The assay is based on the generic amplification of a region within the CP coding region of all known PVY isolates by nucleic acid sequence-based amplification (NASBA) and the differentiation of the detected viral types by MBs.

PVY^{NTN} isolates are identified by detecting a chimerical sequence, previously associated with the tuber necrotic pathotype, which could have formed as a result of a rearrangement between a PVY^{N} and a PVY^{O} genome. Four MBs labeled with different fluorophores were applied. They bind to PVY^{N}- and $PVY^{O/C}$-specific sequences corresponding to the regions flanking the presumed recombination site. Thus, each viral type is signaled by two MBs. The sequences of two MBs were modified, so that they could be expected to tolerate minor sequence polymorphisms present in the target region.

The assay exhibited high specificity toward the subgroups of PVY in both single and mixed infections. The probes were tested for their abilities to tolerate a single mismatch. They gave positive, but reduced signal in all the cases tested but one, thus the MBs might serve not

only for the detection, but also for the identification of the divergent isolates. The sensitivity of the assay was found to be 10^2 target molecules, using *in vitro* transcribed RNA as template.

The technique was validated by the use of 47 PVY isolates originating from 6 countries. The results of the AmpliDet RNA assay were identical or consistent with those of biological characterization in the decisive majority of the cases.

A calculation method was proposed for the prediction of MB binding properties in AmpliDet RNA assay. The assay conditions provide a unique environment for nucleic acid interactions in several respects: a preset, relatively low temperature (41 °C) and the presence of large amount of dimethylsulphoxide, nucleotides and proteins. The probes were characterized by the free energy changes associated with beacon structure formation, and with probe-target molecule interaction. For the prediction of these parameters, thermodynamic models were combined with experimental data, which enabled extrapolations for the conditions of the assay.

The free energy values describing the stabilities of beacon structure and the binding strengths were determined experimentally for 14 MBs, via the fluorescence change accompanying the transitions. The predicted and measured values showed good agreement, within an average error of approximately 10 %, which is a good result, considering the complexity of the system.

The ranges of free energy values characterizing the formation of beacon structure, and that of the probe-target duplex, were determined and found to be wide. To evaluate MB specificity in AmpliDet RNA, an experimental system was created. Six MBs were synthesized with highly overlapping target-complementary regions of various lengths, ranging from 19 to 25 nucleotides and they possessed similar, 6 nucleotide-long stem sequences. MB specificity was tested with RNA templates containing single mutations that would result in the expectedly most and least stabile types of mismatches.

The possibility to design a point mutation specific or a mismatch tolerant probe was demonstrated, regardless of the type of the mismatch. MBs with 'intermediate' specificities were also found, giving positive signals only with the targets possessing the more stabile mismatches.

In addition, nucleotide analogues were tested for their abilities to increase the mismatch tolerance of MBs. Universal pyrimidine nucleotides were shown to be very promising for increasing MB tolerance, resulting in strong signals with the two possible cognate targets.

In the present thesis studies with both practical and theoretical purposes were described, which were aimed to advance the diagnostic methodology for plant virus detection. Beside assay development, we attempted to characterize the properties of MB on a theoretical basis, which might help the MB-design process.

Összefoglaló

Nukleinsav amplifikáción alapuló diagnosztikai eljárásokat fejlesztettünk ki két gazdasági jelentőséggel bíró növényi vírus, a szilvahimlő vírus (PPV) és a burgonya Y vírus (PVY) kimutatására és az izolátumok jellemzésére. Mindkettő veszedelmes és széles körben elterjedt kártevő. A növényi szaporítóanyagok rendszeres szűrése elengedhetetlenül szükséges a vírusmentesség biztosításához. A kidolgozott módszerek nagy érzékenységet és specifitást biztosítanak, és alkalmasak nagyszámú minta tesztelésére. Az AmpliDet RNA *assay*-ben alkalmazott molekuláris *beacon* (MB) próbák tervezéséhez javasoltunk egy termodinamikai modelleken és kísérletes adatokon alapuló predikciós módszert. Vizsgáltuk továbbá az MB próbák specifitásának a spektrumát.

A szilvahimlő vírus kimutatására és törzseinek (PPV-D, PPV-M, PPV-EA és PPV-C) elkülönítésére egy RT-PCR/*nested* PCR eljárást dolgoztunk ki. A köpenyfehérje (CP) szekvencia N-terminális részében, melyet antigén tulajdonságú régióként írtak le, az egyes törzsekre jellemző aminosav mintázatokat azonosítottunk, és a megfelelő nukleinsav szekvenciák alapján törzs-specifikus oligonukleotid primereket terveztünk. A diagnosztikus régiót határoló genomiális szekvenciákban konzervált részeket azonosítottunk a vírus-specifikus kimutatáshoz.

A kifejlesztett eljárás során az általános RT-PCR reakcióban kimutatható a vírus jelenléte. A reakció terméken végrehajtott négy, törzs-specifikus reakcióval azonosíthatjuk a fertőző törzset, vagy törzseket. A módszer működését, és az oligonukleotid primerek specifitását biológiailag jellemzett vírus mintákon, és az azokat reprezentáló, klónozott cDNS templátokon teszteltük. Az kidolgozott eljárás specifikusnak bizonyult, keresztreakciót nem figyeltünk meg.

A kimutatás érzékenységét egy korábban leírt, a 3' nem-kódoló régió specifikus mintázatát kimutató, általános PCR módszerével hasonlítottuk össze, 40 tünetes fáról

begyűjtött minta vizsgálata során. Az új módszer érzékenysége jobbnak bizonyult a korábbiénál.

Kilencvenkettő, főként Magyarországról származó PPV izolátumot jellemeztünk a kifejlesztett eljárással. Párhuzamosan ELISA ill. RsaI-RFLP tipizálásokat is végeztünk. A módszerünk adta diagnózis magas korrelációt mutatott a másik két eljárás eredményével, azonban sokkal gyakrabban jelezte PPV törzsek kevert fertőzését. Az eredmény minden esetben konzisztens volt: az egyik komponens megegyezett a másik két módszer által azonosított típussal. Mivel a primerek specifikusságát ellenőriztük, sokkal valószínűbb, hogy ez az eredmény a kifejlesztett eljárás nagyobb érzékenységére utal a törzs-specifikus azonosításban, főként kevert fertőzések esetén. A vizsgálat a PPV-D törzs meglepően magas gyakoriságát jelezte Magyarországon.

Multiplex AmpliDet RNA eljárást dolgoztunk ki a burgonya Y vírus kimutatására, és a PVY^{N}, $PVY^{O/C}$ törzsek, valamint a gumónekrózist okozó izolátumok (PVY^{NTN}) elkülönítésére. Az eljárás során a CP kódoló szekvencia egy szakaszát, a fertőző izolátum törzsétől függetlenül, NASBA (*nucleic acid sequence-based amplification*) reakcióban felszaporítjuk, míg a vírus típusának azonosítása a termékhez kötődő MB próbákkal történik.

A gumónekrózist okozó izolátumok specifikus kimutatásához a CP régióban leírt, feltételezett génátrendeződést használtuk fel. A PVY^{NTN} CP szekvencia kiméra-jellegű, mind a PVY^{N}, mind a PVY^{O} törzsre jellemző szekvenciát tartalmaz. Diagnosztikus régióként a feltételezett rekombinációs pontot tartalmazó genom szakaszt választottuk: PVY^{N}- és $PVY^{O/C}$-specifikus MB próbákat terveztünk a töréspontot határoló szekvenciákhoz. A reakcióelegy így 4 próbát tartalmaz, és bármely kimutatott típus jelenlétét 2 MB jelzi. Két próba szekvenciáját módosítottuk a célrégiók ismert polimorfizmusának tolerálása végett.

Az eljárás az egyes vírus típusokat nagy specifitással azonosította, mind egyszeres, mind kevert fertőzések esetén. A próbák *mismatch* toleranciáját ellenőriztük. Az MB próbák

egy eset kivételével a nukleotid eltérést tolerálták: pozitív, de kisebb erősségű jelet adtak a célrégióban mutációt hordozó izolátumokkal. Ezért nemcsak a vírus típusának azonosítására, de a divergensebb izolátumok jelzésére is szolgálhatnak. A módszer érzékenysége 10^2 célmolekulának adódott, *in vitro* átírt RNS templáttal.

Az eljárást 6 országból származó, 47 PVY vírus vizsgálatával teszteltük. Az AmpliDet RNA eljárás eredménye az esetek túlnyomó részében egyezett, ill. konzisztens volt a biológiai módszerekkel megállapított típussal.

Az MB próbák AmpliDet RNA *assay*-ben megfigyelt kötődési tulajdonságainak jellemzésére és predikciójára, azaz a próbák tervezésére, egy eljárást dolgoztunk ki. A termodinamikai modellek alkalmazása mellett kísérletes eredményeket is felhasználtunk, amely lehetővé tette a reakció speciális körülményeinek és a reakcióelegy összetételének a figyelembevételét. A próbákat a *beacon* struktúra kialakulását és a kötődést kísérő szabad energia változásokkal jellemeztük. Tizennégy MB esetében ezen paramétereket a konformáció változásokat kísérő fluoreszcencia változás alapján kísérletesen meghatároztuk. A predikált és mért értékek jó egyezést mutattak, 10 % körüli átlagos eltéréssel, amely, a rendszer komplexitását tekintve, jó eredménynek számít.

A működőképes, jó próbák esetében a *beacon* struktúra kialakulását és a próba kötődését jellemző mért szabad energia értékek széles tartományban helyezkedtek el. Az MB próbák AmpliDet RNA *assay*-ben megfigyelhető specifitásának a jellemzésére egy kísérleti rendszert hoztunk létre. Hat átfedő, de eltérő hosszúságú célrégióval (19-25 nukleotid), és hasonló vagy azonos *stem* szekvenciával rendelkező MB próbát szintetizáltunk. A specifitásukat egyetlen nukleotidban eltérő templát RNS molekulákkal teszteltük. Vizsgáltuk a várhatóan erősen destabilizáló ill. a relatíve stabil egyszeres *mismatch*-ek hatását a kötődés erősségére és a fluoreszcens jel intenzitására. Igazoltuk, hogy lehetséges mind pontmutáció-specifikus, mind *mismatch*-toleráló MB próbák létrehozása, a nukleotid eltérés típusától

függetlenül. Megfigyeltünk azonban 'köztes' specifitással bíró próbákat is, melyek a stabilabb kötődést eredményező eltéréseket tolerálták, míg az erősebben destabilizáló *mismatch*-ek esetén gyakorlatilag nem kötődtek.

Megvizsgáltuk a nukleotid analógok alkalmazásának a lehetőségét a *mismacth*-tolerancia növelésére, polimorf szekvenciák AmpliDet RNA *assay*-ben történő kimutatásához. Az univerzális pirimidin (P) analóg erős kötődést tett lehetővé; mindkét illeszkedő célmolekulával az analóg nélküli tökéletesen komplementer próbához hasonló intenzitású jelet eredményezett.

A dolgozatomban a nukleinsav amplifikáción alapuló diagnosztikai eljárások körébe tartozó, mind elméleti, mind gyakorlati jellegű munkákat mutattam be. Diagnosztikai eljárások fejlesztése mellett, a nukleinsav interakciók modelljének felhasználásával, a kimutatás elméleti alapon nyugvó jellemzését és tervezését is megkíséreltük.

Acknowledgement

I would like to thank my supervisor, Dr László Dorgai for his guidance and for his continuous support to my work. I also thank Dr Cor D. Schoen, who acquainted me with the latest developments in the field of diagnostic technology, and helped me both professionally and personally to be able to profit the most from my training periods at IPO-DLO (presently Plant Research International, Wageningen, The Netherlands). I thank my colleagues, Andrea Vörös, Aranka Bálint, Dr Endre Kiss-Tóth, Edit Rutkai and Béla Szamecz in Bay Zoltán Institute, and Michel M. Klerks, Dr Jan van der Wolf, Jose van Beckhoven at Plant Research International, for their help, for the inspiring discussions and the helpful suggestions. I am grateful to Dr Mária Kölber, who introduced me into the world of plant viruses and Dr Harm Huttinga for the possibility to participate in the high-level work at IPO-DLO.

I thank Dr Miklós Kálmán and the Bay Zoltán Foundation for Applied Research for the opportunity to pursue PhD studies, and DLO and Nuffic for the fellowships that enabled my participation in research in other institutes.

I would like to express my thanks to Dr Thierry Candresse, Dr László Palkovics, Dr Lev Nemchinov, Dr István Wolf, Dr Steen Nielsen, Dr Rudra P. Singh, Dr Jan van der Wolf and Michel M. Klerks, who kindly shared inocula of the viruses they isolated or the MB probes they designed.

The companies Isogen Bioscience BV and Organon Teknika (The Netherlands) greatly contributed to my work by providing molecular beacon probes and NASBA reagents, respectively.

References

1. Ahsen, v.N., Oellerich, M., Armstrong, V.W., and Schütz, E. 1999. Application of a thermodynamic nearest-neighbor model to estimate nucleic acid stability and optimize probe design: Prediction of melting points of multiple mutations of apolipoprotein B-3500 and Factor V with a hybridization probe genotyping assay on the LightCycler. Clin. Chem. 45:2094-2101.
2. Albretsen, C., Haukanes, B-I., Aasland, R., Kleppe, K. 1988. Optimal conditions for hybridization with oligonucleotides: a study with myc-oncogene DNA probes. Anal. Biochem. 170:193-202.
3. Allawi, H.T., SantaLucia, J., Jr. 1997. Thermodynamics and NMR of internal G·T mismatches in DNA. Biochemistry 36:10581-10594.
4. Allawi, H.T., SantaLucia, J., Jr. 1998a Nearest-neighbor thermodynamics of internal A·C mismatches in DNA: sequence dependence and pH effects. Biochemistry 37:9435-9444.
5. Allawi, H.T., SantaLucia, J., Jr. 1998b Thermodynamics of internal C·T mismatches in DNA. Nucl. Acids Res. 26:2694-2701.
6. Allawi, H.T., SantaLucia, J., Jr. 1998c Nearest neighbor thermodynamic parameters for internal G·A mismatches in DNA. Biochemistry 37:2170-2179.
7. Atanasoff, D., 1932. Plum pox. A new virus disease. Yearbook. University of Sofia, Faculty of Agriculture, 11:49-69.
8. Atanasoff, D., 1935. Mosaic of stone fruits. Phytopathol. Z. 8:259–284.
9. Badenes, M.L., Asins, M.J., Carbonell, E.A., Llácer, G., 1996. Genetic diversity in apricot, Prunus armeniaca, aimed at improving resistance to plum pox virus. Plant Breed. 115:133–139.
10. Barany, F. 1991. Genetic disease detection and DNA amplification using cloned thermostable ligase. PNAS 88:189-193.
11. Bawden, F.C., Pirie, N.W. 1937. The isolation and some properties of liquid crystalline substances from solanaceous plants infected with three strains of tobacco mosaic virus. – Proceedings of the Royal Society London (Series B) 123:274-320.
12. Beczner, L., Horváth, J., Romhányi, I., Förster, H., 1984. Studies on the etiology of tuber necrotic ringspot disease in potato. Potato Res. 27:339-352.

13. Beijerinck, M. W., 1898. Over een contagium vivum fluidum als oorzaak van de vlekziekte der tabaksbladeren. – Verslagen van de Gewone Vergaderingen Wis- en Natuurkunde Afdeeling Koninklijke Akademie van Wetenschappen, Amsterdam, 1898:229-235. (English translation: On a contagium vivum fluidum as the cause of fleck disease of tobacco leaves. – Phytopathological classics, American Phytopathological Society 7, 1942:32-53.)

14. Bonnet, G., Tyagi, S., Libchaber, A., Kramer, F.R. 1998. Thermodynamic basis of the enhanced specificity of structured DNA probes. PNAS 96:6171-6176.

15. Bos, L. 1999. Plant viruses, unique and intriguing pathogens – a textbook of plant virology. Backhuys Publishers, Leiden, 358 pp.

16. Boscia, D., Zeramdini, H., Cambra, M., Potere, O., Gorris, M.T., Myrta, A., DiTerlizzi, B., Savino, V. 1997. Production and characterization of a monoclonal antibody specific to the M serotype of plum pox potyvirus. Eur. J. Plant Pathol. 103:477-480.

17. Brandes, J., Wetter, C. 1959. Classification of elongated plant viruses on the basis of particle morphology. Virology 8:99-115.

18. Brown, D.M., Lin, P.K. 1991. Synthesis and duplex stability of oligonucleotides containing adenine-guanine analogues. Carbohydr Res. 216:129-139.

19. Cambra, M., Asensio, M., Gorris, M.T., Pérez, E., Camarasa, E., García, J.A., Moya, J.J., López-Abella, D., Vela, C., Sanz, A. 1994. Detection of plum pox potyvirus using monoclonal antibodies to structural and non-structural proteins. EPPO Bull. 24:569-577.

20. Candresse, T., Macquaire, G., Lanneau, M., Bousalem, M., Quiot-Douine, L., Quiot, J. B., Dunez., J. 1995. Analysis of plum pox virus variability and development of strain-specific PCR assays. Acta Hort. 386:357-369.

21. Candresse, T., Rafia, P., Dunez, J., Cambra, M., Asensio, M., Navrátil, M., Garcia, J.A., Boscia, D., Pasquini, G., Barba, M. 1998. Characterization of plum pox virus coat protein epitopes using fusion proteins expressed in E. coli. Acta Hort. 472:461-469.

22. Chachulska, A.M., Chrzanowska, M., Robaglia, C., Zagorski, W. 1997. Tobacco veinal necrosis determinants are unlikely to be located within the 5' and 3' terminal sequences of the potato virus Y genome. Arch. Virol. 142:765-779.

23. Chen, J., Iannone, M.A., Li, M.S., Taylor, J.D., Rivers, P., Nelsen, A.J., Slentz-Kesler, K.A., Roses, A., Weiner, M.P. 2000. A microsphere-based assay for multiplexed single

nucleotide polymorphism analysis using single base chain extension. Genome Res. 10:549-557.

24. Compton, J. 1991. Nucleic acid sequence-based amplification. Nature 350:91-92.

25. Crothers, D.M., Zimm, B.H. 1964. Theory of the melting transition of synthetic polynucleotides: Evaluation of the stacking free energy. J.Mol.Biol. 9:1-9.

26. da Camara Machado, A., Knapp, E., Pühringer, H., Seifert, G., Hanzer, V., Weiss, H., Wang, Q., Katinger, H., Laimer da Camara Machado, M. 1995. Gene transfer methods for the pathogen-mediated resistance breeding in fruit trees. Acta Hort. 392:193-202.

27. De Bokx, J.A., Huttinga, H. 1981. Potato virus Y. In: CMI/AAB Descriptions of plant viruses. No 242.

28. Devereux, J., Haeberly, P., Smithies, O. 1984. A comprehensive set of sequence analysis programs for the VAX. Nucl. Acid Res. 12:387-395.

29. DeVoe, H., Tinoco, I., Jr. 1962. The stability of helical polynucleotides: Base contributions. J. Mol. Biol. 4:500-517.

30. Dosba, F., Orliac, S., Dutrannoy, F., Maison, P., Massonie, G., Audergon, J.M. 1992. Evaluation of resistance to plum pox virus in apricot trees. Acta Hort. 309:211-217.

31. Dunez, J. 1988. Plum pox disease of stone fruit in Egypt. Report of a mission to Egypt. PCP/EGY/6756.

32. Edwardson, Christie, 1991. The Potyvirus group Vol. 1-4. Florida Ag. Sta. Monograph 16.

33. Felsenstein, J. 1993. PHYLIP (Phylogeny Inference Package) version 3.5c. Distributed by the author. Department of Genetics, University of Washington, Seattle.

34. Gingeras, T.R., Whitfield, K.M., Kwoh, D.Y. 1990. Unique features of the self-sustained sequence replication (3SR) reaction in the in vitro amplification of nucleic acids. Ann Biol Clin (Paris). 48:498-501.

35. Glais, I., Kerlan, C., Tribodet, M., Marie-Jean Tordo, V., Robaglia, C., Astier-Manifacier, S. 1996. Molecular characterization of potato virus Y^N isolates by PCR-RFLP. Eur. J. Plant Pathol. 102:655-662.

36. Gutierrez-Campos, R., Torres-Acosta, J.A., Saucedo-Arias, L.J., Gomez-Lim, M.A. 1999. The use of cysteine proteinase inhibitors to engineer resistance against potyviruses in transgenic tobacco plants. Nat Biotechnol. 17:1223-1226.

37. Hammond, J., Pühringer, H., da Camara Machado, A., Laimer da Camara Machado, M. 1998. A broad-spectrum PCR assay combined with RFLP analysis for detection and differentiation of plum pox virus isolates. Acta Hort. 472:483-490.

38. Han, S.J., Cho, H.S., You, J.S., Nam, Y.W., Park, E.K., Shin, J.S., Park, Y.I., Park, W.M., Paek, K.H. 1999. Gene silencing-mediated resistance in transgenic tobacco plants carrying potato virus Y coat protein gene. Mol. Cells. 9:376-383.

39. Heim, A., Grumbach, I.M., Zeuke, S., Top, B. 1998. Highly sensitive detection of gene expression of an intronless gene: amplification of mRNA, but not genomic DNA by nucleic acid sequence based amplification (NASBA). Nucl. Acids Res. 26:2250-2251.

40. Higuchi, R., Fockler, C., Dollinger, G., Watson, R. 1993. Kinetic PCR: real time monitoring of DNA amplification reactions. Biotechnology 11:1026-1030.

41. Hill, F., Loakes, D., Brown, D.M. 1998. Polymerase recognition of synthetic oligodeoxyribonucleotides incorporating degenerate pyrimidine and purine bases. PNAS 95:4258-4263.

42. Ho, S.N., Hunt, H.D., Horton, R.M., Pullen, J.K., Pease, L.R. 1989. Site-directed mutagenesis by overlap extension using the polymerase chain reaction. Gene 77:51-59.

43. Holland, P.M., Abramson, R.D., Watson, R., Gelfand, D.H. 1991. Detection of specific polymerase chain reaction product by utilizing the 5' to 3' exonuclease activity of Thermus aquaticus DNA polymerase. PNAS 88:7276-7280.

44. Howley, P.M., Israel, M.A., Law, M.F., Martin, M.A. 1979. A rapid method for detecting and mapping homology between heterologous DNAs. J. Biol. Chem. 254:4876-4883.

45. Iannone, M.A., Taylor, J.D., Chen, J., Li, M.S., Rivers, P., Slentz-Kesler, K.A., Weiner, M.P. 2000. Multiplexed single nucleotide polymorphism genotyping by oligonucleotide ligation and flow cytometry. Cytometry 39:131-140.

46. Ivanovsky, D. 1892. Ueber die Mosaikkrankheit der Tabakspflanze. – Bulletin de l'Académie Impérial des Sciences, St. Petersburg 35:67-70. (English translation: On the mosaic disease of the tobacco plant. - Phytopathological classics, American Phytopathological Society 7, 1942:27-30.)

47. Johnson, J. 1927. The classification of plant viruses. Research Bulletin Washington Agricultural Experimental Station 76:1-16.

48. Jordan, A.J. 2000. Real-time detection of PCR products and microbiology. Trends in Microbiol. 61-66.

49. Kausche, G.A., Pfankuch, E., Ruska, H. 1939. Die Sichtbarmachung von pflanzlichem virus im Übermikroskop. – Naturwissenschaften 27:292-299.

50. Kerlan, C., Dunez, J. 1976. Some properties of plum pox virus and its nucleic acid and protein components. Acta Hort. 67:185-192.

51. Kerlan, C., Dunez, J. 1979. Differenciation biologique et serologique du souches du virus de la sharka. Annales de Phytopathologie 11:541-250.

52. Kerlan, C., Tribodet, M. 1996. Are all PVY^N isolates able to induce potato tuber necrotic ringspot disease? In: The 13th Triennial Conf. of Eur. Assoc. Potato Res. Veldhoven. The Netherlands. pp. 65-66.

53. Kievits, T., van Gemen, B., van Strijp, D., Schukkink, R., Dircks, M., Adriaanse, H., Malek, L., Sooknanan, R., Lens, P. 1991. NASBA isothermal enzymatic in vitro nucleic acid amplification optimized for HIV-1 diagnosis. J. Virol. Methods 35:273-286.

54. Korschineck, I., Himmler, G., Sagl, R., Steinkellner, H., Kattinger, H.W.D. 1991. A PCR membrane spot assay for the detection of plum pox virus RNA in bark of infected trees. J. Virol. Methods 31:139-146.

55. Kurian, K.M., Watson, C.J., Wyllie, A.H. 1999. DNA chip technology. J. Pathol. 187:267-271.

56. Kwoh, D.Y., Davis, G.R., Whitfield, K.M., Chappelle, H.L., DiMichele, L.J. Gingeras, T.R. 1989. Transcription-based amplification system and detection of amplified human immunodeficiency virus type 1 with a bead-based sandwich hybridization format. PNAS 86:1173-1177.

57. Lay, M.J., Wittwer, C.T. 1997. Real-time fluorescence genotyping of factor V Leiden during rapid-cycle PCR. Clin. Chem. 43:2262-2267.

58. Le Romancer, M., Kerlan, C., Nedellec, M. 1994. Biological characterization of various geographical isolates of potato virus Y inducing superficial necrosis on potato tubers. Plant Pathol. 43:138-144.

59. Lee, L.G., Livak, K.J., Mullah, B., Graham, R.J. Vinayak, R.S., Woudenberg, T.M. 1999. Seven-color, homogeneous detection of six PCR products. BioTechniques 27:342-349.

60. Leone, G., Van Schijndel, H., Van Gemen, B., Kramer, F.R., Schoen, C.D. 1998. Molecular beacon probes combined with amplification by NASBA enable homogeneous, real time detection of RNA. Nucl. Acids Res. 26:2150-2155.

61. Levy, L., Hadidi, A. 1994. A simple and rapid method for processing tissue infected with plum pox potyvirus with specific 3' non-coding region RT-PCR assays. EPPO Bull. 24:595-604.

62. Lin, P.K.T., Brown, D.M. 1989. Synthesis and duplex stability of oligonucleotides containing cytosine-thymine analogues. Nucl. Acids Res. 17:10373-10383.

63. Livak, K.J., Flood, S.J.A., Marmaro, J., Giusti, W., Deetz, K. 1995. Oligonucleotides with fluorescent dyes at opposite ends provide a quenched probe system useful for detecting PCR product and nucleic acid hybridization. PCR Methods and Appl. 4:357-362.

64. Loakes, D., Brown, D.M., Linde, S., Hill, F. 1995. 3-Nitropyrrole and 5-nitroindole as universal bases in primers for DNA sequences and PCR. Nucl. Acids Res. 23:2361-2366.

65. López-Moya, J. J., Fernández-Fernández, M. R., Cambra, M., García, J. A. 2000. Biotechnological aspects of plum pox virus. J. Biotech.76:121-136.

66. Lunel, F., Cresta, P., Vitour, D., Paya, C., Dumont, B., Frangeul, L., Reboul, D., Brault, C., Piette, J.C., Huraux, J.M. 1999. Comparative evaluation of hepatitis C virus RNA quantitation by branched DNA, NASBA, and monitor assays. Hepatology 29:528-535.

67. Mathews, D.H., Burkard, M.E., Freier, S.M., Wyatt, J.R., Turner, D.H. 1999. Predicting oligonucleotide affinity to nucleic acid targets. RNA. 5:1458-1469.

68. McDonald, J.G., Singh, R.P. 1996. Response of potato cultivars to North American isolates of PVY^{NTN}. Am. Potato. J. 73, 317-323.

69. McKay, M.B., Warner, M.F. 1933. Historical sketch of tulip mosaic or breaking. The oldest known plant virus disease. – Nat. Horticultural Magazine 12:179-216.

70. Mullis, K., Faloona, F., Scharf, S.J., Saiki, R., Horn, G., Erlich, H. 1986. Specific enzymatic amplification of DNA in vitro: The polymerase chain reaction. Cold Spring Harb. Symp. Quant. Biol. 51:263-273.

71. Munro, J. 1955. The reactions of certain solanaceous species to strains of potato virus Y. Can. J. Botany 33:355-361.

72. Musielski, H., Mann, W., Laue, R., Michel, S. 1981. Influence of dimethylsulfoxide on transcription by bacteriophage T3-induced RNA polymerase. Z. Allg. Mikrobiol. 21:447-456.

73. Myrta, A., Di Terlizzi, B., Boscia, D., Çaglayan, K., Gavriel, I., Ghanem, G., Varveri, C., Savino, V. 1998a Detection and serotyping of Mediterranean plum pox virus isolates by means of strain-specific monoclonal antibodies. Acta Virol. 42:251-254.

74. Myrta, A., Potere, O., Boscia, D., Candresse, T., Cambra, M., Savino, V. 1998b Production of a monoclonal antibody specific to the El Amar strain of Plum Pox Virus. Acta Virol. 42:248-251.

75. Myrta, A., Potere, O., Crescenzi, A., Nuzzaci, M., Boscia, D. 2001. Properties of two monoclonal antibodies specific to the cherry strain of plum pox virus. J. of Plant Pathol. (in press).

76. Nakano, S., Fujimoto, M., Hara, H., Sugimoto, N. 1999. Nucleic acid duplex stability: influence of base composition on cation effects. Nucl. Acids Res. 27:2957-2965.

77. Nazarenko, I., Bhatnagar, S., Hohman, R. 1997. A closed tube format for amplification and detection of DNA based on energy transfer. Nucl. Acids Res. 25:2516-2521.

78. Nemchinov, L., Hadidi, A., Maiss, E., Cambra, M., Candresse, T., Damsteegt, V. 1996. Sour cherry strain of plum pox potyvirus (PPV): Molecular and serological evidence for a new subgroup of PPV strains. Mol. Plant Pathol. 86:1215-1221.

79. Németh, M. 1963. Field and greenhouse experiments with plum pox virus. Phytopath. Medit. 2:162-166.

80. Németh, M., Kölber M. 1994. History and importance of plum pox in stone-fruit production. EPPO Bull. 24:525-536.

81. Németh, M., Kölber, M. 1981. GF31, a reliable myrobalan field indicator for rapid detection of plum pox virus. Acta Hort. 94:207-214.

82. Olmos, A., Dasí, M.A., Candresse, T., Cambra, M. 1996. Print capture PCR: a simple and highly sensitive method for the detection of plum pox virus (PPV) in plant tissues. Nucl. Acids Res. 24:2192–2193.

83. Olmos. A., Cambra, M., Dasi, M.A., Candresse, T., Esteban, O., Gorris, M.T., Asensio, M. 1997. Simultaneous detection and typing of plum pox potyvirus (PPV) isolates by heminested-PCR and PCR-ELISA. J. Virol. Methods 68:127-137.

84. Palkovics, L., Burgyán, J., Balázs, E. 1993. Comparative sequence analysis of four complete primary structures of plum pox virus strains. Virus Genes 7:339-347.

85. Palkovics, L., Wittner, A., Balázs, E. 1995. Pathogen-derived resistance induced by integrating the plum pox virus coat protein gene into plants of Nicotiana benthamiana. Acta Horticult. 386:311–317.

86. Peyret, N.P., Seneviratne, A., Allawi, H.T., SantaLucia, J. Jr. 1999. Nearest-neighbor thermodynamics and NMR of DNA sequences with internal A·A, C·C, G·G, and T·T mismatches. Biochemistry 38:3468-3477.

87. Poggi-Pollini, C., Giunchedi, L., Bissani, R. 1997. Specific detection of D- and M-isolates of plum pox virus by immunoenzymatic determination of PCR products. J. Virol. Methods 67:127-133.

88. Pribék, D., Gáborjányi, R. 1997. Hungarian Plum pox virus isolates represent different serotypes. Acta Phytopathol. and Enthomol. Hung. 32:281-288.

89. Pribék, D., Palkovics, L., Gáborjányi, R. 1998. A hazai szilvahimlő vírus izolátumok genetikai polimorfizmusának bizonyítása RT-PCR módszerrel. Növényvédelem 34:601-605.

90. Ratcliff, F., Harrison, B.D., Baulcombe, D.C. 1997. A similarity between viral defense and gene silencing in plants. Science 276:1558-1560.

91. Ravelonandro, M., Monsion, M., Delbos, R., Dunez, J. 1993. Variable resistance to plum pox virus and potato virus Y infection in transgenic plants expressing plum pox virus coat protein. Plant Sci. 91:157-169.

92. Ravelonandro, M., Scorza, R., Bachelier, J.C., Labonne, G., Levy, L., Damsteegt, V., Callahan, A.M., Dunez, J., 1997. Resistance of transgenic Prunus domestica to plum pox virus infection. Plant Dis. 81:1231-1235.

93. Regner, F., da Camara Machado, A., Laimer da Camara Machado, M., Steinkellner, H., Mattanovich, D., Hanzer, V., Weiss, H., Kattinger, H., 1992. Coat protein mediated resistance to plum pox virus in Nicotiana cle6elandii and Nicotiana benthamiana. Plant Cell Rep. 11:30-33.

94. Revers, F., Le Gall, O., Candressse, T., Le Romancer, M., Dunez, J., 1996. Frequent occurrence of recombinant potyvirus isolates. J. Gen. Virol. 77:1953-1965.

95. Rose, T.M., Schultz, E.R., Henikoff, J.G., Pietrokovski, S., McCallum, C.M., Henikoff, S. 1998. Consensus-degenerate hybrid oligonucleotide primers for amplification of distantly related sequences. Nucl. Acids Res. 26:1628-1635.

96. Rychlik, W., Spencer, W.J., Rhoads, R.E. 1990. Optimization of the annealing temperature for DNA amplification *in vitro*. Nucl. Acids Res. 18:6409-6412.

97. Saenz, P., Cervera, M.T., Dallot, S., Quiot, L., Quiot, J.B., Riechmann, J.L., Garcia, J.A. 2000. Identification of a pathogenicity determinant of Plum pox virus in the sequence encoding the C-terminal region of protein P3+6K(1). J. Gen. Virol. 81:557-566.

98. Salminen, M.O., Carr, J.K., Burke, D.S., McCutchan, F.E. 1995. Identification of breakpoints in intergenotypic recombinants of HIV type 1 by bootscanning. AIDS Res Hum Retroviruses11:1423-1425.

99. SantaLucia, J., Jr. 1998. A unified view of polymer, dumbbell, and oligonucleotide DNA nearest-neighbor thermodynamics. PNAS 95:1460-1465.

100. Schweitzer, B., Kingsmore, S. 2001. Combining nucleic acid amplification and detection. Curr. Op. in Bitechnol. 12:21-27.

101. Shukla, D.D., Stike, P.M., Tracy, S.L., Gough, K.H., Ward, C.W. 1988. The N and C termini of the coat proteins of potyviruses are surface located and the N terminus contains the major virus specific epitopes. J. Gen. Virol. 69:1497-1508.

102. Singh, M., Singh, RP. 1996. Nucleotide sequence and genome organization of a Canadian isolate of the common strain of potato virus Y (PVY^{O}). Can. J. of Plant Pathol. 18:209-224.

103. Smith, K. M. 1931. Composite nature of certain potato viruses of the mosaic group. Nature 127:702.

104. Smits, H.L., van Gemen, B., Schukkink, R., van der Velden, J., Tjong-A-Hung, S.P., Jebbink, M.F., ter Schegget, J. 1995. Application of the NASBA nucleic acid amplification method for the detection of human papillomavirus type 16 E6-E7 transcripts. J Virol Methods. 54:75-81.

105. Spiegel, S., Scott, S.W., Bowman-Vance, V., Tam, Y., Galiakparov, N.N., Rosner, A. 1996. Improved detection of Prunus necrotic ringspot virus by the polymerase chain reaction. Eur. J. Plant Pathol. 102:681-685.

106. Stanley, W.M. 1935. Isolation of crystalline protein possessing the properties of tobacco mosaic virus. Science 81:644-645.

107. Stanley, W.M., Valens, E.G. 1961. Viruses and the Nature of Life. Dutton, New York, 224 pp.

108. Steemers, F.J., Ferguson, J.A., Walt, D.R. 2000. Screening unlabeled DNA targets with randomly ordered fiber-optic gene arrays. Nat. Biotechnol. 18:91-94.

109. Sugimoto, N., Nakano, S., Katoh, M., Matsumura, A., Nakamuta, H., Ohmichi, T., Yoneyama, M., Sasaki, M. 1995. Thermodynamic parameters to predict stability of RNA/DNA hybrid duplexes. Biochemistry 34:11211-11216.

110. Svanvik, N., Westman, G., Wang, D., Kubista M. 2000. Light-up probes: thizaole orange-conjugated peptide nucleic acid for detection of target nucleic acid in homogeneous solution. Anal. Biochem. 281:26-35.

111. Szirmai, J. 1948. A kajszi vírusbetegsége. Magyar bor és gyümölcs. 3(17):7-8.

112. Täpp, I., Malmberg, L., Rennel, E., Wik, M., Syvänen, A-C. 2000. Homogeneous scoring of single-nucleotide polymorphisms: comparison of the 5'-nuclease TaqMan® assay and Molecular Beacon probes. Biotechniques 28:732-738.

113. Thelwell, N., Millington, S., Solinas, A., Booth, J., Brown, T. 2000. Mode of action and application of Scorpion primers to mutation detection. Nucl. Acids Res. 28:3752-3761.

114. Thompson, J.D., Higgins, D.G., Gibson, T.J. 1994. CLUSTAL W: improving the sensitivity of progressive multiple sequence alignment through sequence weighting, position-specific gap penalties and weight matrix choice. Nucl. Acids Res. 22:4673-4680.

115. Tyagi, S., Bratu, D.P., Kramer, F.R. 1998. Multicolor molecular beacons for allele discrimination. Nat. Biotechnol. 16:49-53.

116. Tyagi, S., Kramer, F.R. 1996. Molecular beacons; probes that fluoresce upon hybridization. Nat. Biotechnol. 14:303-308.

117. van den Heuvel, J.F.J.M., van der Vlugt, R.A.A., Verbeek, M., de Haan, P.T., Huttinga, H. 1994. Characteristics of a resistance-breaking isolate of potato virus Y causing tuber necrotic disease. Eur. J. of Plant Pathol. 100:347-356.

118. van Gemen, B., Kievits, T., Schukkink, R., van Strijp, D., Malek, L.T., Sooknanan, R., Huisman, H.G., Lens, P. 1993. Quantification of HIV-1 RNA in plasma using NASBA during HIV-1 primary infection. J. Virol. Methods 43:177-187.

119. van Regenmortel, M.H.V. 1990. Virus species, a much overlooked but essential concept in virus classification. – Intervirology 31:241-254.

120. van Regenmortel, M.H.V., Fauquet, C.M., Bishop, D.H.L. (eds) 1999. Virus Taxonomy. Seventh Report of the International Committee on Taxonomy of Viruses. Academic Press, London, UK, 1024 pp.

121. Walker, G.T., Fraiser, M.S., Schramm, J.L., Little, M.C., Nadeau, J.G., Malinowski, D.P. 1992. Strand displacement amplification – an isothermal in vitro DNA amplification technique. Nucl. Acids Res. 20:1691-1696.

122. Wallace, R.B., Shaffer, J., Murphy, R.F., Bonner, J., Hirose, T., Itakure, K. 1979. Hybridization of synthetic oligodeoxyribonucleotides to phi chi 174 DNA: the effect of single base pair mismatch. Nucl. Acids Res. 6:3543-3547.

123. Walsh, K., North, J., Barker, I., Boonham, N. 2001. Detection of different strains of Potato virus Y and their mixed infections using competitive fluorescent RT-PCR. J. Virol. Methods 91:167-173.

124. Wang, C., Altieri, F., Ferraro, A., Giartosio, A., Turano, C. 1993. The effect of polyols on the stability of duplex DNA. Physiol Chem Phys Med NMR. 25:273-280.

125. Wang, D.G, Fan, J-B., Siao, C-J., Berno, A., Young, P., Sapolsky, R., Ghandour, G., Perkins, N., Winchester, E., Spencer, J., Kruglyak, L., Stein, L., Hsie, L., Topaloglou, T., Hubbell, E., Robinson, E., Mittmann, M., Morris, M.S., Shen, N., Kilburn, D., Rioux, J., Nusbaum, C., Rozen, S., Hudson, T.J., Lipshutz, R., Chee, M., Lander, E.S. 1998. Large-scale identification, mapping, and genotyping of single-nucleotide polymorphisms in the human genome. Science 280:1077-1082.

126. Weilguny, H., Singh, R.P. 1998. Separation of Slovenian isolates of PVY^{NTN} from the North American isolates of PVY^{N} by a 3-primer PCR. J. Virol. Methods 71:57-68.

127. Wetzel, T., Candresse, T., Macquaire, G., Ravelonandro, M., Dunez, J. 1992. A highly sensitive immunocapture polymerase chain reaction method for plum pox potyvirus detection. J. Virol. Methods 39:27-37.

128. Wetzel, T., Candresse, T., Ravelonandro, M., Dunez, J. 1991. A polymerase chain reaction assay adapted to plum pox virus detection. J. Virol. Methods 33:355-365.

129. Whitcombe, D., Theaker, J., Guy, S.P., Brown, T., Little, S. 1999. Detection of PCR products using self-probing amplicons and fluorescence. Nat. Biotechnol. 17:804-807.

130. Wolf, I., Horváth, S. 2001. A burgonya Y vírus (Potato Y Potyvirus, PVY) törzseinek előfordulása burgonya termőterületeken Magyarországon. Növényvédelem, in press.

131. Xia, T., SantaLucia, J., Jr., Burkard, M.E., Kierzek, R., Shroeder, S.J., Jiao, X., Cox, C., Turner, D.H. 1998. Thermodynamic parameters for an expanded nearest-neighbor model for formation of RNA duplexes with Watson-Crick base pairs. Biochemistry 37:14719-14735.

132. Zuker, M. 2000. Calculating nucleic acid secondary structure. Curr Opin Struct Biol. 10:303-310.